5-24-2010

Mechanism of yeast prion portein aggregation and strain formation

Tejas Baba Kalastavadi
Washington University in St. Louis

WASHINGTON UNIVERSITY

Division of Biology and Biomedical Sciences

Program in Molecular Genetics and Genomics

Dissertation Examination Committee
Dr. Heather L. True-Krob, Chairperson
Dr. John Cooper
Dr. Marc Diamond
Dr. Jin Moo-Lee
Dr. Petra Levin
Dr. Rohit Pappu

Mechanism of yeast prion protein aggregation and strain formation

By

Tejas Baba Chandrashekar Kalastavadi

A dissertation presented to the
Graduate School of Arts and Sciences
Of Washington University
in partial fulfillment of the
requirements for the degree of
Doctor of Philosophy

August 2010
Saint Louis, Missouri

ABSTRACT OF THE DISSERTATION

Mechanism of yeast prion protein aggregation and strain formation

By

Tejas Baba Chandrashekar Kalastavadi

Doctor of Philosophy in Biology and Biomedical Sciences

(Molecular Genetics and Genomics)

Washington University in Saint Louis, 2010

Professor Heather L. True, Chairperson

Misfolding and aggregation of the prion protein (PrP) causes fatal neurodegenerative diseases in many mammalian species, including humans. Mutations in the gene encoding PrP are associated with ~15% of the incidences, while, the vast majority of the cases are sporadic. Interestingly, prion diseases also display pathological variation, suggesting that there are multiple different strains.

To elucidate the mechanism of prion protein aggregation and strain formation, I have taken advantage of the yeast prions [*PSI*+] and [*RNQ*+] and their protein determinants Sup35p and Rnq1p, respectively. Using a Sup35-PrP chimera, I have investigated the effect of the disease associated oligopeptide repeat domain (ORD) expansions of PrP, on prion propagation and amyloid fiber formation. We previously determined that these chimeric proteins maintain the [*PSI*+] yeast prion phenotype. Interestingly, we noted that the repeat expanded chimeric prions maintained a stronger strain of [*PSI*+]. Investigations of the chimeric proteins in vitro revealed that repeat-expansions also increase aggregation propensity. However, despite the increased

aggregation propensity of the repeat expanded proteins, there was no corresponding increase in the stability of the fibers. Therefore, we predicted that the repeat expansions may spontaneously convert to [*PRION*+] with a much higher frequency. Contrary to our prediction, we observed that enhanced conversion of the repeat expanded chimeras only occurred in the presence of another prion, [*RNQ*+] prion.

The [*RNQ*+] prion has previously been implicated in the de novo induction of the [*PSI*+] prion, and therefore also is referred to as [*PIN*+] for ***P***SI ***In***ducible. However, the interaction of [PSI+] and [RNQ+] prions has not been clearly defined and the physical basis for the strains of [*RNQ*+] has been largely unexplored. I have, for the first time, been able to create different strains of [*RNQ*+] in vitro. Rnq1p prion forming domain (Rnq1p PFD) can form fibers that template the conversion of monomeric protein into amyloid fibers. Further, Rnq1p PFD has a shorter lag phase for fiber formation at 37°C when compared to 25°C. Surprisingly, increasing the temperature at which fibers are formed also increased the stability of these fibers. Additionally, the morphology of the fibers is dramatically altered at different temperatures. These distinct biochemical properties manifest as different distributions of [*RNQ*+] strains when the fibers are transformed into yeast cells. Transformants of Rnq1p PFD fibers resulted in weak, medium and strong [*RNQ*+] strains. The amount of aggregated protein and the ability to propagate the prion increased with the strength of the prion strain. However, the [*PIN*+] prion phenotype did not correlate with the [*RNQ*+] prion strength. The weak and strong [*RNQ*+] both induced the [*PSI*+] prion with equally higher efficiencies when compared to the medium [*RNQ*+]. Coincidently, the weak [*RNQ*+] strain has very similar properties

to the previously identified very high [*PIN*+] strain suggesting an incongruent relationship between [RNQ+] and [PIN+] associated phenotypes.

Determining the biochemical properties of the Rnq1p PFD fibers and their ability to induce specific distributions of prion strains has enabled us to dissect the mechanism for the [*RNQ*+] prion strains. Additionally, I have been able to distinguish the mechanisms involved in determining the [*PIN*+] prion strains from the [*RNQ*+] strains. Incorporating the mechanism of strain formation elucidated by investigating [*RNQ*+] strains, with the previously proposed model for [*PSI*+] strains, has provided us a framework to understand both general and specific properties of prion disease strains.

Acknowledgements

I would like to thank Heather True for allowing me to join her laboratory for my thesis work. She has been very patient with my progress in the lab and has provided me with all the encouragement and support I've needed to grow as a scientist. I can honestly say that I may have not been able to finish my Ph.D. had it not been for her mentorship.

I want to thank the True Lab for providing a wonderful environment to work in for almost six years. I would like to thank past members of the lab, Sarah Simpson and Lisa Strawn who were here before I joined the lab. I would like to thank Elizabeth Tank for showing me what it is to have good work ethic. The other members of the lab: Rachel Bouttenot for insights and entertainment, Patrick Bardill for his wit and humor. Adeline Lin, Jen Dulle, Donell Carey, Kevin Stein for being patient with me and all the help and support they have provided. I would like to thank Erin Straight for allowing me to live vicariously through her the last few months of graduate school. I would also like to thank the undergraduate students who have worked with me over the years for their help and for dealing with me.

My experience in Saint Louis would not have been the same had I not met Abhishek Saharia. We were roommates for five and a half years. In him I have found a brother I've never had. I would like to thank all my other friends and family who have made the past few years memorable.

I am greatly indebted to my parents Dr. P. Chandrashekar and R. Jayalakshmi for providing me with all the opportunities in life and more. I would like to thank my extended family for all the love and support I've received from them throughout my life.

Finally, my life has never been the same since I met Fiorella Ghisays. She believed in me and gave me a chance. If not for her, I would not have finished my thesis in a timely fashion. She has provided me in her a passion for hard work, success and respect. Any success I achieve in life here on, I bet will be due to her motivation and belief she has in me.

TABLE OF CONTENTS

LIST OF TABLES AND FIGURES

Chapter 1: Background and Significance

1.1 Overview: Protein misfolding and aggregation-based diseases

A vast number of diseases in humans have been linked to misfolding and aggregation of a functionally and sequentially diverse set of endogenously expressed proteins (Table 1.1) (1). Many fatal neurodegenerative disorders are part of this class of protein misfolding diseases (2). The cause for misfolding and aggregation of these proteins is not clearly understood in most cases and as such, the onset of disease is considered to be sporadic (1). A subset of these diseases is linked to specific mutations in the gene encoding the protein that is aggregated. An interesting feature of these proteins is that they do not form non-specific amorphous aggregates but instead self-assemble into ordered amyloid fibers (2). The consequence that most of these mutations have on protein misfolding, conformational conversion and eventual aggregation (amyloid formation) is not clearly defined, however.

The original introduction of the term "amyloid" and description for macroscopic deposits in human tissue was provided by Virchow in 1854 (3). It was later determined that these inclusions were proteinaceous in nature and associated with various clinical symptoms (3). Major advancements since then have provided clues toward understanding the mechanisms by which they are formed and the role they play in physiology and pathology of various organisms from bacteria to humans (1). Many important questions remain, however, including the effect that disease-associated mutations have on amyloid fiber formation and disease onset, physical basis and consequence of conformational diversity of amyloid fibers, and properties that bestow certain amyloid-like aggregates to be infectious.

Table 1.1 Human diseases associated with amyloid deposition

Disease Name	**Fibril protein/ peptide**
Prion disease (CJD, GSS, FFI, Kuru)	Prion Protein
Alzheimer's disease (AD)	Amyloid β (Aβ)
Parkinson's disease (PD)	α-synuclein
Frontotemporal lobar dementia (FLTD)	Tau and TDP-43
Amyotrophic lateral sclerosis (ALS)	Superoxide dismutase (SOD), TDP-43
Huntington disease (HD)	Huntingtin exon-1 with polyQ expansion
Spinocerebellar ataxias (SCAs)	Ataxins with polyQ expansion
Senile systemic amyloidosis	Transthyretin
Reactive systemic AA amyloidosis	Serum amyloid A protein
Haemodialysis amyloidosis	$\beta_2$microglobulin

Table 1.2 *Saccharomyces cerevisiae* prion proteins

Prion	Protein determinant	Function of protein (modified from (4))
[URE3]	Ure2p	Nitrogen catabolism
[*PSI*+]	Sup35p	Translation termination
[*RNQ*+]	Rnq1p	Unknown function, promotes induction of [PSI+]
[*SWI*+]	Swi1p	Transcriptional regulation
[MCA]	Mca1p	Regulation of apoptosis
[*OCT*+]	Cyc8p	Transcriptional repression
[*MOT3*+]	Mot3p	Transcriptional regulation

The most common protein-aggregation based neurodegenerative diseases are Alzheimer's Disease (AD) and Parkinson's Disease (PD) (2). The onset of these diseases is very strongly age dependent, which may be a consequence of a decreased functionality of the quality control machinery. Diseases caused by expansion of a poly-glutamine tract in the protein, such as Huntington's disease, show a strong inverse correlation between the age of onset and the length of the poly-glutamine expansion (5). This may be due to an increase in the intrinsic ability of the mutant proteins to aggregate and cause disease. Although, neurodegenerative diseases tend to show strong age-dependence, there is considerable variation in clinical and pathological manifestation of several human amyloid disorders including prion disease (6). Self-propagating variation in the conformation of the aggregated amyloid fibers has been proposed to be the molecular basis for this phenotypic variation (7).

Various models have been suggested to explain the effect of protein aggregates on cellular function that results in disease. Both loss-of-function of the aggregated protein as well as toxic gain-of-function of the aggregates have been considered for some diseases. Interestingly, some evidence suggests that it is actually on-pathway oligomers that are toxic to cells and that the amyloid fibers may provide a protective effect by sequestering the oligomers (8,9). Deciphering the structural information of amyloid fibers has been fairly successful. In comparison elucidating the structure of the transient oligomers has been quite challenging, although, recent biophysical experiments show promising results (10).

Intriguingly, not all protein aggregates are disease-causing. Some amyloid-like aggregates of proteins are thought to have functional roles (1). In the yeast,

Saccharomyces cerevisiae, many different protein aggregates have been proposed to have roles in cellular physiology and adaptation (Table 1.2) (4). Investigation of these yeast proteins and their properties has provided important insights into the mechanisms of protein aggregation.

In this chapter, I will focus on protein misfolding and the ability of proteins to form amyloid fibers. Subsequently, I will discuss prion diseases specifically and features of the prion protein that are unlike other protein misfolding disorders. I will place special emphasis on two topics 1) specific class of inherited prion disease, and 2) the phenomenon of prion strains and the ability of certain proteins to be infectious in nature. Finally, I will discuss work done in yeast using endogenous prion proteins to understand various aspects of protein misfolding disorders and specifically with respect to prion disease.

1.2 Protein misfolding and amyloid fiber formation

Proper folding of proteins is critical for cellular function and physiology and the cell has developed many mechanisms to deal with misfolded proteins (11). The problem of how proteins fold into their native structure has been a long-standing question. In 1973 Christian Anfinsen and colleagues postulated that the native structure of a protein is the thermodynamically stable structure and that it only depends on the amino acid sequence and conditions of the solution (12). More recently, Dobson and colleagues have provided evidence to suggest that most polypeptide chains, irrespective of the specific amino acid sequence, have the ability to form amyloid fibers given the

appropriate solution conditions (13). However, the propensity and the ability of a specific protein to form fibers in vivo is dependens on the amino-acid sequence (14).

Various models have been proposed to explain the formation of amyloid fibers from otherwise folded proteins (illustrated in Figure 3) (1). Proteins that are normally in their native conformation, through an as yet unknown mechanism, form predominantly β-sheet rich amyloid fibers. It has yet to be determined whether the monomeric, natively-folded protein undergoes a conformational change prior to oligomerizing and forming amyloid fibers, or if the monomers oligomerize initially and then acquire a different conformation. It is possible that both these pathways are utilized, but the specific pathway that a protein takes toward forming fibers is dependent on the specific properties of the polypeptide in question. In addition, certain mutations associated with protein aggregation diseases have been shown to destabilize the native conformation of the protein and thereby promote aggregation, at least in vitro (15,16).

Although the precise timing of the conformational change that occurs in the proteins that form amyloid fibers is not known, it has been well-established that amyloid formation occurs through a nucleation-dependent pathway (1). The time course for fiber formation as assayed by Thioflavin-T (Th-T), typically follows a sigmoidal growth curve consisting of a lag phase, followed by an exponential growth phase, and finally a plateau phase that indicates the end of the reaction (17,18). The lag phase is considered to be the rate-limiting step during which the nucleus is formed. The lag phase can be eliminated by adding preformed fibers to a reaction containing monomeric protein, thereby nucleating or seeding the reaction (1). Very little is known about the changes that may be

Figure 1 Model for protein aggregation pathways (from Chiti and Dobson, Annu. Rev. Biochem. 2006. 75:333-66)

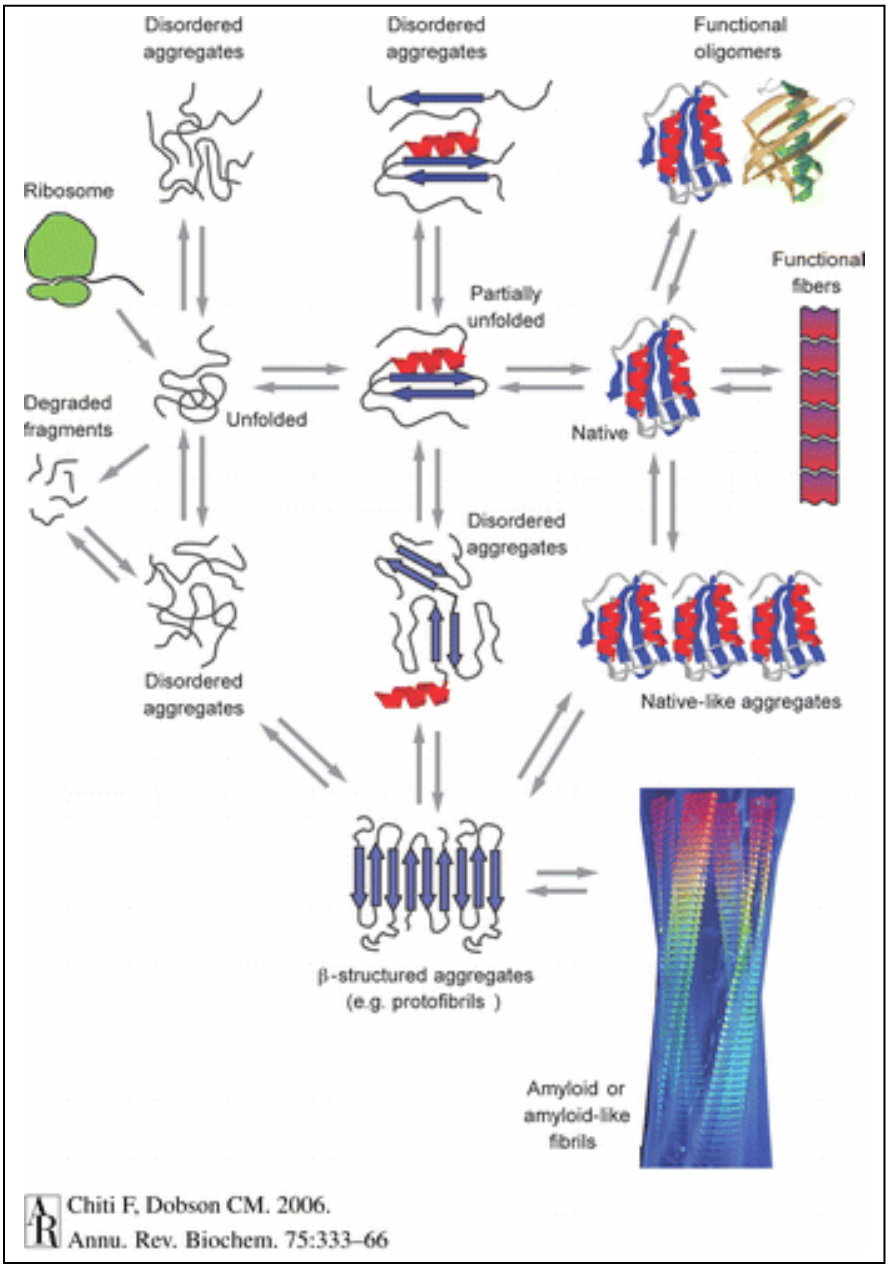

occurring during the lag phase and this has proven to be a very interesting and challenging area of research.

The amyloid fibers formed in vitro by the various polypeptides and proteins have a common set of characteristics. They can be imaged using either transmission electron microscopy (TEM) or atomic force microscopy (AFM). The amyloid fibers are ~10 nm in diameter and can assemble with other fibers to form higher-order structures (19). X-ray diffraction experiments have shown that individual protofibrils are composed of assembled monomeric proteins or peptides such that the polypeptide chain forms β-strands that run perpendicular to the axis of the fibril (Figure 1A and 1B) (20). The fibers can bind dyes such as thioflavin-T (ThT) and Congo Red (CR) (21). Recent attempts to solve the structure of amyloid fibers have been successful. The use of solid-state NMR (SSNMR) and X-ray crystal diffraction analysis of nano- and microcrystals using peptide fragments from amyloidogenic proteins have proven useful in defining the structural details of the fibers (22-25). A peptide (GNNQQNY) derived from Sup35p, a yeast prion protein, formed three-dimensional crystals that possessed the characteristics of amyloid fibers (25). For this specific peptide, each individual peptide molecule formed a single β-strand and stacked in-parallel and in-register to form a single β-sheet (Figure 1C and 1D). The β-sheets are also packed in pairs in parallel to each other (25). Since the discovery of the amyloid structure of the Sup35p derived peptide, other peptides obtained from the sequence of a milieu of proteins have shown a range of atomic architectures for amyloid fibers (26). These diverse structures provide a plausible molecular explanation for the existence of the strain phenomena in amyloid-related disorders.

Figure 2 Structure of amyloid fibril (from Baxa, U. Curr Alzheimer Res. 2008 June; 5(3): 308-318)

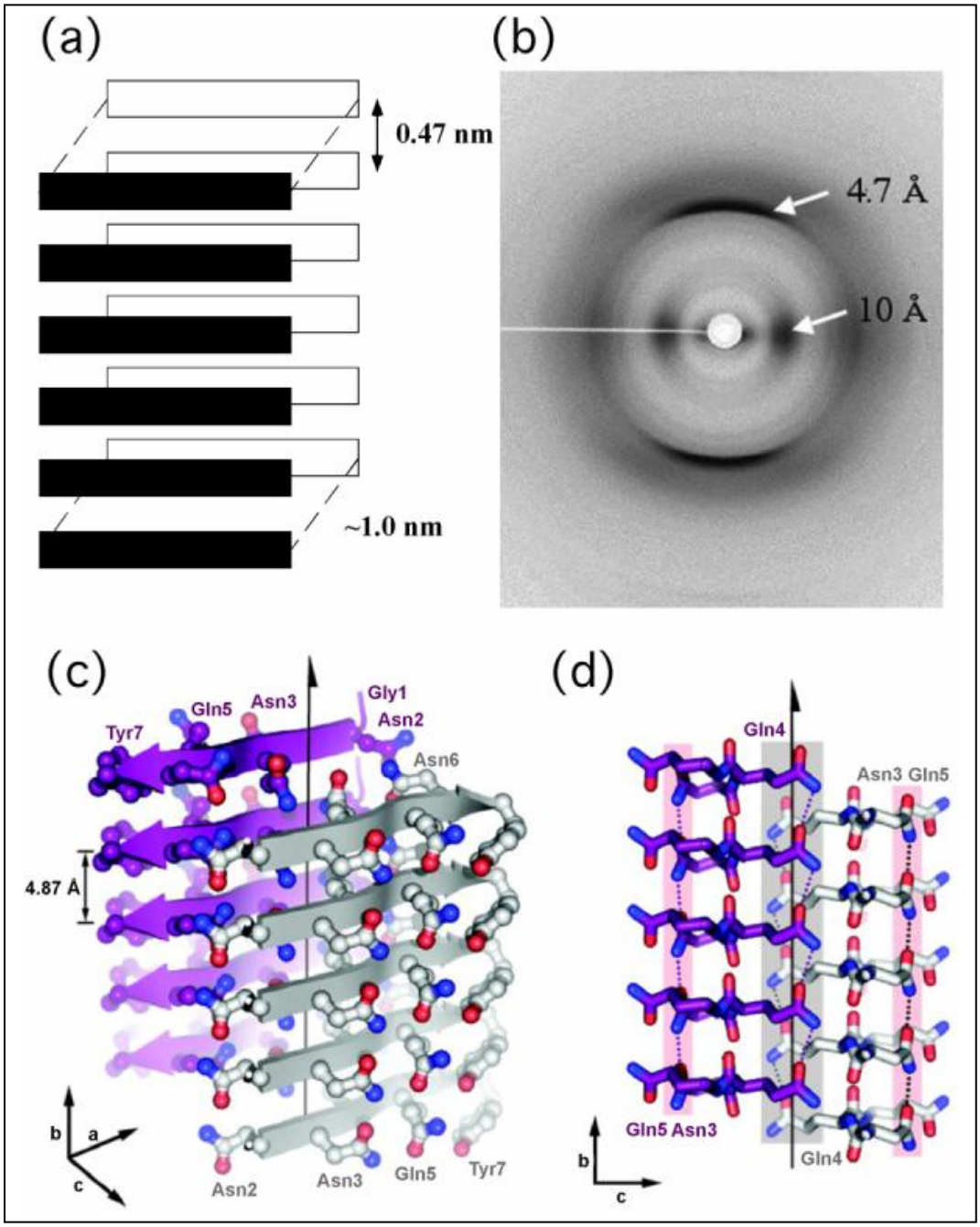

In contrast to the progress made towards unraveling the structure of the amyloid fiber, there is little known about what may prove to be the most interesting of species in the pathway of amyloid formation, the oligomers that act as the intermediates between monomers and fibers. There is growing evidence to suggest that such oligomers are the toxic species that result in cell death and cause disease (9). The discovery of an antibody that specifically recognizes oligomers and does so with oligomers formed from multiple proteins suggested common structural characteristics of these species (27). However, there is data suggesting the existence of low molecular weight oligomers that are relatively disorganized prior to the formation of a structure that can be recognized by the oligomer specific antibodies (28). Considering the information currently available, one can imagine many different pathways a protein can take to go from natively-folded protein to amyloid fibers that constitute protein deposits associated with various diseases.

1.3 Repeat expansion proteins and neurodegenerative disease

Expansion of the CAG codon that encodes the amino acid glutamine has been associated with various neurodegenerative diseases (29). These so called "polyglutamine" diseases, due to the nature of the expanded glutamine tract, include Huntington disease (HD), several spinocerebellar ataxias (SCAs) and spinal bulbar muscular atrophy (SBMA) (29). Large inclusions of the proteins with the expanded glutamine tract have been associated with disease and were thought to be the cause of neurodegeneration (30). However, there is evidence to suggest that these aggregated protein inclusions may not be obligatorily associated with disease (31). Cases of disease

in the absence of protein aggregates, as well as the absence of any disease pathology in the presence of aggregates have been observed (32,33).

Expanded polyglutamine proteins have an increased propensity to aggregate and form ordered amyloid fibers in vitro (34). Additionally, the poly-Q length seems to play a critical role in aggregation potential and toxicity (35). There is a strong inverse correlation between age of onset of disease and length of poly-Q expansion (36). Loss-of-function, toxic gain-of-function, or altered function have been attributed as mechanisms that can result in the onset of the growing number of repeat expansion related neurodegenerative diseases (30). Although the poly-Q expansion has been the main focus of research and has bared the brunt of blame for disease, it is becoming increasing clear that sequence around the poly-Q expansion is a crucial determinant in pathogenesis (37).

In the case of prion disease, insertion mutations that expand an octapeptide repeat domain (ORD) from the endogenous number of five repeats to and additional two to nine repeats causes a dominantally inherited form of prion disease in humans (38). Significant effort has been placed on understanding the effect of the poly-Q insertion mutations on protein folding and aggregation, however, not much is known about the effect of the ORD expansion mutations on protein folding with the prion protein. In chapter two, I discuss work done to address this question and provide a plausible biochemical explanation for the onset of disease due to expansion in the ORD in PrP.

1.4 Prion proteins and disease

Transmissible spongiform encephalopathies (TSEs or prion diseases) have been one of the most intriguing and enigmatic diseases. This disease first presented itself as Kuru among the Fore tribe in Papua New Guinea and was studied extensively by D. Carleton Gajdusek (39). It was initially thought to be caused by a slow viral infection with long incubation times and progressive pathology that ended in fatality (40). Subsequently, many other neurodegenerative diseases similar to Kuru, such as scrapie in sheep and Creutzfeldt-Jakob disease in humans (CJD) were grouped together based on their similarities (41). More interestingly, both scrapie and CJD were also shown to be transmissible (42,43).

Human prion disease presents itself as many different disorders. As mentioned earlier, Kuru and CJD are two types of prion disease. Gerstmann-Straussler syndrome (GSS), variant CJD (vCJD) and Fatal Familial Insomnia (FFI) are also disorders that are referred to as prion diseases (44). Prion disease itself may have genetic, infectious or sporadic origins but all cases present with spongiform degeneration.

Based on various lines of evidence Stanley Prusiner proposed that the transmissible agent in these diseases was not a virus, but a small *pro*teinaceous *in*fectious particle he termed "prion" (45). He noted that the infectious agent was protease sensitive, but agents that modified nucleic acids failed to cause inactivation. It was later shown that prion particles are primarily composed of an abnormal conformation of the prion protein (PrP), a ~27 kDa protein encoded by the *PRNP* gene, endogenously expressed in mammalian cells (46). PrP is a membrane-anchored protein that undergoes cleavage of its signal peptide and glycosylation at two different sites (47). It is processed through the

Figure 3 Disease associated mutations in PrP (from van der Kamp, M. W. et al. Protein Engineering, Design and Selection 2009 22:461-468)

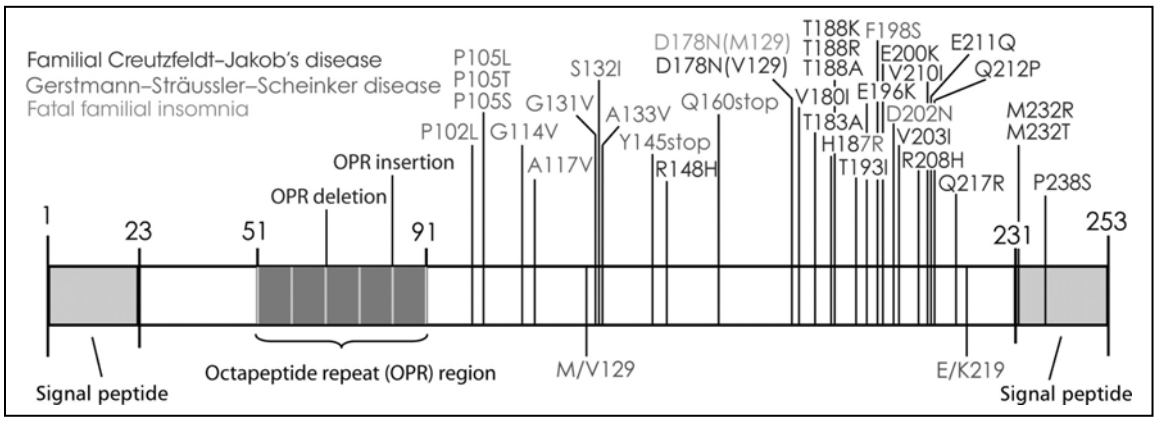

secretory pathway and anchored to the cell surface via the GPI anchor. Although the ultimate proof for prion diseases to be propagated solely by misfolded protein is still incomplete, there is growing evidence to suggest that this model infact is accurate (48).

At least 30 mutations of the *PRNP* gene (Figure 2) are now known to cause inherited forms of human prion diseases (47). Approximately 10-15% of the incidence of prion disease can be accounted for by the presence of inherited mutation (49). Although the biological function of PrP has not yet been determined, mutations in this gene presumably influence the stability, processing and/or cellular interactions of the protein to cause disease (50). There is evidence to suggest that there are different ways that different mutations effect PrP, however, and many questions remain about the mechanisms by which many mutations cause disease. In the second chapter of my thesis I will specifically discuss work I did to elucidate the mechanism by which one class of mutations in PrP, repeat expansions, affects amyloid fiber formation and stability.

In a manner similar to other protein misfolding amyloid based diseases, PrP can undergo a conformational change from its native, globular state to an aggregated,-structurally distinct form (51). During this conformational change PrP^{c} (cellular) which is sensitive to protease treatment shifts from having some α-helical structure to one that is predominantly β-sheet rich and resistant to protease treatment, called PrP^{Sc} (Scrapie) (40,50,52). Several mutations associated with prion disease significantly destabilize the PrP^{c} conformer that may then proceed to form PrP^{Sc} (53). The converted PrP^{Sc} is believed to propagate by binding to PrP^{c} and acting template for PrP^{c} to refold into the abnormal isoform. The development of the protein misfolding cyclic amplification assay (PMCA) has provided substantial evidence to suggest a templated conversion model (54).

The specific mechanisms that the protein follows to convert from a natively folded structure to an abnormal structure, and subsequently convert native protein to join the aggregate, are still a mystery. Recombinant full-length PrP can be induced to form amyloid fibers in vitro under various conditions (51). However, these fibers formed from recombinant PrP does not lead to an infectious PrP^{Sc} conformation unless it is in the presence of lipids or RNA (48).

The PrP protein contains an octapeptide repeat domain (ORD) in the N-terminal region of the protein between amino acids 51 and 91 (47). In the wild type protein, there are five repeats in the ORD (49). Insertion of more than two additional octapeptide repeats in this region causes inherited prion disease (49). Considerable variability in clinical phenotype has been reported for this group of mutations, with age of onset ranging from 21-82 years of age and duration of disease ranging from 3 months to 21 years (49). In addition, pathological features of families that have been reported to have ORD expansions have been highly variable. Despite this variability, it has been shown by Croes and colleagues that there is a negative correlation, albeit a weak one, between age of onset and duration of disease with size of the insertion in the ORD (55). In chapter two of this thesis, I discuss in detail work done to elucidate the effect that ORD expansions that result in a total of eight, 11, and 14 repeats have on amyloid fiber formation and stability.

The diversity in clinical symptoms and pathology of prion disease that arise either just from the wild type protein or within families harboring the same mutant provides a basis for the significance and existence of multiple prion "strains" (40,50,56). Various experiments have shown that when different prion strains are injected to identical hosts,

they develop distinct prion-disease phenotypes (57). Traits that have been used to classify prion strains include aggregate deposition, incubation times, tissue pathology and cellular targets (44). There is growing evidence to suggest that specificity of strains arises from conformational changes in the aggregated protein and that the strains are defined by the tertiary or supramolecular structure of the prion particle.

1.5 Infectious and non-infectious amyloids

The nucleated conformation conversion model for amyloid fiber formation previously described may be a common feature for all amyloidogenic proteins (17,18). As mentioned earlier, amyloidogenesis of many proteins leads to protein misfolding disorders (1). In fact, the similarity is quite uncanny, in that, the features of the fibers such as β-sheet content, dye-binding and protease resistance are all shared (58). The ability of preformed seeds to template the conformational change of previously unconverted monomer and form amyloid fibers is analogous to the propagation of prions (19).

Recent studies have shown that, in cell culture, poly-Q aggregates and tau aggregates can be internalized by cells (59,60). Thus, tt is theoretically possible that the internalized aggregates can convert soluble cytoplasmic proteins and stimulate aggregation. It is conceivable that all protein misfolding disorders have the potential to be "infectious", however, other than PrP^{Sc}, none of the other protein misfolding disorders have had detectable naturally-occuring infectivity and none have given rise to disease epidemics such as Kuru and BSE.

The closest any other disease has come to being "prion-like" is AA amyloidosis. In mammals that have AA amyloidosis, the N-terminal-derived serum amyloid A (SAA) is accumulated in multiple organs such as the spleen and liver when the levels of blood SAA are chronically elevated (44). The "infectivity" of AA amyloidosis may explain the high prevalence of this disease in captive cheetahs (61). AA amyloidosis and Alzheimer's disease (AD) have both been shown to be infectious in laboratory animals as long as the recipient animals have elevated levels of SAA or Aβ (44,62).

Although the role of protein misfolding and amyloid fiber formation has been unequivocally implicated in many diseases, it remains to be seen as to how many of them have a prion-like mechanism of disease transmission. More importantly, understanding what differences distinguish protein aggregates that are infectious versus others that are not is very intriguing. Chapter four of this thesis discusses a model I have developed that provides a means of addressing this question from a structural as well as a biochemical perspective.

1.6 Yeast prions

Although only one prion protein, PrP, has been identified in mammals, many different proteins in the yeast *Saccharomyces cerevisiae* have been shown to have prion-like properties (Table 2) (4). In yeast however, prion proteins do not cause disease, but act as epigenetic elements of heredity (63). They may play a role in modifying phenotypes in a manner that allows the yeast adapt to changing environmental conditions (64,65).

The [*PSI*+] factor was initially identified in 1965 (66), it was not until almost another 30 years later that Reed Wickner suggested that [*PSI*] and [URE3], another yeast cytoplasmic factor, were in fact prions (67). He proposed four criteria that need to be fulfilled for prion-based phenotypic properties. First, the phenotype should be inherited cytoplasmically suggesting that the determinant is not a genetic mutation. Second, the prion state was dependent on the expression of the protein determinant. Third, mutations in the genetic determinant of the prion displayed the prion phenotype. Fourth, the genetic mutation was recessive; however, the prion state was dominant (66).

The [PSI^{+}] prion is one of the most well -characterized prions in yeast (68). It is encoded by the Sup35p, the eukaryotic release factor 3 (eRF3) in yeast and is an essential protein that functions in translation termination (69-71). It was initially identified in a genetic screen as a mutant that enhanced suppression of stop codons by *SUP16* (*SUQ5*) (72). One can assay for the prion state of a cell by the suppression of the nonsense allele *ade1-14*. In the [psi^{-}] state, Sup35p is in its normal soluble form and there is no nonsense suppression of the *ade1-14* allele resulting in the accumulation of a red pigment in the colonies. In the [PSI+] state, Sup35p is aggregated and non-functional, allowing for nonsense suppression (73,74). This provides for expression of full length Ade1p, resulting in a complete adenine biosynthetic pathway and the colonies are white.

The Sup35p can be divided into three domains: the N-terminal domain (N), amino acids 1-123, the middle domain (M), amino acids 124-253, and the carboxy-terminal domain (C), amino acids 254-685 (68). The NM region is dispensable for viability, but the N domain is necessary and sufficient for [*PSI*+] propagation (75-77). The C-terminal domain is essential for viability and is necessary for the translation termination function

of the protein (75,78). The N domain of Sup35p can be further dissected into the QN-rich domain, amino acids 1-40 and the oligopeptide repeat domain (ORD), amino acids 41-97 (66,79,80). Mutations of polar residues in the QN-rich domain can have profound effects on [*PSI*+] propagation including loss of the prion state, forming of "cryptic" [*PSI*+] and "Psi no more" (PNM) forms (81,82). The ORD contains five copies and one incomplete copy of an oligopeptide. The number of repeats within the ORD is very important and the loss of even a single repeat results in the loss of the prion (76,83,84). In contrast, increasing the number of repeats by the addition of two repeats increases the rate of spontaneous conversion of [*psi*-] cells to [*PSI*+] (83).

The prion domain of Sup35p has been shown to form amyloid fibers in vitro (85,86). In addition a nucleated polymerization model has been suggested based on the ability of preformed "seeds" to enhance the formation of these amyloid fibers (18,85,86). Lysates obtained from [*PSI*+] cells, but not [*psi*-] cells, are also capable of seeding amyloid fiber formation (85). Fibers formed from recombinant of Sup35NM protein when introduced into [*psi*-] cells convert and acquire the [*PSI*+] phenotype, providing conclusive evidence that Sup35p amyloid fibers are in fact *bona fide* infectious particles (87,88).

Sup35p fractionates to the pellet fraction when lysates from [*PSI*+] cells are subjected to high speed centrifugation because it is present as high molecular weight aggregates in these cells. In [*psi*-] cells, Sup35p is soluble and therefore does not pellet and is present in the soluble fraction (73,74). Additionally, the NM domain of Sup35 when fused to GFP mediates the aggregation of GFP into punctuate foci specifically in [*PSI*+] cells and displays a diffuse patter in in [*psi*-] cells (73).

The structural analysis of Sup35NM amyloid fibers has proven to be extremely challenging and the proposed structures are a hotly debated topic in the field. The two proposed structures suggest either an in-register parallel β-sheet or a β-helix (89). So far techniques including fluorescence labeling, solid-state NMR and (H/D) exchange NMR have been used to probe the structure of Sup35NM amyloid fibers (90-92). There is compelling evidence for both structures, and additional work is needed to identify the biologically relevant structure.

Interestingly, the repeats from Sup35p (consensus: PQGGYQQYN) bear a striking resemblance to the oligopeptide repeats present in PrP (consensus: PHGGGWGQ) (93). In our lab, we previously assayed the affect of the wild type ORD from PrP as well as repeat expansions of the ORD associated with prion disease on [*PSI*+] prion state in vivo (94). In chapter 2 of this thesis, I discuss the effect that the wild type as well as disease-associated ORDs of PrP had within the context of Sup35NM amyloid fiber formation in vitro.

1.7 Yeast prion strains

Analogous to the perplexing property of mammalian prions being able to exist as different "strains" of PrP^{Sc}, a subset of yeast prions including [*PSI*+] can maintain and propagate distinct strains, although yeast strains are generally referred to as "variants", since the term "strain" is used to distinguish different genetic backgrounds (40,66).

The hypothesis that a protein can aggregate and form a number of different ordered, self-propagating conformational states is very exciting. There is growing evidence, especially from the yeast prion field, to suggest that this is in fact the case. In

chapter 3 of this thesis I discuss work done to provide a framework on which to base a universal physical basis for the formation of prion strains based on the yeast prion [*RNQ*+].

Extensive work done with Sup35p and variants of [*PSI*+] has provided a wealth of information towards understanding the molecular mechanisms of prion variant formation. Amyloid fibers of Sup35NM with different physical properties can be transformed into yeast to induce distinct [*PSI*+] phenotypes (88,95). The physical properties of Sup35NM fibers can be simply influenced by changing the temperature at which the fibers are formed. The thermostability of the fibers formed at different temperatures is distinct. For example, Sup35NM fibers formed at 4°C have a lower melting point than those formed at 25°C, suggesting that there are gross structural differences between them. Additionally, when 4°C fibers were transformed into [*psi*-] yeast, they gave primarily strong [*PSI*+] variants and 25°C fibers transformed gave weak [*PSI*+] variants (88).

Several studies using multiple techniques have been conducted to identify structural differences of fibers formed at different temperatures (90,91). Cysteine mutant studies using fluorescent dyes identified differences in the length of the amyloid core, i.e. the amino acids in the protein that are buried and protected from the solvent, and the amino acids involved in forming either inter- or intra-molecular contacts necessary for amyloid fiber formation. Fibers formed at 4°C had a smaller amyloid core (amino acids 31-86) and 25°C fibers had a longer core (amino acides 21-121). The amyloid core as determined by another technique, H/D exchange NMR, suggested that 4°C fibers have a core spanning amino acids 4-40 and 37°C fibers have a core spanning amino acids 4-70. Although the H/D exchange NMR results do not agree with the fluorescence assay based

results quantitatively, i.e. the specific amino acid positions, both techniques agree with each other qualitatively, i.e. the length of the amyloid core changes and a shorter core yields stronger [*PSI*+] variants. The thermostabilities of the fibers are consistent with the length of the amyloid core of the fibers formed at the different temperatures. The amyloid fiber with longer cores are more stable than the fibers with weaker cores (88,89,96). It is reasonable to speculate that fibers that are stronger in vitro produce weaker prion pheotypes in vivo because the aggregates in this conformation are harder to break apart and therefore have fewer ends (or contacts) to template conversion of soluble protein. Consequently, weaker fibers may be easier to fragment, providing more ends for templating and subsequent propagation to daughter cells. Furthermore, specific inter-molecular contacts have been shown to be responsible for certain prion variants (90). Although differences in variants of [*PSI*+] have relatively large structural changes, recent crystallographic studies with amyloid forming peptides suggest that subtle changes may be sufficient for prion variant formation (26).

In chapter three of this thesis, we discuss pioneering work done toward understanding biochemical and structural properties of another prion [*RNQ*+]. We hope this and future studies will help illustrate universalities amongst prion strain nucleation and propagation.

[*RNQ*+]/ [*PIN*+] *prion* The [*PIN*+] prion was initially identified as a non-Mendelian trait of *S. cerevisiae* that is required for efficient [*PSI*+] induction when Sup35p is overexpressed (97,98). Many different proteins were identified as potential factors that when overexpressed made yeast cells [*PIN*+] (99). However, the most commonly found [*PIN*+] element in strains of yeast is that propagated by Rnq1p. As

such, in most cases, [*PIN*+] and [*RNQ*+] are used synonymously and refer to the prion state of the Rnq1p. Rnq1p does not have a known biological function in its globular or soluble state, however, the [*RNQ*+] prion influences the induction of [*PSI*+]. Interestingly, Rnq1p was independently identified as a prion because it contained a glutamine (Q) and asparagine (A) rich domain (similar to prion forming domains of Sup35p and Ure2p) (100). The prion state of Rnq1p is represented as [*RNQ*+] and the non-prion state is [*rnq*-] (100).

Rnq1p is a 42.5 kDa protein that can be divided into primarily two domains: amino acids 1-152 constitute the non-Q/N rich domain and 153-405 constitutes the Q/N-rich domain (100). The Q/N-rich domain has been shown to be sufficient for prion propagation and hence is considered as the prion forming domain (PFD) for Rnq1p (100,101). This domain has also been shown to form amyloid fibers (100,101). Additionally, a fragment of Rnq1p containing amino acids 133-405 has been shown to be sufficient for "infectivity", that is, fibers generated from this fragment, when transformed into yeast cells, convert the cells from [*rnq*-] to [*RNQ*+] (102). The non-prion forming domain of Rnq1p has been suggested to be involved in self-regulation of the QN-rich aggregation prone domain (103). Further, multiple mutants in the N-terminal non-prion forming domain of Rnq1p have been shown to inhibit the propagation of the [*RNQ*+] prion (104).

The [RNQ^{+}] prion has also been shown to modulate toxicity of poly-Q expansion proteins when expressed in yeast cells (105). It has been shown that modulation of poly-Q toxicity by both cis- and trans-acting polypeptide sequences depends entirely on the prion state of the Rnq1p (106). As such, the [RNQ^{+}] prion and Rnq1p provides a unique

system for the investigation of the effect of pre-existing misfolded proteins on the aggregation of other cellular proteins and its subsequent consequence on cellular physiology.

Interestingly, the [*RNQ*+] prion can also propagate multiple variants (102,107). The original isolates of [*RNQ*+] variants were obtained spontaneously (107). These variants showed differences in their ability to induce the [*PSI*+] prion (107). They also had varied solubilities when subjected to high speed centrifugation (107). Variants of [*RNQ*+] were also obtained when, Rnq1p aggregates were transformed into yeast (102). Previous work has shown very interesting interactions between variants of [*PSI*+] and [*PIN*+] (108,109). In particular, certain variants destabilize stable inheritance of the variants of the other prion (108).

In this thesis, the focus of Chapter three is the biochemical and physical properties of the variants of [*RNQ*+] and a comparison of the physical basis of these variants with that suggested for [*PSI*+] variants (96).

1.8 Interplay of chaparones and yeast prions

Increased stress in cells caused by various environmental conditions, especially temperature, leads to the induced expression of a group of proteins called heat shock proteins (110). Many of these heat shock proteins are molecular chaperones that function in protein folding, unfolding and refolding of misfolded proteins, and disaggregation of aggregated proteins. More interestingly, the maintenance and propagation of yeast prions has been intimately linked with various chaperone systems (110).

Both the yeast prions discussed earlier in this chapter, [*PSI*+] and [*RNQ*+] depend entirely on the presence of the yeast chaperone, Hsp104p (98,111). Interestingly, for the [*PSI*+] prion, either overexpression or inactivation of Hsp104p causes the loss of the prion state (111). However, certain variants of [*PSI*+] are maintained only when Hsp104p is overproduced (112). In contrast, [*RNQ*+] propagation is not affected in the presence of high levels of Hsp104p but reverts back to [*rnq*-] when *HSP104* is deleted (77). Interestingly, there are certain mutants of *HSP104* that differentially affect [*PSI*+] and [*RNQ*+] prions (109,113).

It is thought that Hsp104p functions in the propagation of prions by facilitating the break down of prion aggregates into smaller "seeds" or "propagons" that can be inherited by daughter cells. This model suggests that it is the disaggregation activity of Hsp104p that is required for prion propagation in yeast (114,115). It is possible that excess Hsp104p breaks down [*PSI*+] aggregates to soluble non-templating conformers and thereby rids the cell of the prion state. However, it is yet to be determined as to how overproduction of Hsp104p cures the [*PSI*+] prion as the cells initially expression higher levels of Hsp104p seems to increase the size of the aggregates (114,115). Various mutational analyses have been conducted by other labs in the past and novel mutational studies are being conducted in our lab currently to dissect the mechanism of Hsp104 action on protein aggregation and prion maintenance (116,117).

Other chaperones that have secondary roles in prion maintenance include the Hsp70s, Hsp40s and small Hsps (110,118,119). Hsp70 family members Ssa1 and Ssa2 when overproduced have been shown to enhance the *de novo* induction of [*PSI*+] and prevent curing by Hsp104p overproduction (120,121). In fact, a direct physical

association of Sup35p and Ssa has been shown both in vivo and in vitro (121). Members of the Ssa subfamily have been also shown to modulate poly-Q aggregation and toxicity when overproduced (122,123). In contrast to Ssa proteins, Ssb proteins antagonize [*PSI*$^{+}$] propagation when overexpressed in combination with Hsp104p (124). Additionally, loss of *SSB1* and *SSB2* genes increased the spontaneous formation of [*PSI*$^{+}$] (124).

The Hsp40 protein, Ydj1p has been shown to promote the loss of certain variants of [*RNQ*+] (107). Ydj1p overexpression in combination with Ssa1 has been shown to cure weak [*PSI*+] strains (125). Sis1p, an essential Hsp40 protein in yeast has been shown to be required for the propagation of [*RNQ*+] and [*PSI*+] (126,127).

The effect of yeast chaperones on protein aggregation and prion maintenance is complex. Considering that the chaperones interact differently with prion aggregates obtained from different proteins and variants of the same prions, the specific effects that the various chaperones have on the aggregates (both prion and non-prion) probably depends on the specific properties of aggregates themselves. Elucidating the details of these mechanisms may prove vital in developing strategies and/ or targets for therapeutics in protein misfolding disorders.

1.9 Amyloid fiber polymorphisms: Effect of different solution conditions

A very intriguing feature of amyloid fibers (that may reflect some of the differences between prion variants) is that the fibers formed from the same polypeptide can occur in a range of structurally different morphologies. This variation has been found in both in vitro preparations and biological samples (128,129). Variation in clinical and pathological manifestations of several human amyloid disorders has been

suggested to be caused by diversity of structures of the amyloid fibers (130). We suggest in Chapter 4 of this thesis that this diversity may also be responsible for differences in the ability of certain amyloidoses to be infectious and other to not. Additionally, we suggest in Chapter 5 that some the variation within diverse fibers created from the same polypeptide sequence may be due to changes in environmental conditions under which protein aggregation was initiated. It is important to mention here that in spite of all the variation, at least a small portion of the polypeptides form a cross β-sheet structure. This preserves the common properties of amyloid fibers.

Three possibilities have been proposed as means for gross structural differences to arise in amyloid (131): 1) the number of protofibrils that make up the fibers, 2) relative orientation of the protofibrils and 3) the protofibril substructure may differ by changes in the underlying conformation of the subunits. As such, sequences and specific interactions involved in the formation of the cross β-core may be distinct in amyloid fibers with different morphologies. As mentioned earlier, the physico-chemical environment can substantially influence the fiber morphology created from the same polypeptide. Various environmental factors have been studied in the past, such as pH of the solution, temperature, agitation, salts and other co-solutes (132-135). It has been clearly demonstrated that for β_2-m temperature and pH profoundly affect heterogeneity of aggregation (136). To add to this complexity, even within the same sample, significant variations in fiber morphology can be detected. Previously, it has been shown that certain salt conditions favor a specific ensemble of fibril structures (135). However, fibrils have also proven difficult to classify based on morphology due to the variation between structures being more of a continuum, rather than discrete steps (137).

From a disease perspective, intermediates that proteins go through in order form amyloid fibers are a very interesting species because it is these structures that have been implicated in causing toxicity to cells. These oligomeric assemblies may present an avenue to either increase or decrease the variations in the structure of the amyloid fibers that result. Additionally, certain structures may be susceptible to manipulation by small molecules to prevent toxicity.

Many interesting questions arise from the above set of observations. 1) How does a specific polypeptide chain acquire the different structures? 2) Is there a specific relationship between the morphologies and polypeptide sequences? 3) How do environmental factors affect the specific morphology and interact with different amyloidogenic proteins?

In chapter 5 of this thesis, I discuss work we have done to begin to answer these questions. We have utilized six different environmental conditions and two different amyloidogenic proteins, Sup35p and Rnq1p to address these issues.

2.0 Summary and Significance

Protein misfolding and aggregation has been shown to play a major role in many diseases, including a large group of fatal neurodegenerative diseases. In many of these diseases, misfolding and aggregation of the protein leads to the formation of ordered structures called amyloid fibers. Phenotypic variation in some of the diseases is thought to be caused, in part, due to polymorphisms in the protein aggregate structures. In spite of these common features, only subsets of amyloid fiber aggregates are infectious.

The initiating events of protein misfolding, aggregation and formation of amyloid fibers are not well defined. Additionally, the effect of certain mutations in genes that encode proteins that participate in these diseases is not well understood. Furthermore the basis for polymorphisms in amyloid fibers and their correlation to environmental conditions are also not known. Most intriguingly, the differences between protein aggregates that are infectious and those that are benign have only started to recently be explored.

The four different facets of this thesis investigate specific aspects of the above unanswered important questions. In this thesis, I discuss 1) the role of a specific group of mutations in PrP that cause a dominant, inherited form of prion disease, 2) the physical basis for prion variant formation using the yeast prion [*RNQ*+], 3) the effect that various conditions have on amyloid fiber formation of the proteins, Sup35NM and Rnq1PFD, and 4) the biochemical properties of a mutant form of Rnq1PFD, Rnq1PFDΔHot that is capable of forming amyloid fibers that are both infectious and benign.

References:

1. Chiti, F., and Dobson, C. M. (2006) *Annu Rev Biochem* **75**, 333-366

2. Koo, E. H., Lansbury, P. T., Jr., and Kelly, J. W. (1999) *Proc Natl Acad Sci U S A* **96**, 9989-9990

3. Sipe, J. D., and Cohen, A. S. (2000) *J Struct Biol* **130**, 88-98

4. Halfmann, R., Alberti, S., and Lindquist, S. *Trends Cell Biol* **20**, 125-133

5. Snell, R. G., MacMillan, J. C., Cheadle, J. P., Fenton, I., Lazarou, L. P., Davies, P., MacDonald, M. E., Gusella, J. F., Harper, P. S., and Shaw, D. J. (1993) *Nat Genet* **4**, 393-397

6. Collins, S. J., Lawson, V. A., and Masters, C. L. (2004) *Lancet* **363**, 51-61

7. Safar, J., Wille, H., Itri, V., Groth, D., Serban, H., Torchia, M., Cohen, F. E., and Prusiner, S. B. (1998) *Nat Med* **4**, 1157-1165

8. Arrasate, M., Mitra, S., Schweitzer, E. S., Segal, M. R., and Finkbeiner, S. (2004) *Nature* **431**, 805-810

9. Haass, C., and Selkoe, D. J. (2007) *Nat Rev Mol Cell Biol* **8**, 101-112

10. Ohhashi, Y., Ito, K., Toyama, B. H., Weissman, J. S., and Tanaka, M. *Nat Chem Biol* **6**, 225-230

11. Dobson, C. M. (1999) *Trends Biochem Sci* **24**, 329-332

12. Anfinsen, C. B. (1973) *Science* **181**, 223-230

13. Guijarro, J. I., Sunde, M., Jones, J. A., Campbell, I. D., and Dobson, C. M. (1998) *Proc Natl Acad Sci U S A* **95**, 4224-4228

14. Chiti, F., Webster, P., Taddei, N., Clark, A., Stefani, M., Ramponi, G., and Dobson, C. M. (1999) *Proc Natl Acad Sci U S A* **96**, 3590-3594

15. Booth, D. R., Sunde, M., Bellotti, V., Robinson, C. V., Hutchinson, W. L., Fraser, P. E., Hawkins, P. N., Dobson, C. M., Radford, S. E., Blake, C. C., and Pepys, M. B. (1997) *Nature* **385**, 787-793

16. Raffen, R., Dieckman, L. J., Szpunar, M., Wunschl, C., Pokkuluri, P. R., Dave, P., Wilkins Stevens, P., Cai, X., Schiffer, M., and Stevens, F. J. (1999) *Protein Sci* **8**, 509-517

17. Jarrett, J. T., and Lansbury, P. T., Jr. (1993) *Cell* **73**, 1055-1058

18. Serio, T. R., Cashikar, A. G., Kowal, A. S., Sawicki, G. J., Moslehi, J. J., Serpell, L., Arnsdorf, M. F., and Lindquist, S. L. (2000) *Science* **289**, 1317-1321

19. Baxa, U. (2008) *Curr Alzheimer Res* **5**, 308-318

20. Serpell, L. C., Sunde, M., Benson, M. D., Tennent, G. A., Pepys, M. B., and Fraser, P. E. (2000) *J Mol Biol* **300**, 1033-1039

21. Nilsson, M. R. (2004) *Methods* **34**, 151-160

22. Petkova, A. T., Ishii, Y., Balbach, J. J., Antzutkin, O. N., Leapman, R. D., Delaglio, F., and Tycko, R. (2002) *Proc Natl Acad Sci U S A* **99**, 16742-16747

23. Jaroniec, C. P., MacPhee, C. E., Astrof, N. S., Dobson, C. M., and Griffin, R. G. (2002) *Proc Natl Acad Sci U S A* **99**, 16748-16753

24. Makin, O. S., Atkins, E., Sikorski, P., Johansson, J., and Serpell, L. C. (2005) *Proc Natl Acad Sci U S A* **102**, 315-320

25. Nelson, R., Sawaya, M. R., Balbirnie, M., Madsen, A. O., Riekel, C., Grothe, R., and Eisenberg, D. (2005) *Nature* **435**, 773-778

26. Sawaya, M. R., Sambashivan, S., Nelson, R., Ivanova, M. I., Sievers, S. A., Apostol, M. I., Thompson, M. J., Balbirnie, M., Wiltzius, J. J., McFarlane, H. T., Madsen, A. O., Riekel, C., and Eisenberg, D. (2007) *Nature* **447**, 453-457

27. Kayed, R., Head, E., Thompson, J. L., McIntire, T. M., Milton, S. C., Cotman, C. W., and Glabe, C. G. (2003) *Science* **300**, 486-489

28. Bitan, G., Kirkitadze, M. D., Lomakin, A., Vollers, S. S., Benedek, G. B., and Teplow, D. B. (2003) *Proc Natl Acad Sci U S A* **100**, 330-335

29. Zoghbi, H. Y., and Orr, H. T. (2000) *Annu Rev Neurosci* **23**, 217-247

30. Gatchel, J. R., and Zoghbi, H. Y. (2005) *Nat Rev Genet* **6**, 743-755

31. Slow, E. J., Graham, R. K., Osmand, A. P., Devon, R. S., Lu, G., Deng, Y., Pearson, J., Vaid, K., Bissada, N., Wetzel, R., Leavitt, B. R., and Hayden, M. R. (2005) *Proc Natl Acad Sci U S A* **102**, 11402-11407

32. Dickson, D. W., Crystal, H. A., Mattiace, L. A., Masur, D. M., Blau, A. D., Davies, P., Yen, S. H., and Aronson, M. K. (1992) *Neurobiol Aging* **13**, 179-189

33. Dickson, D. W., Crystal, H. A., Bevona, C., Honer, W., Vincent, I., and Davies, P. (1995) *Neurobiol Aging* **16**, 285-298; discussion 298-304

34. Scherzinger, E., Lurz, R., Turmaine, M., Mangiarini, L., Hollenbach, B., Hasenbank, R., Bates, G. P., Davies, S. W., Lehrach, H., and Wanker, E. E. (1997) *Cell* **90**, 549-558

35. Schaffar, G., Breuer, P., Boteva, R., Behrends, C., Tzvetkov, N., Strippel, N., Sakahira, H., Siegers, K., Hayer-Hartl, M., and Hartl, F. U. (2004) *Mol Cell* **15**, 95-105

36. Chen, S., Ferrone, F. A., and Wetzel, R. (2002) *Proc Natl Acad Sci U S A* **99**, 11884-11889

37. Tsuda, H., Jafar-Nejad, H., Patel, A. J., Sun, Y., Chen, H. K., Rose, M. F., Venken, K. J., Botas, J., Orr, H. T., Bellen, H. J., and Zoghbi, H. Y. (2005) *Cell* **122**, 633-644

38. Vital, C., Gray, F., Vital, A., Parchi, P., Capellari, S., Petersen, R. B., Ferrer, X., Jarnier, D., Julien, J., and Gambetti, P. (1998) *Neuropathol Appl Neurobiol* **24**, 125-130

39. Gajdusek, D. C. (1977) *Science* **197**, 943-960

40. Prusiner, S. B. (1998) *Proc Natl Acad Sci U S A* **95**, 13363-13383

41. Klatzo, I., Gajdusek, D. C., and Zigas, V. (1959) *Lab Invest* **8**, 799-847

42. Gajdusek, D. C., Gibbs, C. J., Jr., Asher, D. M., and David, E. (1968) *Science* **162**, 693-694

43. Gibbs, C. J., Jr., Gajdusek, D. C., Asher, D. M., Alpers, M. P., Beck, E., Daniel, P. M., and Matthews, W. B. (1968) *Science* **161**, 388-389

44. Aguzzi, A., and Calella, A. M. (2009) *Physiol Rev* **89**, 1105-1152

45. Prusiner, S. B. (1982) *Science* **216**, 136-144

46. Prusiner, S. B. (1991) *Science* **252**, 1515-1522

47. van der Kamp, M. W., and Daggett, V. (2009) *Protein Eng Des Sel* **22**, 461-468

48. Wang, F., Wang, X., Yuan, C. G., and Ma, J. *Science* **327**, 1132-1135

49. Mead, S. (2006) *Eur J Hum Genet* **14**, 273-281

50. Collinge, J. (2001) *Annu Rev Neurosci* **24**, 519-550

51. Cobb, N. J., and Surewicz, W. K. (2009) *Biochemistry* **48**, 2574-2585

52. Caughey, B., and Chesebro, B. (2001) *Adv Virus Res* **56**, 277-311

53. Apetri, A. C., Surewicz, K., and Surewicz, W. K. (2004) *J Biol Chem* **279**, 18008-18014

54. Castilla, J., Saa, P., Hetz, C., and Soto, C. (2005) *Cell* **121**, 195-206

55. Croes, E. A., Theuns, J., Houwing-Duistermaat, J. J., Dermaut, B., Sleegers, K., Roks, G., Van den Broeck, M., van Harten, B., van Swieten, J. C., Cruts, M., Van Broeckhoven, C., and van Duijn, C. M. (2004) *J Neurol Neurosurg Psychiatry* **75**, 1166-1170

56. Weissmann, C. (2004) *Nat Rev Microbiol* **2**, 861-871

57. Pattison, I. H., and Millson, G. C. (1961) *J Comp Pathol* **71**, 101-109

58. Luheshi, L. M., and Dobson, C. M. (2009) *FEBS Lett* **583**, 2581-2586

59. Frost, B., Jacks, R. L., and Diamond, M. I. (2009) *J Biol Chem* **284**, 12845-12852

60. Ren, P. H., Lauckner, J. E., Kachirskaia, I., Heuser, J. E., Melki, R., and Kopito, R. R. (2009) *Nat Cell Biol* **11**, 219-225

61. Zhang, B., Une, Y., Fu, X., Yan, J., Ge, F., Yao, J., Sawashita, J., Mori, M., Tomozawa, H., Kametani, F., and Higuchi, K. (2008) *Proc Natl Acad Sci U S A* **105**, 7263-7268

62. Lundmark, K., Westermark, G. T., Nystrom, S., Murphy, C. L., Solomon, A., and Westermark, P. (2002) *Proc Natl Acad Sci U S A* **99**, 6979-6984

63. True, H. L., and Lindquist, S. L. (2000) *Nature* **407**, 477-483

64. True, H. L., Berlin, I., and Lindquist, S. L. (2004) *Nature* **431**, 184-187

65. Shorter, J., and Lindquist, S. (2005) *Nat Rev Genet* **6**, 435-450

66. Tuite, M. F., and Cox, B. S. (2003) *Nat Rev Mol Cell Biol* **4**, 878-890

67. Wickner, R. B. (1994) *Science* **264**, 566-569

68. Serio, T. R., and Lindquist, S. L. (1999) *Annu Rev Cell Dev Biol* **15**, 661-703

69. Stansfield, I., Jones, K. M., Kushnirov, V. V., Dagkesamanskaya, A. R., Poznyakovski, A. I., Paushkin, S. V., Nierras, C. R., Cox, B. S., Ter-Avanesyan, M. D., and Tuite, M. F. (1995) *EMBO J* **14**, 4365-4373

70. Zhouravleva, G., Frolova, L., Le Goff, X., Le Guellec, R., Inge-Vechtomov, S., Kisselev, L., and Philippe, M. (1995) *EMBO J* **14**, 4065-4072

71. Doel, S. M., McCready, S. J., Nierras, C. R., and Cox, B. S. (1994) *Genetics* **137**, 659-670

72. Cox, B. S. (1971) *Heredity* **26**, 211-232

73. Patino, M. M., Liu, J. J., Glover, J. R., and Lindquist, S. (1996) *Science* **273**, 622-626

74. Paushkin, S. V., Kushnirov, V. V., Smirnov, V. N., and Ter-Avanesyan, M. D. (1996) *EMBO J* **15**, 3127-3134

75. Ter-Avanesyan, M. D., Kushnirov, V. V., Dagkesamanskaya, A. R., Didichenko, S. A., Chernoff, Y. O., Inge-Vechtomov, S. G., and Smirnov, V. N. (1993) *Mol Microbiol* **7**, 683-692

76. Ter-Avanesyan, M. D., Dagkesamanskaya, A. R., Kushnirov, V. V., and Smirnov, V. N. (1994) *Genetics* **137**, 671-676

77. Derkatch, I. L., Chernoff, Y. O., Kushnirov, V. V., Inge-Vechtomov, S. G., and Liebman, S. W. (1996) *Genetics* **144**, 1375-1386

78. Kushnirov, V. V., Ter-Avanesian, M. D., Dagkesamanskaia, A. R., Chernov Iu, O., Inge-Vechtomov, S. G., and Smirnov, V. N. (1990) *Mol Biol (Mosk)* **24**, 1037-1041

79. Kushnirov, V. V., Ter-Avanesyan, M. D., Telckov, M. V., Surguchov, A. P., Smirnov, V. N., and Inge-Vechtomov, S. G. (1988) *Gene* **66**, 45-54

80. Osherovich, L. Z., Cox, B. S., Tuite, M. F., and Weissman, J. S. (2004) *PLoS Biol* **2**, E86

81. DePace, A. H., Santoso, A., Hillner, P., and Weissman, J. S. (1998) *Cell* **93**, 1241-1252

82. McCready, S. J., Cox, B. S., and McLaughlin, C. S. (1977) *Mol Gen Genet* **150**, 265-270

83. Liu, J. J., and Lindquist, S. (1999) *Nature* **400**, 573-576

84. Parham, S. N., Resende, C. G., and Tuite, M. F. (2001) *EMBO J* **20**, 2111-2119

85. Glover, J. R., Kowal, A. S., Schirmer, E. C., Patino, M. M., Liu, J. J., and Lindquist, S. (1997) *Cell* **89**, 811-819

86. King, C. Y., Tittmann, P., Gross, H., Gebert, R., Aebi, M., and Wuthrich, K. (1997) *Proc Natl Acad Sci U S A* **94**, 6618-6622

87. Sparrer, H. E., Santoso, A., Szoka, F. C., Jr., and Weissman, J. S. (2000) *Science* **289**, 595-599

88. Tanaka, M., Chien, P., Naber, N., Cooke, R., and Weissman, J. S. (2004) *Nature* **428**, 323-328

89. Tessier, P. M., and Lindquist, S. (2009) *Nat Struct Mol Biol* **16**, 598-605

90. Krishnan, R., and Lindquist, S. L. (2005) *Nature* **435**, 765-772

91. Toyama, B. H., Kelly, M. J., Gross, J. D., and Weissman, J. S. (2007) *Nature* **449**, 233-237

92. Shewmaker, F., Wickner, R. B., and Tycko, R. (2006) *Proc Natl Acad Sci U S A* **103**, 19754-19759

93. Weissmann, C. (1999) *J Biol Chem* **274**, 3-6

94. Tank, E. M., Harris, D. A., Desai, A. A., and True, H. L. (2007) *Mol Cell Biol* **27**, 5445-5455

95. King, C. Y., and Diaz-Avalos, R. (2004) *Nature* **428**, 319-323

96. Tanaka, M., Collins, S. R., Toyama, B. H., and Weissman, J. S. (2006) *Nature* **442**, 585-589

97. Derkatch, I. L., Bradley, M. E., Masse, S. V., Zadorsky, S. P., Polozkov, G. V., Inge-Vechtomov, S. G., and Liebman, S. W. (2000) *EMBO J* **19**, 1942-1952

98. Derkatch, I. L., Bradley, M. E., Zhou, P., Chernoff, Y. O., and Liebman, S. W. (1997) *Genetics* **147**, 507-519

99. Derkatch, I. L., Bradley, M. E., Hong, J. Y., and Liebman, S. W. (2001) *Cell* **106**, 171-182

100. Sondheimer, N., and Lindquist, S. (2000) *Mol Cell* **5**, 163-172

101. Vitrenko, Y. A., Gracheva, E. O., Richmond, J. E., and Liebman, S. W. (2007) *J Biol Chem* **282**, 1779-1787

102. Patel, B. K., and Liebman, S. W. (2007) *J Mol Biol* **365**, 773-782

103. Kurahashi, H., Ishiwata, M., Shibata, S., and Nakamura, Y. (2008) *Mol Cell Biol* **28**, 3313-3323

104. Shibata, S., Kurahashi, H., and Nakamura, Y. (2009) *Prion* **3**, 250-258

105. Meriin, A. B., Zhang, X., He, X., Newnam, G. P., Chernoff, Y. O., and Sherman, M. Y. (2002) *J Cell Biol* **157**, 997-1004

106. Duennwald, M. L., Jagadish, S., Giorgini, F., Muchowski, P. J., and Lindquist, S. (2006) *Proc Natl Acad Sci U S A* **103**, 11051-11056

107. Bradley, M. E., Edskes, H. K., Hong, J. Y., Wickner, R. B., and Liebman, S. W. (2002) *Proc Natl Acad Sci U S A* **99 Suppl 4**, 16392-16399

108. Bradley, M. E., and Liebman, S. W. (2003) *Genetics* **165**, 1675-1685

109. Bardill, J. P., and True, H. L. (2009) *J Mol Biol* **388**, 583-596

110. Rikhvanov, E. G., Romanova, N. V., and Chernoff, Y. O. (2007) *Prion* **1**, 217-222

111. Chernoff, Y. O., Lindquist, S. L., Ono, B., Inge-Vechtomov, S. G., and Liebman, S. W. (1995) *Science* **268**, 880-884

112. Borchsenius, A. S., Muller, S., Newnam, G. P., Inge-Vechtomov, S. G., and Chernoff, Y. O. (2006) *Curr Genet* **49**, 21-29

113. Kurahashi, H., and Nakamura, Y. (2007) *Mol Microbiol* **63**, 1669-1683

114. Wegrzyn, R. D., Bapat, K., Newnam, G. P., Zink, A. D., and Chernoff, Y. O. (2001) *Mol Cell Biol* **21**, 4656-4669

115. Kryndushkin, D. S., Alexandrov, I. M., Ter-Avanesyan, M. D., and Kushnirov, V. V. (2003) *J Biol Chem* **278**, 49636-49643

116. Shorter, J., and Lindquist, S. (2006) *Mol Cell* **23**, 425-438

117. Romanova, N. V., and Chernoff, Y. O. (2009) *Protein Pept Lett* **16**, 598-605

118. Jones, G. W., and Tuite, M. F. (2005) *Bioessays* **27**, 823-832

119. Masison, D. C., Kirkland, P. A., and Sharma, D. (2009) *Prion* **3**, 65-73

120. Newnam, G. P., Wegrzyn, R. D., Lindquist, S. L., and Chernoff, Y. O. (1999) *Mol Cell Biol* **19**, 1325-1333

121. Allen, K. D., Wegrzyn, R. D., Chernova, T. A., Muller, S., Newnam, G. P., Winslett, P. A., Wittich, K. B., Wilkinson, K. D., and Chernoff, Y. O. (2005) *Genetics* **169**, 1227-1242

122. Gokhale, K. C., Newnam, G. P., Sherman, M. Y., and Chernoff, Y. O. (2005) *J Biol Chem* **280**, 22809-22818

123. Muchowski, P. J., Schaffar, G., Sittler, A., Wanker, E. E., Hayer-Hartl, M. K., and Hartl, F. U. (2000) *Proc Natl Acad Sci U S A* **97**, 7841-7846

124. Chernoff, Y. O., Newnam, G. P., Kumar, J., Allen, K., and Zink, A. D. (1999) *Mol Cell Biol* **19**, 8103-8112

125. Kushnirov, V. V., Kochneva-Pervukhova, N. V., Chechenova, M. B., Frolova, N. S., and Ter-Avanesyan, M. D. (2000) *EMBO J* **19**, 324-331

126. Sondheimer, N., Lopez, N., Craig, E. A., and Lindquist, S. (2001) *EMBO J* **20**, 2435-2442

127. Higurashi, T., Hines, J. K., Sahi, C., Aron, R., and Craig, E. A. (2008) *Proc Natl Acad Sci U S A* **105**, 16596-16601

128. Meinhardt, J., Sachse, C., Hortschansky, P., Grigorieff, N., and Fandrich, M. (2009) *J Mol Biol* **386**, 869-877

129. Jimenez, J. L., Tennent, G., Pepys, M., and Saibil, H. R. (2001) *J Mol Biol* **311**, 241-247

130. Seilheimer, B., Bohrmann, B., Bondolfi, L., Muller, F., Stuber, D., and Dobeli, H. (1997) *J Struct Biol* **119**, 59-71

131. Kodali, R., and Wetzel, R. (2007) *Curr Opin Struct Biol* **17**, 48-57

132. Pedersen, J. S., Dikov, D., Flink, J. L., Hjuler, H. A., Christiansen, G., and Otzen, D. E. (2006) *J Mol Biol* **355**, 501-523

133. Petkova, A. T., Leapman, R. D., Guo, Z., Yau, W. M., Mattson, M. P., and Tycko, R. (2005) *Science* **307**, 262-265

134. Makarava, N., and Baskakov, I. V. (2008) *J Biol Chem* **283**, 15988-15996

135. Klement, K., Wieligmann, K., Meinhardt, J., Hortschansky, P., Richter, W., and Fandrich, M. (2007) *J Mol Biol* **373**, 1321-1333

136. Piazza, R., Pierno, M., Iacopini, S., Mangione, P., Esposito, G., and Bellotti, V. (2006) *Eur Biophys J* **35**, 439-445

137. Fandrich, M., Meinhardt, J., and Grigorieff, N. (2009) *Prion* **3**, 89-93

Chapter 2: Prion Protein Insertional Mutations Increase Aggregation Propensity but not Fiber Stability

Tejas Kalastavadi and Heather L. True

This chapter has been published in March of 2008 in the journal BMC Biochemistry Volume 9**:**7

Abstract

Background: Mutations in the *PRNP* gene account for ~15% of all prion disease cases. Little is understood about the mechanism of how some of these mutations in *PRNP* cause the protein to aggregate into amyloid fibers or cause disease. We have taken advantage of a chimeric protein system to study the oligopeptide repeat domain (ORD) expansions of the prion protein, PrP, and their effect on protein aggregation and amyloid fiber formation. We replaced the ORD of the yeast prion protein Sup35p with that from wild type and expanded ORDs of PrP and compared their biochemical properties *in vitro*. We previously determined that these chimeric proteins maintain the [PSI^+] yeast prion phenotype *in vivo*. Interestingly, we noted that the repeat expanded chimeric prions seemed to be able to maintain a stronger strain of [PSI^+] and convert from [psi^-] to [PSI^+] with a much higher frequency. In this study we have attempted to understand the biochemical properties of these chimeric proteins and to establish a system to study the properties of the ORD of PrP both *in vivo* and *in vitro* conveniently.

Results: Investigation of the chimeric proteins *in vitro* reveal that repeat-expansions increase aggregation propensity and that the kinetics of fiber formation depends on the number of repeats. The fiber formation reactions are promiscuous in that the chimeric protein containing 14 repeats can readily cross-seed fiber formation of proteins that have the wild type number of repeats. Morphologically the amyloid fibers formed by repeat-expanded proteins associate with each other to form large clumps that were not as prevalent in fibers formed by proteins containing the wild type number of repeats. Despite the increased aggregation propensity and lateral association of the repeat expanded proteins, there was no corresponding increase in the stability of the fibers

formed. Therefore, we predict that the differences in fibers formed with different repeat lengths may not be due to gross changes in the amyloid core.

Conclusion: The biochemical observations presented here explain the properties of these chimeric proteins previously observed in yeast. More importantly, they suggest a mechanism for the observed correlation between age of onset and disease severity with respect to the length of the ORD in humans.

Background

The aggregation of various proteins is implicated in many diseases, including neurodegenerative disorders [1]. Many of the aggregating proteins form amyloid fibers that are the hallmark of diseases such as Alzheimer's, Parkinson's and Huntington's disease [2]. Amyloid fibers are also associated with prion diseases. The prion protein (PrP) can misfold and aggregate to form amyloid fibers, leading to neurodegenerative prion diseases [3, 4]. The three primary means of acquiring prion diseases are as follows: 1) infection – can be transmitted by the ingestion of meat obtained from diseased animals, 2) spontaneous – occurs sporadically via unknown mechanism(s) and 3) inherited – mutations in the *PRNP* gene encoding PrP [4, 5]. About 15% of prion disease cases are associated with mutations in the *PRNP* gene and ~85% of the cases are classified as sporadic [5]. A unique characteristic of prion diseases is that an aggregated form of the PrP protein can be infectious [6], however infectious forms of prion disease are rare in comparison to inherited and sporadic cases. Although the mechanism of pathogenesis of prion diseases is not well understood, this process does not necessarily result from a genetic mutation [3, 7, 8]. It is hypothesized that the aggregated form of PrP is infectious and acts as a template to change the native conformation of PrP and

cause it to also aggregate [8]. Familial forms of prion diseases include Creutzfeldt-Jakob disease (CJD), Gerstmann-Sträussler-Scheinker syndrome (GSS), and Fatal Familial Insomnia (FFI). Several different mutations in *PRNP* are associated with prion diseases, but the mechanisms by which the various mutations cause disease are not always clearly understood [5]. In this study, we use a model system created to investigate some aspects of an inherited form of prion disease that results from insertional mutations in *PRNP* to cause diseases such as GSS and CJD [9].

PrP is a 23 kD protein that can be divided into two major domains. The C terminus is the prion-forming domain (PFD) and is implicated in the formation of amyloid fibers in the infectious form of the disease [10, 11]. The N-terminal domain is largely unstructured; however, some mutations in this domain are linked to disease and influence PrP fibrillization and amyloid propagation *in vitro* [12]. The N-terminal region contains an oligopeptide repeat domain (ORD) that consists of five repeats of an eight amino acid peptide with the consensus sequence PHGGGWGQ [13]. Expansion of the ORD by the addition of two to nine extra repeats causes a dominantly inherited form of prion disease [5, 14-18]. The number of repeats present is inversely correlated, albeit weakly, with the age of onset of disease [19]. In addition, recombinant PrP peptides with expansions of the ORD display increased aggregation *in vitro* [20]. A transgenic mouse model of one such ORD expansion, Tg(PG14), in which the number of repeats in the ORD is increased to 14, develops a fatal neurodegenerative disorder [21, 22]. The disease manifests spontaneously, and although not infectious, the Tg(PG14) mice develop neurological illness that features ataxia, neuropathological abnormalities and the accumulation of PrP in the brain [21, 23]. However if infectious prion particles are

introduced into the brains of mice expressing the transgene, there is accumulation of PrP in the brain and the brain homogenate is actually infectious and can propogate the disease [22, 23]. Furthermore, the ORD has been shown to bind many divalent cations such as copper, manganese and zinc [24, 25]. It has been proposed that binding of these metals to the ORD may affect the structural properties of PrP and thereby affect disease progression [24]. Thus, many lines of evidence from human, mouse and biochemical studies illustrate a vital role for the ORD in some prion diseases.

Prion proteins also exist in yeast [26]. However, unlike the mammalian prion protein that causes disease when aggregated, yeast prions function as epigenetic factors of phenotypic inheritance [27-29]. One well-studied prion in yeast is the [*PSI*$^+$] prion, whose protein determinant is Sup35p [30-32]. Sup35p is the *Saccharomyces cerevisiae* eRF3 (eukaryotic release factor 3) involved in modulating translation termination at stop codons in messenger RNAs. When Sup35p is in the prion conformation ([*PSI*$^+$]), the aggregated protein is presumably no longer functional in translation termination, resulting in nonsense suppression [32, 33].

Sup35p is a 76.5 kD protein that can be divided into three domains. The C-terminal domain is necessary and sufficient for the function of the protein in translation termination [30, 34, 35]. The amino-terminal region of Sup35p (NM) is considered the PFD [30, 35]. However, the minimum region required for maintainance of the prion [*PSI*$^+$] is amino acids 1-93 [36, 37] The N-terminal domain (N) is rich in glutamine and asparagine (Q/N) residues. The middle domain (M) is rich in charged amino acids [35]. Interestingly, the N-terminal domain of Sup35p contains an ORD that consists of five and a half repeats with the consensus sequence PQGGYQQYN [38] that is similar to the

ORD in PrP. Deletion of even one repeat from the wild type Sup35 protein prevents efficient formation of the [*PSI*$^{+}$] prion [36]. Expansion of the Sup35p repeats increases the frequency of conversion from the [*psi*$^{-}$] to the [*PSI*$^{+}$] state [38]. Previous studies have shown that the [*PSI*$^{+}$] prion phenotype can be maintained *in vivo* when the Sup35p repeat region is replaced by the PrP repeat sequence [36, 39]. The Sup35p repeats were replaced with five, eight, 11 or 14 PrP repeats to generate chimeras referred to as SP5 (Sup35 with 5 PrP repeats), SP8, SP11, and SP14, respectively [39]. All chimeras were capable of propagating a prion and maintained translation termination function in the non-prion state. Interestingly, the SP14 chimeric protein spontaneously converted cells from the non-prion [*sp14*$^{-}$] state to the [*SP14*$^{+}$] prion state at a frequency that is approximately four orders of magnitude higher than that of the spontaneous conversion of wild type Sup35p from the [*psi*$^{-}$] to the [*PSI*$^{+}$] state. This increase in the spontaneous conversion of the repeat-expanded chimera to the prion state may be due to an increase in the inherent propensity of the repeat-expanded proteins to aggregate and form amyloid fibers. However, the interpretation of the data is complicated by the requirement for the [*RNQ*$^{+}$] prion for the enhanced induction *in vivo*.

Here, we take advantage of the chimeric Sup35-PrP prion protein system to study the effect of the PrP repeat expansions on the *in vitro* aggregation of the prion protein. The advantage of using the Sup35-PrP chimera lies in the ability to readily study properties of protein aggregation both *in vitro* and *in vivo*. By using the chimeric Sup35-PrP protein system, the effects of mutations associated with prion disease can be assessed by fiber formation *in vitro* and compared to their *in vivo* behavior in yeast, and vice versa.

In this study, we investigate the properties of the PrP ORD and disease-associated repeat expansion on amyloid fiber formation in an effort to distinguish between the properties of an ORD with non-pathological versus pathological repeat lengths. To this end, we have purified recombinant protein that encompasses the NM region of wild type Sup35p (Sup35NM) and that of chimeras with five (SP5NM), eight (SP8NM), 11 (SP11NM) or 14 (SP14NM) repeats of PrP precisely substituted for the Sup35p ORD and characterized their kinetic, morphological and biochemical properties.

RESULTS

The expanded ORD of PrP decreases the lag phase of fiber formation – We purified the NM region of wild type Sup35p (Sup35NM) and chimeras with five (SP5NM), eight (SP8NM), 11 (SP11NM), and 14 (SP14NM) repeats. The purified recombinant proteins were used to assess the influence of ORD repeat expansion on amyloid fiber formation by monitoring the change in Thioflavin-T (Th-T) fluorescence over time. Wild type Sup35NM had a lag phase of ~5,000 seconds followed by a logarithmic growth phase (Fig. 1A). However, in the presence of seeds (sonicated preformed fibers 2.5% w/w), the lag phase was completely eliminated and fiber formation occurred rapidly (Fig. 1A) as reported previously [40]. We then assayed fiber formation of the chimeric proteins SP5NM, SP8NM, SP11NM and SP14NM. The formation of chimeric SP5NM fibers in an unseeded reaction showed a lag phase (~5,000 seconds; Fig. 1B) similar to that observed with wild type Sup35NM (Fig. 1A). The repeat-expanded chimeras SP8NM, SP11NM, and SP14NM had a negligible lag phase in unseeded reactions (Fig. 1B).

Figure 1

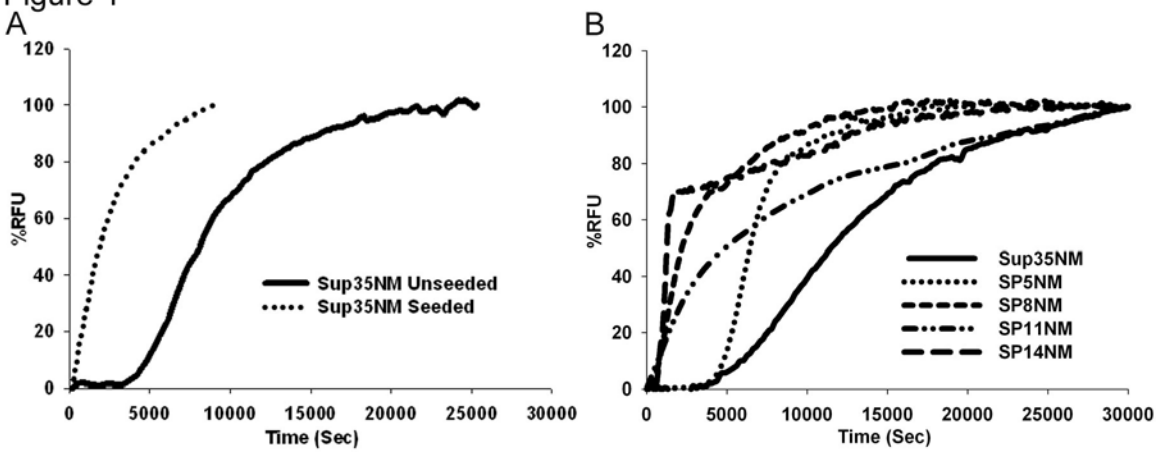

Figure 1. Fiber formation of ORE chimeras is faster than that with the wild type ORD of PrP. Recombinant protein was diluted from denaturant (120 x) to 2.5µM and fiber formation was followed by Th-T fluorescence. Graphs are plotted as %RFU (Relative fluorescence units) versus time. (A) Sup35NM unseeded (solid line) and Sup35NM seeded with sonicated preformed fibers (dotted line). Reaction was seeded with 2.5% (w/w) of preformed sonicated fibers. (B) Unseeded reactions Sup35NM (solid line), SP5NM (dotted line), SP8NM (short dashed line), SP11NM (dotted and dashed line) and SP14NM (long dashed line).

Strikingly, the kinetics of fiber formation of the expanded ORD chimeric proteins in the unseeded reactions was similar to the kinetics of fiber formation of Sup35NM in the presence of pre-formed fiber seeds. In an effort to determine if the lack of lag phase associated with SP14NM fiber formation was simply due to seeds forming in the presence 6M GdHCl, we resuspended SP14NM protein in 8M urea instead. When protein was diluted out from 8M urea, we observed the same rate of fiber formation and no lag phase (data not shown).

Another widely used method that enables detection of infectious prion seeds is protein transformation. We tested for the presence of infectious seeds by transforming [*psi*$^-$] yeast cells with purified SP14NM in 6M GdHCl or SP14NM sonicated fibers. Cells transformed with SP14NM protein that was not allowed to form fibers did not acquire the [*PSI*$^+$] phenotype (Fig. 2) in over 200 colonies tested while 25%-30% of cells transformed with fibers acquired the [*PSI*$^+$] phenotype (Fig. 2, data not shown). These data suggest that preformed seeds of SP14NM did not exist in the presence of 6M GdHCl. However, formally the possibility exists that seeds are formed that are resistant to both denaturants and cause the reaction to appear as a seeded reaction. We observed that cells transformed with SP14NM fibers formed at 4°C and 25°C acquired strong [*PSI*$^+$] (Fig. 2) and weak [*PSI*$^+$] (Fig. 2), respectively. This illustrates the infectious nature of the *in vitro* formed SP14NM fibers. The appearance of strong and weak [*PSI*$^+$] strains in cells that were transformed with fibers formed at different temperatures is in agreement with previously published results for Sup35NM [41]. The concept of yeast prion strain variants and their basis of structural variability has been studied extensively [41-43] and is presumably recapitulated with our repeat expansion chimeras.

In order to verify that the repeat-expanded proteins form fibers faster than the wild type proteins, we visualized the formation of Sup35NM and SP14NM fibers over a time course using transmission electron microscopy (TEM). We were able to detect very few significant structures (above background) at five minutes with Sup35NM by TEM (Fig. 3A). Short fibers of Sup35NM became visible at 30 minutes and the formation of longer fibers was observed by 150 minutes (Fig. 3B, 3C). The TEM images obtained with Sup35NM at 400 minutes (Fig. 3D) were similar to images obtained after 24 hours of fiber formation (Fig. 7A), suggesting that the reaction had reached completion by 400 minutes. The TEM images supported the Th-T data which indicated that the reaction with wild type plateaued by ~200 minutes (Fig. 1A). In contrast to Sup35NM, we observed that the repeat-expanded SP14NM formed visible short fibers as early as five minutes and longer fibers by 30 minutes (Fig. 3E, 3F). TEM images of SP14NM suggest that fiber formation remains unchanged between 150 minutes (Fig. 3G) and 24 hours (Fig. 7E).

Repeat-expanded prion protein cross-seeds the amyloid fiber formation of protein containing wild type repeat numbers efficiently – Prion diseases caused by oligopeptide repeat expansion (ORE) are inherited in an autosomal dominant manner. Patients who suffer from inherited prion disease typically express one copy of the repeat-expanded allele and one copy of the wild type allele [7, 9]. Protein aggregates in these patients sometimes contain both the mutant and wild type protein [9]. One reason for the presence of both proteins in the aggregates could be that repeat-expanded PrP aggregates readily and cross-seeds the aggregation of the wild type protein. Therefore, we tested whether SP14NM seeds could enhance amyloid fiber formation of either Sup35NM or

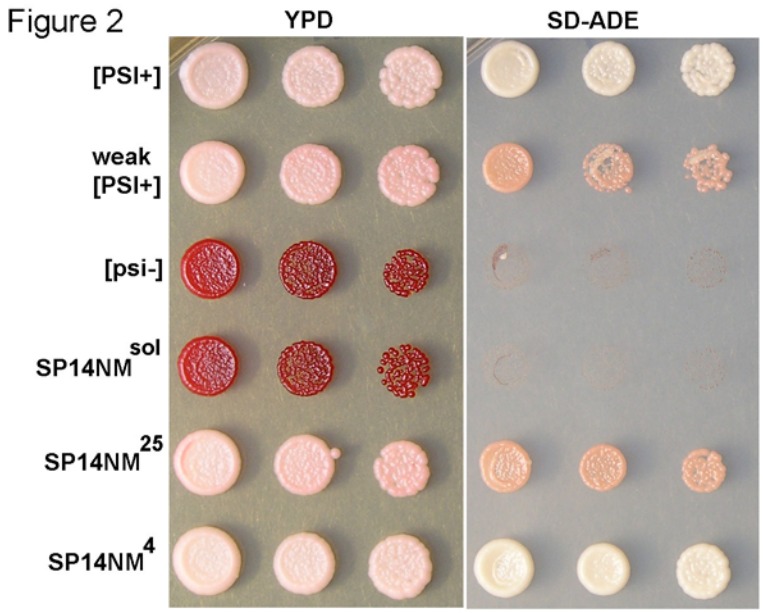

Figure 2. The [*PSI*$^{+}$] phenotype was assayed by color on YPD, growth on SD-ADE and curability (not shown). Control protein transformations show that protein harvested from either strong or weak [*PSI*$^{+}$] cells transformed in to [*psi*$^{-}$] cells induces the corresponding prion phenotype while protein harvested from [*psi*$^{-}$] cells does not induce the prion state. Soluble SP14NM protein (SP14NM^{sol}) does not induce the [*PSI*$^{+}$] prion phenotype prior to fiber formation. SP14NM protein was able to induce the [*PSI*$^{+}$] prion phenotype after fiber formation either at 4ºC (SP14NM^{4}, strong strain) or 25ºC (SP14NM^{25}, weak strain).

SP5NM monomers. We observed that SP14NM does cross-seed the aggregation of both Sup35NM (Fig. 4A) and SP5NM (Fig. 4B) efficiently. These data also support the previous suggestion that co-aggregation of wild type PrP and ORE PrP is a plausible factor in prion disease progression [9, 20].

Increasing repeat length in the ORD increases both incorporation of monomer and lateral association of amyloid fibers– Since the SP14NM amyloid fiber formation occurs almost instantaneously upon dilution from denaturant, we next asked whether there was any effect of adding seeds. We observed a sharp spike in fluorescence when SP14NM seeds were added to soluble SP14NM monomers (Fig. 5A), suggesting that fiber formation did occur by templating off of the pre-formed fiber seeds added. However, this spike was followed by a drop in fluorescence to a steady state level that was similar to that observed in the unseeded reaction. This was a very intriguing observation as no such drop in fluorescence was observed in the seeded Sup35NM fiber formation reaction (Fig. 1A). One possible reason for the tendency of the reaction to rapidly reach a steady state would be the inability of the fibers to incorporate additional soluble protein. In order to determine if the fiber ends were still competent for addition of soluble protein, we added fresh SP14NM monomer to a fiber formation reaction that had already reached the steady state level of Th-T fluorescence. The addition of SP14NM monomer at the reaction plateau caused another spike in fluorescence (Fig. 5B), suggesting that the fibers are still capable of adding soluble protein. Therefore, the plateau in fluorescence observed in seeded SP14NM fiber formation reactions was not likely due to an inability to incorporate additional monomer.

Figure 3

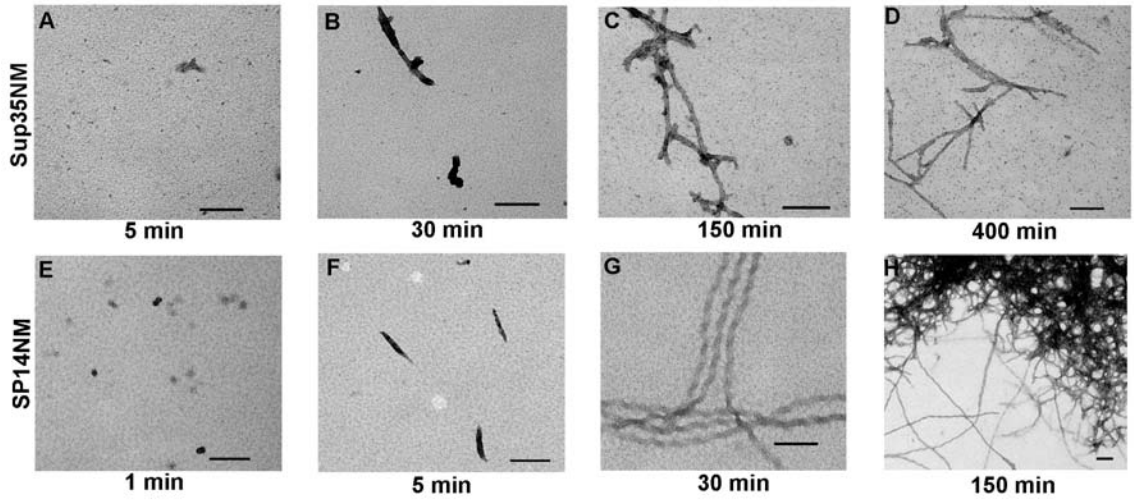

Figure 3. Unseeded SP14NM fiber formation is faster than Sup35NM fiber formation as monitored by TEM. Length of scale bar represents 100 nm. Sup35NM (5μM) after (A) 5 min, (B) 30 min, (C) 150 min, (D) 400 min and SP14NM (5μM) after (E) 1 min, (F) 5 min, (G) 30 min, (H) 150 min.

Figure 4

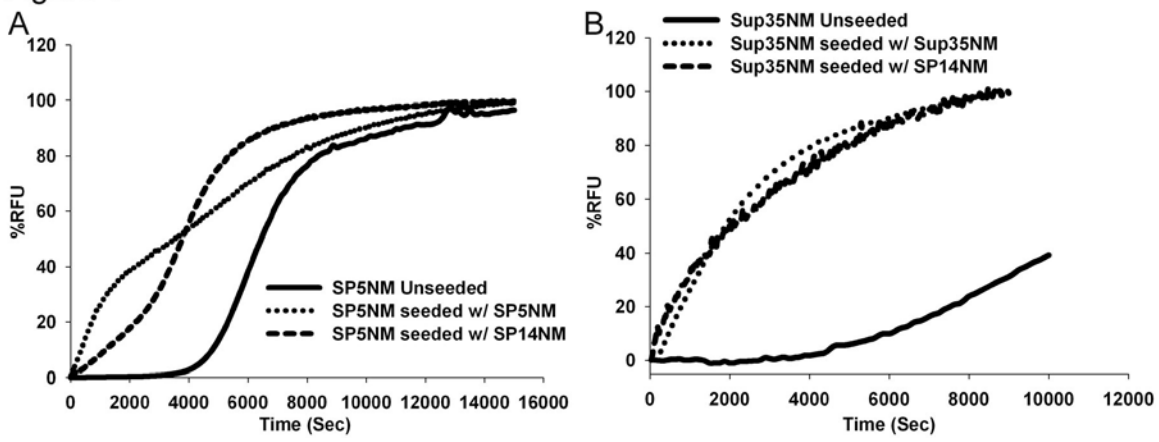

Figure 4. Sup35NM and SP5NM are efficiently cross-seeded by SP14NM seeds. Recombinant protein was diluted from denaturant (120 x) to 2.5μM and fiber formation was followed by Th-T fluorescence. Reactions were seeded with 2.5% (w/w) of preformed sonicated fibers as indicated. Graphs are plotted as %RFU versus time. (A) Fiber formation of Sup35NM. (B) Fiber formation of SP5NM.

Alternatively, the initial spike observed in the seeded SP14NM reaction could arise due to fibers forming at the instant the seed is added, while the ensuing drop in fluorescence could result from dissociation of protein from the fibers. The plateau would then be a result of the reaction reaching an equilibrium state. To address this hypothesis, we assessed the amount of soluble protein at the end-point of fiber formation using a centrifugation assay. First, all chimeras were allowed to form fibers overnight. Then we separated the amyloid fibers from the soluble protein by centrifugation and examined the protein in the fractions by SDS-PAGE and western blot. We observed that the amount of remaining soluble protein decreased as the number of repeats increased (Fig. 6). The amyloid fiber formation reaction of either SP5NM or SP8NM showed a considerable amount of soluble protein after an overnight incubation, as seen by the protein in the supernatant fraction. However, there was little and no detectable protein in the supernatant from either SP11NM or SP14NM fiber formation reactions, respectively. The lack of soluble protein remaining in the SP14NM fiber formation reaction negated the hypothesis that the drop in fluorescence in seeded SP14NM reactions occurred as a result of dissociation of protein from the amyloid fibers over time.

This led us to hypothesize that the spike and drop pattern of Th-T fluorescence seen in seeded SP14NM fiber formation reactions might be due to exclusion of Th-T binding over time. The increase in fluorescence occurs as Th-T initially binds the rapidly forming fibers and the drop may result from Th-T being occluded from the fibers as the reaction progresses. In order to address this hypothesis, we returned to TEM in order to examine the morphology of the fibers of wild type Sup35NM and the chimeric proteins. Interestingly, TEM revealed a morphological difference between the Sup35NM and

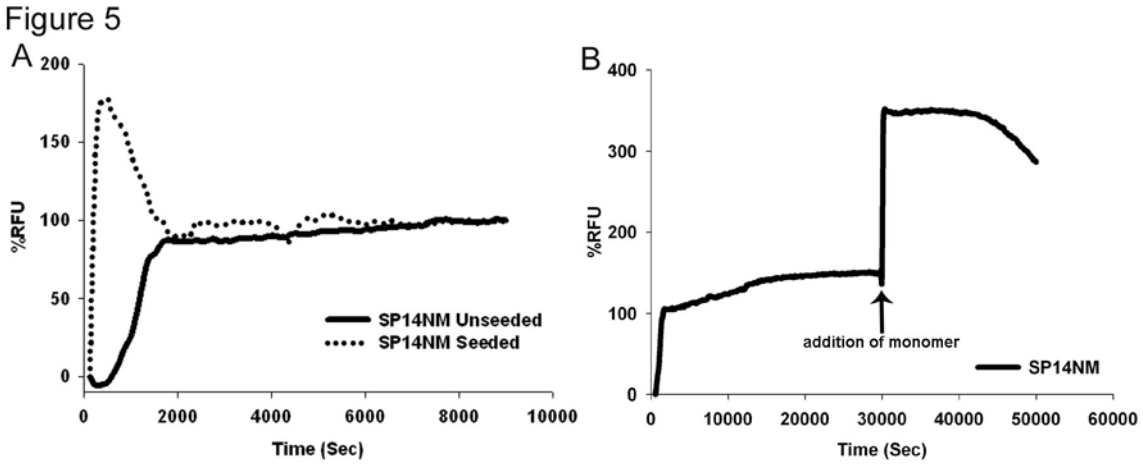

Figure 5. The addition of preformed seeds causes a spike in SP14NM fiber formation. Recombinant protein was diluted from denaturant (120 x) to 2.5μM and fiber formation was followed by Th-T fluorescence. Graphs are plotted as %RFU versus time. (A) SP14NM unseeded (solid line) and SP14NM seeded (dotted line). (B) Another spike in Th-T fluorescence is observed after the addition of more monomer (2.5μM) after the SP14NM fiber formation reached a plateau.

Figure 6

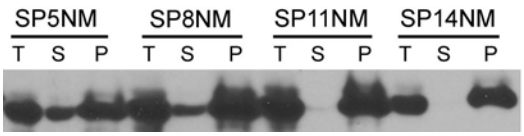

Figure 6. Soluble protein is incorporated into fibers more efficiently in chimeras with increased number of repeats in the ORD. Fiber formation reactions (5μM) were separated into supernatant (S) and pellet (P) fractions by high speed centrifugation and analyzed by SDS-PAGE and western blot using α-Sup35 antibodies. Soluble protein remains in the supernatant fraction and the fibers are found in the pellet fraction. (T) is the total reaction prior to centrifugation.

SP14NM fibers. We investigated the morphology of fibers after 24 hours of fiber formation of all the chimeric proteins. We observed that fibers formed from proteins with the wild type number of repeats, Sup35NM and SP5NM did not have a clumped morphology (Fig. 7A, 7B). However, fibers formed from SP8NM, SP11NM, and SP14NM proteins all exhibited a highly clumped morphology by TEM (Fig. 7C, 7D, 7E). The repeat-expanded ORD chimeric proteins showed an increased lateral association of fully formed fibers as compared to the fibers formed with either Sup35NM or SP5NM. Furthermore, when fibers formed overnight by SP14NM were sonicated, there was an increase in Th-T fluorescence (data not shown). This suggests that sonication disrupted the clumps and once again increased the surface area for Th-T to bind the fibers. Such an increase in fluorescence was not observed when the same experiment was done with fibers formed from either Sup35NM or SP5NM (data not shown). These data support the hypothesis that the difference in Th-T fluorescence is due to the morphological differences between the fibers. As the fibers laterally associate and form large clumps, sites that were previously available for Th-T binding may be unable to bind to Th-T as they interact with other fibers. Such Th-T occlusion would cause a drop in fluorescence.

Prion protein repeat expansion allows fiber formation in the presence of denaturant – In the absence of denaturant, fiber formation of Sup35NM and SP5NM exhibits a lag phase of ~5,000 seconds (Fig. 1B). However, SP8NM, SP11NM, and SP14NM form fibers instantaneously without an appreciable lag phase (Fig. 1B). This suggests that expansion of the repeat region increases the propensity of the proteins to aggregate. However, with these data we were unable to discern how the propensity to aggregate increases with the change in repeat length. There may be a gradual increase in aggregation propensity with

an increase in repeat number or there may be a critical number of repeats after which the protein forms fibers without a lag phase. To further characterize the effect that increasing repeat number has on protein aggregation, we assembled fibers in the presence of increasing concentrations of urea. In the presence of 0.5 M urea, fiber formation of unseeded SP5NM had an extended lag phase of approximately 10,000 seconds (compared to 5,000 seconds in the absence of urea). Unseeded SP8NM had a lag phase of approximately 5,000 seconds (compared to no lag phase without urea) while the lag phases of fiber formation of either SP11NM or SP14NM were not affected by 0.5 M urea (Fig. 8A). When the urea concentration was increased to 1 M in fiber formation reactions of SP5NM and SP8NM, the Th-T fluorescence did not reach a plateau within 30,000 seconds (Fig. 8B), suggesting that fiber formation did not reach completion within the same time frame as in the absence of denaturant (Fig. 1B). SP11NM also formed fibers at a much slower rate in the presence of 1 M urea (Fig. 8B). However, the lag phase of SP14NM fiber formation was not affected by 1 M urea. In the presence of 2 M urea, we did not detect fiber formation with any of the proteins by Th-T fluorescence (data not shown). These results suggest that the propensity of the chimeric prion proteins to aggregate is a function of the number of repeats in the protein; as the number of repeats increase, the propensity of the proteins to aggregate gradually increases.

Prion protein repeat expansion does not enhance stability of amyloid fibers – ORD-expanded proteins aggregate to form amyloid fibers much faster than the wild type protein. An interesting question that arises from this is: Do the amyloid fibers formed by

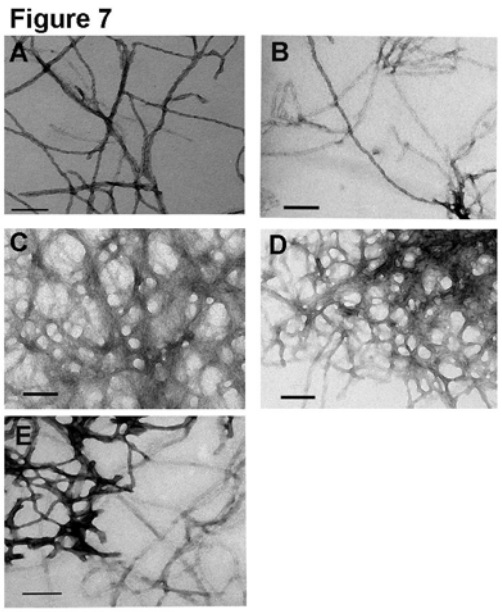

Figure 7. The morphology of amyloid fibers formed from protein containing pathological versus non-pathological repeat lengths is distinct. Unseeded fiber formation reactions (5μM) were imaged by TEM after 16 hours. The length of scale bar represents 100 nm. (A) Sup35NM and (B) SP5NM have uniform dispersed fibers. (C) SP8NM, (D) SP11NM and (E) SP14NM have clumped fibers.

Figure 8

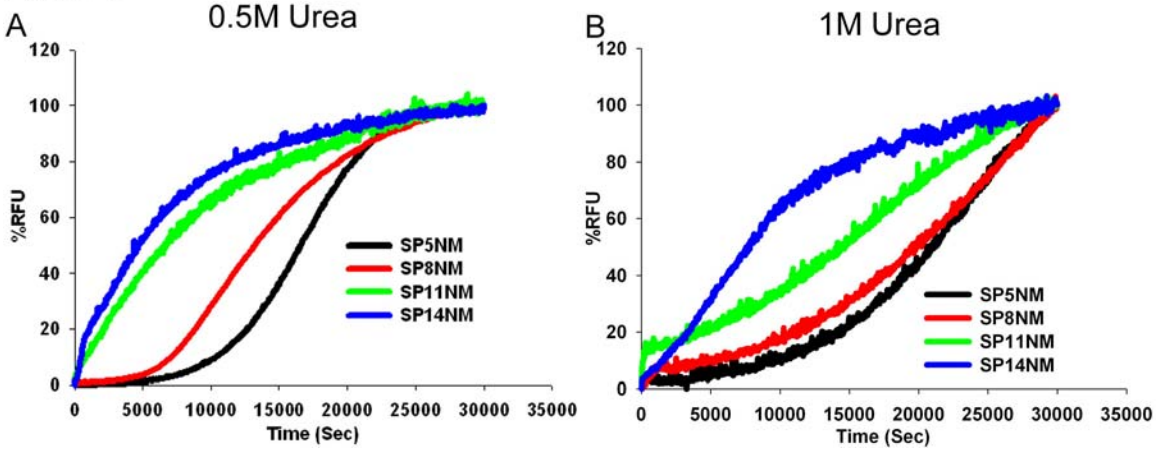

Figure 8. Expansion of the ORD enhances fiber formation in the presence of the denaturant urea. Recombinant protein was diluted from denaturant (120 x) to 2.5µM and fiber formation was followed by Th-T fluorescence. Fiber formation of chimeric proteins SP5NM, SP8NM, SP11NM and SP14NM in (A) 0.5M Urea FFB (B) 1M Urea FFB is shown.

ORD-expanded proteins differ in stability? That is, does the expansion of the ORD enhance fiber stability? It is possible to imagine that mutations that cause proteins to have a greater on-rate for fiber formation may have a slower off-rate and thereby make the amyloid fiber more stable. One way of measuring the stability of amyloid fibers *in vitro* is to examine their denaturation profiles. Amyloid denaturation profiles can be evaluated by treating the fibers with increasing concentrations of denaturant and determining the concentration at which half of the protein is resolubilized. We measured the denaturation profiles of the fibers formed from all of the chimeras by determining the amount of protein remaining aggregated after treatment with increasing concentrations of GdHCl. Using this method, we were able to determine the concentration of GdHCl at which the protein present in the pellet was depleted by approximately 50%. Interestingly, approximately 50% of the pelletable protein was depleted for all the chimeras at GdHCl concentrations between 1.5 - 2 M (Fig. 9A), suggesting that the ORD expansion does not enhance the stability of fibers. We also measured stability of the chimeras by monitoring Th-T fluorescence after treatment with increasing concentrations of GdHCl and observed that the loss of Th-T fluorescence was similar for all chimeric proteins and mirrored the centrifugation results (data not shown). Next, we examined fiber stability in a temperature solublization assay. We treated fibers across a temperature gradient from 25ºC to 95ºC at 10ºC intervals in the presence of 2% SDS. We observed that for all the fibers 50% of the protein becomes soluble between 55ºC - 65ºC (Fig. 9B). Taken together, these data suggest that the stability of the amyloid fibers formed by the chimeric proteins is the same, irrespective of the ORD repeat length.

Figure 9

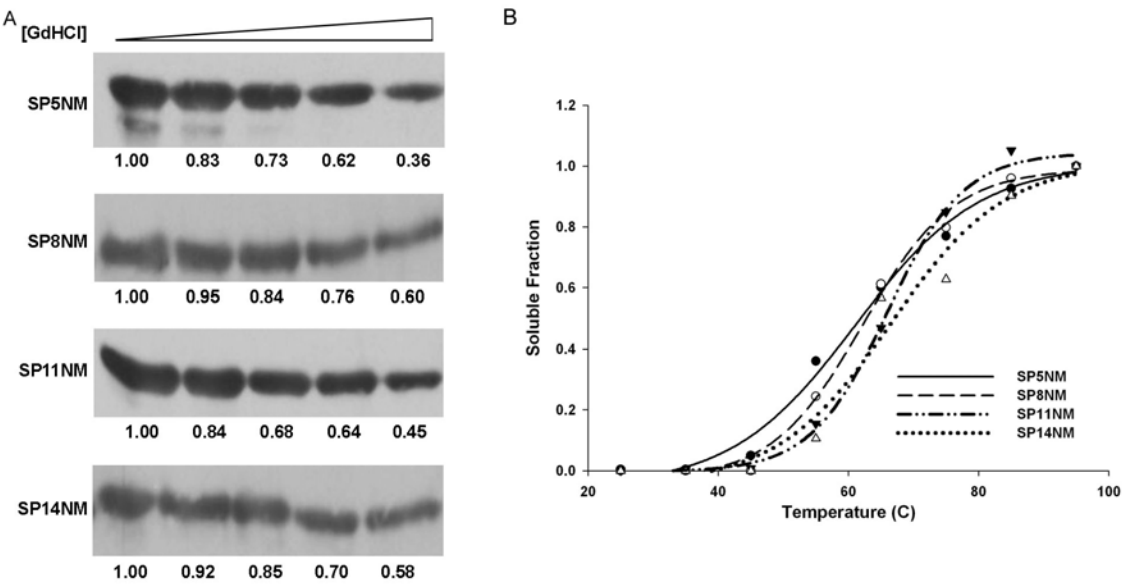

Figure 9. The stability of the prion protein fibers is not enhanced by expansion of the repeat domain. (A) Fibers were formed overnight, treated with GdHCl denaturant and then separated into soluble and pellet fractions by centrifugation (16,000 x g). Samples were analyzed by SDS-PAGE and western blotted using α-Sup35 antibodies. Bands were quantified using ImageJ software. (B) Fibers of SP5NM (●), SP8NM (○), SP11NM (▼) and SP14NM (Δ) were formed overnight, treated across a temperature gradient in the presence of 2% SDS. Following SDS-PAGE and western blot, gel bands were quantified using ImageJ software and and best fit lines were graphed using SigmaPlot software.

DISCUSSION

In this study, we characterized the biochemical properties of a set of chimeric prion proteins wherein the ORD of Sup35p was replaced with that of PrP. The chimeric prion proteins were created by substituting the endogenous Sup35p ORD with the repeat domain of PrP containing five, eight, 11 and 14 oligopeptide repeats [39]. The repeat-expanded proteins show a remarkable set of properties that highlight their enhanced ability to aggregate and form amyloid fibers *in vitro*. These data agree with work done by others in which recombinant PrP (rPrP) with ORD expansions exhibit an enhanced ability to form amyloid fibers with increasing number of repeats [20, 44]. Our data also support previous work done with transgenic mice (Tg(PG14)) that express PrP harboring nine additional octapeptide repeats. These mice manifest a spontaneous form of prion disease [21]. Although the spontaneous form of the disease in the Tg(PG14) mice is not infectious, the protein aggregates and the animals display many of the histopathological hallmarks that are characteristic of prion diseases in mammals [23].

In humans, there is a high degree of heterogeneity with respect to the age of onset and disease progression in people that have mutations in the *PRNP* gene [19, 45, 46]. There is a weak inverse correlation between the number of repeats and the age of onset of disease [19]. Further, repeat-expanded proteins have also been proposed to interact with the wild type PrP protein. Examination of amyloid plaques from patients with one copy of wild type PrP and one copy of mutant PrP demonstrated the presence of both the wild type and the mutant forms of the protein in the same plaques [9]. It has also been shown that mixing repeat-expanded rPrP with wild type rPrP enhances fiber formation of wild type rPrP [20]. These data suggested that there may be co-aggregation or cross-seeding

between the mutant and wild type proteins. Our data also supports the cross-seeding model of disease progression since SP14NM shows efficient cross-seeding of both Sup35NM and SP5NM.

We observed that an increase in the number of repeats enhanced the ability of the protein to form fibers to the extent that the lag phase observed during most amyloid fiber formation reactions was lost. In addition, the proteins harboring repeat expansions had an enhanced ability to form fibers in the presence of denaturant. Interestingly, comparing our data to a recent study suggests that the presence of heterogeneous repeats, that is, a combination of one Sup35p repeat with eight repeats from the PrP protein, forms amyloid fibers slower than having eight repeats from PrP only (Fig. 1B) [25]. This suggests that the enhanced amyloid formation with repeat expansion requires homogenous repeats. Strikingly, our data suggests seeding of fibers with proteins having different (Sup35p or PrP) repeats appears to be as efficient as seeding with proteins that harbor same repeats (Fig. 4B).

Previous work by Serio *et al.* suggested a nucleated conformational conversion model of amyloid fiber formation of Sup35NM [47]. An important aspect of this model is that the rate limiting step for fiber formation, manifested as the lag phase, is the conformational conversion of the nucleus to establish a competent seed. One implication of this model is that rate of fiber formation is not linearly dependent on initial concentration of protein. Serio *et al.* showed that the lag phase of Sup35NM fiber formation was not affected significantly by the initial protein concentration. We observed that the lag phase of SP14NM fiber formation, albeit an extremely short lag phase, is also not affected by initial protein concentration. In fact, even when the

concentration of SP14NM protein was only 0.25 μM in unseeded fiber formation reactions, the lag phase of fiber formation was identical to that of 5 μM protein (data not shown). Our kinetic data suggest that the SP14NM nucleus has an enhanced ability to undergo conformational conversion to the extent that the lag phase of fiber formation is virtually eliminated. As previously suggested [42], one mechanism that could explain the decrease in lag phase for fiber formation is that the expanded ORDs have transient β-sheet structures that are formed due to intramolecular contacts, which may reduce the number of intermolecular contacts required to obtain a stabilized structure to nucleate fiber formation. This would suggest that if a monomer can undergo the appropriate conformational changes and maintain that conformation through intramolecular contacts, then the protein may not need to form oligomers in order to form fibers. Currently, it is unclear if the growth of amyloid fibers in general occurs through linear addition of monomers or intermediate fibers [48, 49]. Different amyloidogenic proteins may have distinct mechanisms for the growth of amyloid fibers. Work done by others suggests that fibers formed by Sup35NM occurs by monomer addition [49], however, in the case of the A-beta peptide, an oligomeric intermediate may be necessary for fiber growth [50, 51]. One current model for the growth of poly-Q peptides suggests that a single molecule, after undergoing conformational conversion, may act as a nucleus capable of templating the addition of monomers, thereby resulting in the growth of amyloid fibers [48]. Therefore, it is plausible that for PrP molecules with expanded ORDs, the mechanism of amyloid fiber assembly and growth changes such that the formation of an oligomer for initiation or growth of fibers is no longer required.

In addition to the ability of repeat-expanded proteins to form a competent seed more readily, a difference in the pathological and non-pathological repeat expansions may be in the efficiency with which monomer is added to the fibers. Our data from the centrifugation assay suggests that the ability of the conformationally-converted nucleus to incorporate soluble protein increases as the number of repeats increase. Currently, a debatable idea in the amyloid field is the existence of a critical concentration in amyloid fiber formation reactions. It has been suggested that the addition of monomer to the fibers may be reversible [52]. Therefore, by assaying the amount of monomer remaining at the end point, we could potentially determine the relative critical concentrations [53]. As such, our data from the centrifugation assay may also suggest that as the number of repeats in the ORD increases, the critical concentration decreases. However, we do not know if these reactions are in fact reversible.

Since the repeat-expanded proteins form fibers faster and incorporate monomer more efficiently, we hypothesized that the fibers formed may also be more stable. However, the increased repeat length did not alter amyloid stability as assessed by denaturation in GdHCl or resolubilization by heat treatment. We observed no significant shift in the concentration of GdHCl or the range of temperature that resolublized 50% of the fibers formed by the chimeras. This suggests that, irrespective of which mutant repeat expansion protein is found from patient to patient, the clearance of the aggregates might be equally challenging to the cellular machinery. One reason for the lack of difference in stability might be that the amyloid core of the fibers does not change significantly between fibers formed with the various repeat-expanded monomers. We crudely assessed changes in the amyloid core of the fibers by treating the fibers with

various proteases and determining the pattern of protease resistant fragments. We observed similar patterns of protease resistant fragments for all of the ORD-expanded proteins (chymotrypsin, V8, proteinase K; data not shown). This suggests that the amyloid core of all the fibers, regardless of the monomer used to form the fibers, might be the same. In order to conclusively determine the amyloid core of all these proteins, however, more sensitive biophysical assays are required.

From our previous *in vivo* experiments [39], we noted that SP14NM can maintain the [$SP14^+$] prion phenotype in weak and strong variants similar to the wild type [PSI^+]. However, a very unique characteristic of the [$SP14^+$] prion lies in its ability to interconvert between weak and strong variants at a high frequency. One explanation for the ability of SP14 to be able to interconvert readily may be that the amyloid core does not change significantly between the two variants. Therefore, the protein would readily be able to adopt either conformation and thereby switch variants at a high frequency. This differs from wild type Sup35p, where weak and strong strains of the [PSI^+] prion have different amyloid cores [42]. However it is important to note that another study suggests that the strain variants may actually not have significantly different amyloid cores [54]. The strain variants observed in yeast can be used as a model to study the phenotypic heterogeneity that is exhibited by strains of prion disease. The ability of [$SP14^+$] prion to interconvert between variants rapidly may provide an avenue to investigate the mechanisms underlying the high degree of phenotypic heterogeneity observed with prion diseases that arise due to repeat expansions in *PRNP*.

Conclusion

In summary, biochemical characterization of the repeat expanded proteins demonstrated that the proteins harboring repeat expansions of pathological length have a greater propensity to aggregate and have a considerably shorter lag phase in fiber formation. The morphology of the fibers is also different between the non-pathological and pathological repeat expansions. Amyloid fibers formed with repeat-expanded proteins clump into large aggregates, whereas the fibers formed by proteins that do not have repeat expansions do not laterally associate to the same extent. Additionally, chimeras with the disease-associated repeat expansions proved to be more efficient at converting soluble protein into the aggregated state than the proteins containing wild type repeat numbers. In spite of the differences between the proteins with respect to fiber formation rate and morphology, the pattern of protease resistance, presumably indicative of the amyloid core, remained the same in all chimeric proteins. In addition, the fibers formed from all proteins showed similar denaturation and solubilization profiles when treated with guanidine hydrochloride (GdHCl) or heat. Together, our data suggest that the expansion of the ORD in PrP results in an increased propensity of the protein to convert from the native conformation to an aggregated conformation, but does not alter the stability of the amyloid fibers formed.

Methods

Protein expression and purification of recombinant proteins – Sup35NM was purified as reported previously [55]. SP5NM, SP8NM, SP11NM and SP14NM were subcloned (from [39]) into the vector pET22. Protein was expressed in BL21(DE3)pLysS *Escherichia coli* cells grown in CircleGrow® medium containing chloramphenicol

(34μg/ml) and ampicillin (100 μg/ml). Protein expression was induced with 1mM IPTG, at OD_{600}~0.6 at 24°C for four and a half hours. The bacterial pellet was resuspended in buffer A (8M urea, 10mM Tris-HCl, pH 7.5) and gently agitated at room temperature for 20 minutes. The cell debris was removed by centrifugation for 30 minutes at 17,000 rpm in a Sorvall SS-34 rotor. The supernatant was loaded onto a Q-Sepharose (GE HealthCare) column and the protein was eluted with a linear gradient of sodium chloride (0 - 1M NaCl). Fractions containing the protein were loaded onto a hydroxyapatite column (BIO RAD) equilibrated with buffer C (8M Urea, 5mM KPO_4, pH 6.8). The protein was eluted with a linear gradient of potassium phosphate (5-500mM). Fractions containing the protein were determined by SDS-PAGE and coomassie staining. The fractions containing the protein were pooled and dialyzed against Buffer A and stored in methanol at -80°C.

Amyloid Fiber Formation Kinetics – Recombinant protein was methanol-precipitated and resuspended in 6M GdHCl. Protein concentration was determined by measuring the OD at 280nm. The protein was diluted 120-fold in FFB buffer (150mM NaCl, 5mM KPO_4, pH 7.5) for fiber formation assays. Fiber formation was followed by monitoring Thioflavin-T binding (100-fold excess). Thioflavin-T fluorescence was continuously measured using PTI Quantamaster spectrofluorometer (Photon Technology International, Inc., Santa Clara, CA).

Electron Microscopy –Samples of fibrillar Sup35NM, SP5NM, SP8NM, SP11NM and SP14NM were allowed to settle onto freshly glow-discharged 200 mesh carbon-formvar coated copper grids for 5 minutes. Grids were then rinsed twice with water and stained

with 1% uranyl acetate (Ted Pella) for one minute. Samples were viewed on a JEOL 1200EX transmission electron microscope (JEOL USA).

Centrifugation Assay – Amyloid fibers were formed by incubating recombinant protein diluted 120-fold in FFB overnight at room temperature while rotating end-over-end. The reaction was separated into pellet and supernatant fractions by centrifugation (16,000 x g, 20 minutes). The total, supernatant and pellet fractions were separated by SDS-PAGE and analyzed by western blot using α-Sup35 antibodies.

GuanidineHydrochloride (GdHCl) denaturation profile – Recombinant protein was diluted 120-fold in FFB and incubated at room temperature on a rotator overnight. The fibers were treated with increasing concentrations (0-2M) of GdHCl for 30 minutes. The treated fibers were then separated into supernatant and pellet fractions by centrifugation (16,000 x g, 20 minutes). The pellet fractions were separated by SDS-PAGE and analyzed by western blot using α-Sup35 antibodies. The band intensities were quantified using ImageJ software.

Temperature resolubilization assay – Recombinant protein was diluted 120-fold in FFB and incubated at room temperature on a rotator overnight. These fibers were then incubated across a temperature gradient (25ºC - 95ºC, 10ºC intervals) for 5 minutes in the presence of 2% SDS. After the heat treatment, the samples were analyzed by SDS-PAGE and western blot. The amount of protein that entered the gel was determined by quantifying the bands using ImageJ software.

Protein transformation – Protein transformation into 74-D694 yeast strain was conducted as described in Ref. [56].

Abbreviations

IPTG: isopropyl-beta-D-thiogalactopyranoside, ORD: Oligopeptide Repeat Domain, ORE: Oligopeptide Repeat Expansion, PFD: Prion Forming Domain, PrP: Prion Protein, SDS-PAGE: Sodium Dodecyl Sulphate- PolyAcrylamide Gel Electrophoresis, TEM: Transmission Electron Microscopy, Th-T: Thioflavin-T.

Authors' contributions

T.K and H.L.T conceived and designed the study. T.K conducted the experiments and together with H.L.T analyzed the results. T.K and H.L.T drafted the manuscript.

Acknowledgments

We thank Brett Pearson for constructing plasmids used in this study, Darcy Gill (EM core facility, Molecular Microbiology department, Washington University School of Medicine) for help with the TEM images and Dr. John Cooper for allowing us to use equipment and providing helpful advice. We thank Rajaraman Krishnan (Whitehead Institute for Biomedical Research, USA) for helpful advice. We thank Dr. Emiliano Bassini, Dr. David Harris, Dr. Rohit Pappu and members of the True Lab for helpful discussions and critical comments on the manuscript. This work was supported by NIH grant GM072228 (H.L.T.) and the Ellison Medical Foundation (H.L.T.).

References

1. Dobson, C.M., *Protein misfolding, evolution and disease.* Trends Biochem Sci, 1999. **24**(9): p. 329-32.

2. Ross, C.A. and M.A. Poirier, *Protein aggregation and neurodegenerative disease.* Nat Med, 2004. **10 Suppl**: p. S10-7.

3. Prusiner, S.B., *Prions.* Proc Natl Acad Sci U S A, 1998. **95**(23): p. 13363-83.

4. Chesebro, B., *Introduction to the transmissible spongiform encephalopathies or prion diseases.* Br Med Bull, 2003. **66**: p. 1-20.

5. Wadsworth, J.D., et al., *Molecular and clinical classification of human prion disease.* Br Med Bull, 2003. **66**: p. 241-54.

6. Prusiner, S.B., *Novel proteinaceous infectious particles cause scrapie.* Science, 1982. **216**(4542): p. 136-44.

7. Collinge, J., *Prion diseases of humans and animals: their causes and molecular basis.* Annu Rev Neurosci, 2001. **24**: p. 519-50.

8. Castilla, J., et al., *In vitro generation of infectious scrapie prions.* Cell, 2005. **121**(2): p. 195-206.

9. Chen, S.G., et al., *Allelic origin of the abnormal prion protein isoform in familial prion diseases.* Nat Med, 1997. **3**(9): p. 1009-15.

10. Baskakov, I.V., et al., *Pathway complexity of prion protein assembly into amyloid.* J Biol Chem, 2002. **277**(24): p. 21140-8.

11. Swietnicki, W., et al., *Aggregation and fibrillization of the recombinant human prion protein huPrP90-231.* Biochemistry, 2000. **39**(2): p. 424-31.

12. Zahn, R., et al., *NMR solution structure of the human prion protein.* Proc Natl Acad Sci U S A, 2000. **97**(1): p. 145-50.

13. Kretzschmar, H.A., et al., *Molecular cloning of a human prion protein cDNA.* DNA, 1986. **5**(4): p. 315-24.

14. Campbell, T.A., et al., *A prion disease with a novel 96-base pair insertional mutation in the prion protein gene.* Neurology, 1996. **46**(3): p. 761-6.

15. Capellari, S., et al., *Familial prion disease with a novel 144-bp insertion in the prion protein gene in a Basque family.* Neurology, 1997. **49**(1): p. 133-41.

16. Goldfarb, L.G., et al., *Transmissible familial Creutzfeldt-Jakob disease associated with five, seven, and eight extra octapeptide coding repeats in the PRNP gene.* Proc Natl Acad Sci U S A, 1991. **88**(23): p. 10926-30.

17. Krasemann, S., et al., *Prion disease associated with a novel nine octapeptide repeat insertion in the PRNP gene.* Brain Res Mol Brain Res, 1995. **34**(1): p. 173-6.

18. Pietrini, V., et al., *Creutzfeldt-Jakob disease with a novel extra-repeat insertional mutation in the PRNP gene.* Neurology, 2003. **61**(9): p. 1288-91.

19. Croes, E.A., et al., *Octapeptide repeat insertions in the prion protein gene and early onset dementia.* J Neurol Neurosurg Psychiatry, 2004. **75**(8): p. 1166-70.

20. Yu, S., et al., *Aggregation of prion protein with insertion mutations is proportional to the number of inserts.* Biochem J, 2007. **403**(2): p. 343-51.

21. Chiesa, R., et al., *Neurological illness in transgenic mice expressing a prion protein with an insertional mutation.* Neuron, 1998. **21**(6): p. 1339-51.

22. Chiesa, R., et al., *Accumulation of protease-resistant prion protein (PrP) and apoptosis of cerebellar granule cells in transgenic mice expressing a PrP insertional mutation.* Proc Natl Acad Sci U S A, 2000. **97**(10): p. 5574-9.

23. Chiesa, R., et al., *Molecular distinction between pathogenic and infectious properties of the prion protein.* J Virol, 2003. **77**(13): p. 7611-22.

24. Choi, C.J., et al., *Interaction of metals with prion protein: possible role of divalent cations in the pathogenesis of prion diseases.* Neurotoxicology, 2006. **27**(5): p. 777-87.

25. Dong, J., et al., *Probing the role of PrP repeats in conformational conversion and amyloid assembly of chimeric yeast prions.* J Biol Chem, 2007. **282**(47): p. 34204-12.

26. Chernoff, Y.O., S.M. Uptain, and S.L. Lindquist, *Analysis of prion factors in yeast.* Methods Enzymol, 2002. **351**: p. 499-538.

27. True, H.L., I. Berlin, and S.L. Lindquist, *Epigenetic regulation of translation reveals hidden genetic variation to produce complex traits.* Nature, 2004. **431**(7005): p. 184-7.

28. True, H.L. and S.L. Lindquist, *A yeast prion provides a mechanism for genetic variation and phenotypic diversity.* Nature, 2000. **407**(6803): p. 477-83.

29. Shorter, J. and S. Lindquist, *Prions as adaptive conduits of memory and inheritance.* Nat Rev Genet, 2005. **6**(6): p. 435-50.

30. Ter-Avanesyan, M.D., et al., *The SUP35 omnipotent suppressor gene is involved in the maintenance of the non-Mendelian determinant [psi+] in the yeast Saccharomyces cerevisiae.* Genetics, 1994. **137**(3): p. 671-6.

31. Doel, S.M., et al., *The dominant PNM2- mutation which eliminates the psi factor of Saccharomyces cerevisiae is the result of a missense mutation in the SUP35 gene.* Genetics, 1994. **137**(3): p. 659-70.

32. Tuite, M.F. and B.S. Cox, *Propagation of yeast prions.* Nat Rev Mol Cell Biol, 2003. **4**(11): p. 878-90.

33. Liebman, S.W. and I.L. Derkatch, *The yeast [PSI+] prion: making sense of nonsense.* J Biol Chem, 1999. **274**(3): p. 1181-4.

34. Ter-Avanesyan, M.D., et al., *Deletion analysis of the SUP35 gene of the yeast Saccharomyces cerevisiae reveals two non-overlapping functional regions in the encoded protein.* Mol Microbiol, 1993. **7**(5): p. 683-92.

35. Serio, T.R. and S.L. Lindquist, *[PSI+]: an epigenetic modulator of translation termination efficiency.* Annu Rev Cell Dev Biol, 1999. **15**: p. 661-703.

36. Parham, S.N., C.G. Resende, and M.F. Tuite, *Oligopeptide repeats in the yeast protein Sup35p stabilize intermolecular prion interactions.* Embo J, 2001. **20**(9): p. 2111-9.

37. Osherovich, L.Z., et al., *Dissection and design of yeast prions.* PLoS Biol, 2004. **2**(4): p. E86.

38. Liu, J.J. and S. Lindquist, *Oligopeptide-repeat expansions modulate 'protein-only' inheritance in yeast.* Nature, 1999. **400**(6744): p. 573-6.

39. Tank, E.M., et al., *Prion protein repeat expansion results in increased aggregation and reveals phenotypic variability.* Mol Cell Biol, 2007.

40. Glover, J.R., et al., *Self-seeded fibers formed by Sup35, the protein determinant of [PSI+], a heritable prion-like factor of S. cerevisiae.* Cell, 1997. **89**(5): p. 811-9.

41. Tanaka, M., et al., *Conformational variations in an infectious protein determine prion strain differences.* Nature, 2004. **428**(6980): p. 323-8.

42. Krishnan, R. and S.L. Lindquist, *Structural insights into a yeast prion illuminate nucleation and strain diversity.* Nature, 2005. **435**(7043): p. 765-72.

43. Derkatch, I.L., et al., *Genesis and variability of [PSI] prion factors in Saccharomyces cerevisiae.* Genetics, 1996. **144**(4): p. 1375-86.

44. Moore, R.A., et al., *Octapeptide repeat insertions increase the rate of protease-resistant prion protein formation.* Protein Sci, 2006. **15**(3): p. 609-19.

45. King, A., et al., *Phenotypic variability in the brains of a family with a prion disease characterized by a 144-base pair insertion in the prion protein gene.* Neuropathol Appl Neurobiol, 2003. **29**(2): p. 98-105.

46. Kovacs, G.G., et al., *Mutations of the prion protein gene phenotypic spectrum.* J Neurol, 2002. **249**(11): p. 1567-82.

47. Serio, T.R., et al., *Nucleated conformational conversion and the replication of conformational information by a prion determinant.* Science, 2000. **289**(5483): p. 1317-21.

48. Ross, C.A., et al., *Polyglutamine fibrillogenesis: the pathway unfolds.* Proc Natl Acad Sci U S A, 2003. **100**(1): p. 1-3.

49. Collins, S.R., et al., *Mechanism of prion propagation: amyloid growth occurs by monomer addition.* PLoS Biol, 2004. **2**(10): p. e321.

50. Fawzi, N.L., et al., *Determining the critical nucleus and mechanism of fibril elongation of the Alzheimer's Abeta(1-40) peptide.* J Mol Biol, 2007. **365**(2): p. 535-50.

51. Nguyen, P.H., et al., *Monomer adds to preformed structured oligomers of Abeta-peptides by a two-stage dock-lock mechanism.* Proc Natl Acad Sci U S A, 2007. **104**(1): p. 111-6.

52. Harper, J.D. and P.T. Lansbury, Jr., *Models of amyloid seeding in Alzheimer's disease and scrapie: mechanistic truths and physiological consequences of the time-dependent solubility of amyloid proteins.* Annu Rev Biochem, 1997. **66**: p. 385-407.

53. O'Nuallain, B., et al., *Thermodynamics of A beta(1-40) amyloid fibril elongation.* Biochemistry, 2005. **44**(38): p. 12709-18.

54. Toyama, B.H., et al., *The structural basis of yeast prion strain variants.* Nature, 2007. **449**(7159): p. 233-7.

55. Serio, T.R., et al., *Yeast prion [psi +] and its determinant, Sup35p.* Methods Enzymol, 1999. **309**: p. 649-73.

56. Tanaka, M. and J.S. Weissman, *An efficient protein transformation protocol for introducing prions into yeast.* Methods Enzymol, 2006. **412**: p. 185-200.

Chapter 3: Analysis of the [*RNQ*$^{+}$] prion reveals stability of amyloid fibers as the key determinant of yeast prion variant propagation

Tejas Kalastavadi and Heather L. True

This chapter is submitted to the Journal of Biological Chemistry and is in revision.

SUMMARY

Variation in pathology of human prion disease is believed to be caused, in part, by distinct conformations of aggregated protein resulting in different prion strains. Several prions also exist in yeast and maintain different self-propagating structures, referred to as prion variants. Investigation of the yeast prion [*PSI*$^+$] has been instrumental in deciphering properties of prion variants and modeling the physical basis of their formation. Here, we describe the generation of specific variants of the [*RNQ*$^+$] prion in yeast transformed with fibers formed in vitro in different conditions. The fibers of the Rnq1p prion-forming domain (PFD) that induce different variants in vivo have distinct biochemical properties. The physical basis of propagation of prion variants has been previously correlated to rates of aggregation and disaggregation. With [*RNQ*$^+$] prion variants, we found that the prion variant does not correlate with the rate of aggregation as anticipated but does correlate with fragility. Interestingly, we found that there are differences in the ability of the [*RNQ*$^+$] prion variants to faithfully propagate themselves and to template the aggregation of other proteins. Incorporating the mechanism of variant formation elucidated in this study with that previously proposed for [*PSI*$^+$] variants has provided a framework to separate general characteristics of prion variant properties from those specific to individual prion proteins.

Prion diseases are fatal neurodegenerative disorders that affect many mammals. Prions are responsible for diseases such as scrapie in sheep, bovine spongiform encephalopathy (BSE) in cows and Creutzfeldt-Jakob disease in humans (1). These diseases are linked to either mutations in the gene encoding the prion protein (*PRNP*) or

aggregation of the prion protein (PrP) itself (2,3). Self-propagating aggregates of PrP are implicated in the infectious transmission of prion disease among mammals (4). One interesting feature of prion diseases lies in the apparent heterogeneity of clinical symptoms and disease pathology (5-7). It has been hypothesized that this heterogeneity in pathology is partly due to the existence of different prion strains (8). The mechanism of prion strain generation is not entirely understood, but is an important aspect of prion disease. Elucidating mechanisms that dictate the generation of prion strains is crucial to understanding the biology underlying prion diseases, protein misfolding, and aggregation.

Naturally occurring prions that exist in fungi such as the budding yeast *Saccharomyces cerevisiae* are not associated with disease, but act as a mechanism to alter phenotype. Recent studies have uncovered several prion-like proteins in yeast (9-13). The three extensively characterized prions in yeast are the [*PSI*$^{+}$], [*RNQ*$^{+}$] and [URE3] prions (14-16). The [*PSI*$^{+}$] prion manifests as a result of the aggregation of Sup35p (17,18), which is the *S. cerevisiae* eukaryotic release factor 3 (eRF3) (19). In the [*psi*$^{-}$] state, Sup35p binds Sup45p and this complex is required for translation termination at stop codons (20). In the [*PSI*$^{+}$] state, however, much of the Sup35p is in the aggregated state and not available to function in translation termination (17). A premature stop codon in a metabolic pathway, such as that in the *ade1-14* allele, provides a convenient method of detecting the [*PSI*] state of yeast cells. Yeast grown on nutrient-rich media that harbor the *ade1-14* allele are white in color in the [*PSI*$^{+}$] state, but red in color in the [*psi*$^{-}$] state due to the accumulation of a metabolic intermediate in the adenine biosynthetic pathway (21). Yeast can maintain different variants of the [*PSI*$^{+}$] prion and these cause different levels of read through of the *ade1-14* premature stop codon that

correlate to the amount of aggregated Sup35p (22-24). This results in different levels of pigment accumulation in cells and weaker strains of [*PSI*$^{+}$] manifest as shades of pink (24). This phenotype has proven very useful in investigating the mechanism of prion variant generation.

The structure of different [*PSI*$^{+}$] prion variants have been revealed by biophysical and nuclear magnetic resonance (NMR) studies on conformationally-distinct fibers of the prion forming domain (PFD) of Sup35p (Sup35NM) formed in vitro at different temperatures (25-28). These studies suggest that the protected amyloid core of the strong variant is short relative to the amyloid core of the weak variant. A model designed to explain the propagation of prion variants related structural and biochemical properties of amyloid fibers to the prion variant phenotype (29). This model suggests that the propagation of prion variants can be explained by differences in the rate of fiber growth and sensitivity to shearing. Since the addition of new protein appears to occur on fiber ends (30,31), it follows that the most efficient propagation requires more free ends to template the addition of new protein. Thus, more free ends may relate to a faster rate of aggregation. The mechanism for prion variant generation has been proposed primarily based on work conducted using Sup35NM and the [*PSI*$^{+}$] prion.

Two other prions in yeast, [URE3] and [*RNQ*$^{+}$], have also been reported to display variant phenotypes (32,33). The [URE3] prion in *S. cerevisiae* is propagated by the Ure2 protein (16). Recombinant Ure2p can form fibers in vitro and when transformed into yeast can induce different variants of the [URE3] prion (33). The [*RNQ*$^{+}$] prion is caused by the aggregation of the Rnq1 protein (34). In the [*rnq*$^{-}$] state, the Rnq1 protein has no known function. However, in the [*RNQ*$^{+}$] state, aggregated

Rnq1p facilitates the induction of the [*PSI*$^+$] prion (35-37). [*RNQ*$^+$] also exists as different variants (38) that appear when recombinant Rnq1p fibers are transformed into yeast (39). However, the generation of specific [*RNQ*$^+$] variants by altering the conditions of in vitro amyloid formation has not been investigated. As such, the physical basis for the generation of [URE3] and [*RNQ*$^+$] variants has not been described and it remains to be determined if the properties described for [*PSI*$^+$] variants can be generalized.

We have taken advantage of the [*RNQ*$^+$] reporter protein (RRP) previously described by our lab to phenotypically assess the [*RNQ*$^+$] prion status as well as [*RNQ*$^+$] variants (40). The RRP molecule is a chimeric protein with the proposed PFD of Rnq1p (amino acids 153-405) fused to the translation termination domain of Sup35p (the MC region, amino acids 124-685) (41,42). The RRP fusion presumably co-aggregates with Rnq1p in the [*RNQ*$^+$] state which results in prion-dependent nonsense suppression. As such, this provides a phenotypic assay for the [*RNQ*] state. This assay allowed us to detect both intragenic and extragenic effectors of [*RNQ*$^+$] propagation (40,43). We found that the level of nonsense suppression afforded by RRP changes with [*RNQ*$^+$] prion variants and this enables us to distinguish variants by phenotype.

In this study, we created and characterized variants of the [*RNQ*$^+$] prion by controlling conditions of fiber formation and transforming the fibers into yeast strains with Rnq1p in the non-prion state, [*rnq*$^-$]. We show that the proposed PFD of Rnq1p forms amyloid fibers with distinct characteristics when generated in different conditions. Additionally, infection of these fibers into yeast induces different [*RNQ*$^+$] prion variants in vivo. Each [*RNQ*$^+$] variant maintains and propagates a unique set of characteristics in

vivo and in vitro. Finally, our data suggests the existence of both similarities and differences between the mechanisms that dictate [*RNQ*$^{+}$] and [*PSI*$^{+}$] variant propagation.

RESULTS

Temperature has a profound effect on the kinetics of Rnq1PFD fiber formation- We purified recombinant Rnq1PFD in 8 M Urea as described in experimental procedures. The purified Rnq1PFD protein formed amyloid fibers when diluted out of denaturant. The length of the lag phase of fiber formation is a parameter that can be used to measure the ability of the protein to aggregate and is one determinant for prion variant formation; a longer lag phase indicates a reduced ability to aggregate. In order to create [*RNQ*$^{+}$] prion variants, we used different temperatures to generate structural variation in the fibers of Rnq1PFD. We followed fiber formation of Rnq1PFD at 25°C and 37°C using a Thioflavin-T fluorescence assay. At 25°C, Rnq1PFD fibers had a lag phase of ~470 minutes followed by a logarithmic growth phase (Fig. 1A). In contrast, fiber formation of Rnq1PFD at 37°C had a shorter lag phase of ~300 minutes.

The ability of seeds to enhance the conversion of monomeric protein into fibers is an important feature of nucleated conformational conversion for amyloid fiber formation (44). We formed Rnq1PFD fibers at 25°C and 37°C and tested the ability of the fibers to act as seeds and template the addition of freshly diluted monomeric Rnq1PFD. Interestingly, even though Rnq1PFD fiber formation occurs with a shorter lag phase at 37°C, the seeds obtained from fibers formed at 25°C were more efficient at templating new fiber formation at both 25°C and 37°C (Fig. 1B and 1C). Seeds obtained from fibers formed at 37°C also enhanced fiber formation reactions but were less efficient at seeding Rnq1PFD monomer at either temperature (Fig. 1B and 1C).

Figure 1

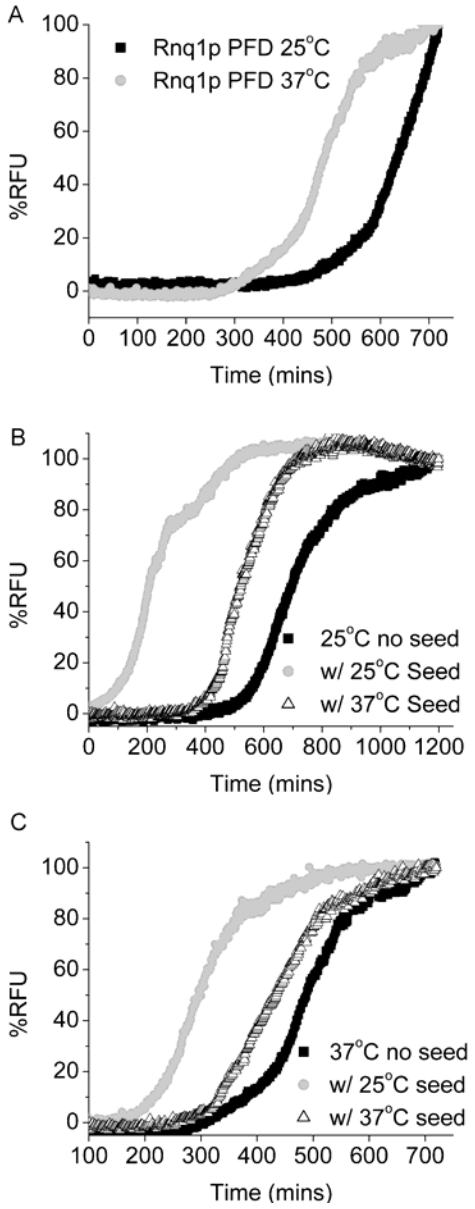

FIGURE 1. **Fiber formation of Rnq1p is faster at higher temperatures and enhanced by the addition of pre-formed seeds.** Purified Rnq1PFD was diluted from denaturant (75-fold) to 4 μM and fiber formation was followed using Th-T fluorescence. Graphs are plotted as %RFU (relative fluorescence units) versus time. (A) Rnq1PFD unseeded at 25°C (black squares) and 37°C (grey circles). (B) Rnq1PFD fiber formation at 25°C unseeded (black squares), with 5% seeds formed at 25°C (grey circles), and with 5% seeds formed at 37°C (open triangles). (C) Rnq1PFD fiber formation at 37°C unseeded (black squares), with 5% seeds formed at 25°C (grey circles) and with 5% seeds formed at 37°C (open triangles). Graphs are representative of at least three independent trials.

Rnq1PFD fibers formed at different temperatures induce distinct distributions of prion variants- Prion proteins in yeast can maintain different variants of the prion state that are a consequence of different self-propagating structures (45). The variants differ from each other based on their phenotype, the ratio of soluble to aggregated protein, and their ability to maintain and propagate the prion (23,24,38). Previous work has extensively characterized variants of the [*PSI*$^+$] prion generated in vitro (25-27,29,46,47). Variants of the [*RNQ*$^+$] prion have also been characterized in vivo and display different abilities to induce the [*PSI*$^+$] prion (38,48). However, these variants arose spontaneously and were originally referred to as [*PIN*$^+$] strains for [*PSI*+] *in*duciblity (37,49). Additionally, some variants of [*PIN*$^+$] were acquired when fibers of Rnq1PFD were transformed into [*rnq*$^-$] yeast, but these were not characterized (39). Characterization of [*RNQ*$^+$] variants has been limited since the only methods to assay the [*RNQ*$^+$]/ [*PIN*$^+$] status of yeast cells involved either [*PSI*$^+$] induction or Rnq1p solubility assays. In our lab, we have been able to circumvent some of these tedious procedures by taking advantage of the previously described RRP ([*RNQ*$^+$] Reporter Protein), which enables the use of a colony color assay to determine the presence of different prion variants of [*RNQ*$^+$]. We found that RRP not only reported on the presence of the [*RNQ*$^+$] prion, but also showed changes in phenotype depending on the [*RNQ*$^+$]/[*PIN*$^+$] variant ((40) and Fig. 2A). High [*PIN*$^+$] and [*pin*$^-$] are readily discernible from low [*PIN*$^+$] and medium [*PIN*$^+$] when RRP-expressing strains are grown on nutrient rich media. Low [*PIN*$^+$] and medium [*PIN*$^+$] strains are phenotypically similar to each other in this assay.

In order to create [*RNQ*$^+$] variants for characterization, we first asked whether amyloid fibers of Rnq1PFD formed at different temperatures corresponded to the

generation of different prion variants, as previously observed with Sup35NM and [*PSI*$^{+}$] (47,50). We transformed [*rnq*$^{-}$] 74-D694 cells expressing both wild type *RNQ1* and the RRP chimeric protein with amyloid fibers of recombinant Rnq1PFD formed at 18°C, 25°C, and 37°C. Transformants were picked, diluted, and spotted on plates to assess phenotype. We scored the transformants that turned white, light pink, or dark pink as strong, medium, or weak [*RNQ*$^{+}$] variants, respectively (Fig. 2B and Table 1). We also correlated the colony color phenotype of the variants to their growth on media lacking adenine (SD-ade). Transformants were also grown on media containing guanidine hydrochloride (GdnHCl), which inactivates Hsp104 (51) and cures all variants of the [*RNQ*$^{+}$] prion. [*RNQ*$^{+}$] variants were verified for curability on media containing GdnHCl using color as an indicator of change in nonsense suppression. [*RNQ*$^{+}$] RRP strains converted from either white or pink to red, and the cured strains remained red upon removal from media containing GdnHCl. Rnq1PFD fibers formed at 18°C only induced strong and medium variants of [*RNQ*$^{+}$] when transformed into [*rnq*$^{-}$] cells (Table 1). Fibers formed at 25°C induced weak, medium, and strong [*RNQ*$^{+}$] variants when transformed into [*rnq*$^{-}$] cells. In contrast, cells infected with fibers formed at 37°C yielded primarily medium and weak [*RNQ*$^{+}$] variants and very few strong [*RNQ*$^{+}$] variants. These data suggest that the temperature at which fibers were formed in vitro influenced the distribution of [*RNQ*$^{+}$] variants propagated in cells. Specifically, increasing the temperature decreased the fraction of strong [*RNQ*$^{+}$] variants and increased the weak variants of [*RNQ*$^{+}$].

Figure 2

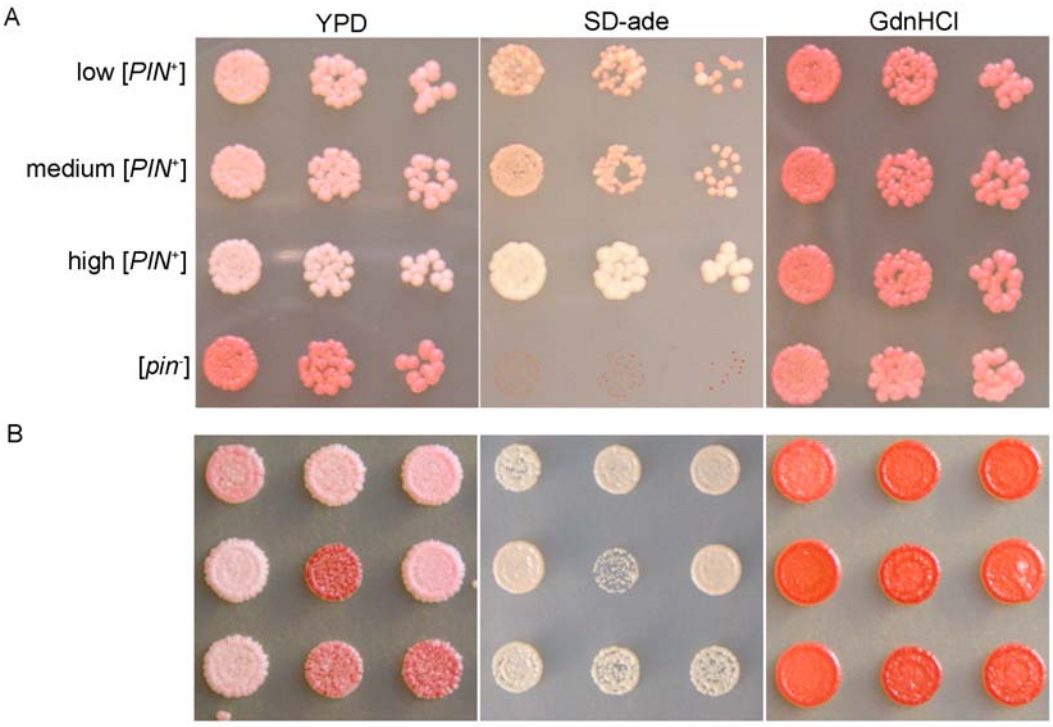

FIGURE 2. **RRP differentiates [*RNQ*$^+$]/ [*PIN*$^+$] variants** (A) Yeast strains expression the RRP reporter display different levels of nonsense suppression in [*PIN*$^+$] variants. (B) Transformation of Rnq1PFD amyloid fibers into [*rnq*$^-$] yeast induces variants of the [*RNQ*$^+$] prion. The [*RNQ*$^+$] phenotype was assayed using the RRP reporter to show color on YPD, growth on SD-ade, and curability by growth on media containing GdnHCl. Colony color on YPD is indicative of different levels of suppression of the *ade1-14* premature stop codon to produce Ade1p. [*RNQ*$^+$] prion variants co-aggregate with RRP and cause different phenotypes (color on YPD). The strength of the variants is also reflected by their ability to grow on SD-ade medium.

Table 1

Distribution of [*RNQ*$^{+}$] variants

	Weak	Medium	Strong
18 ° C	0	25	75
25 ° C	15	46	39
37 ° C	29	68	3

Table 1. **Distribution of [*RNQ*+] prion variants**. Yeast colonies that resulted from infection of Rnq1PFD fibers formed at 18°C, 25°C, and 37°C were grouped into weak, medium, and strong [*RNQ*$^{+}$] strains based on RRP-mediated colony color (on YPD) and growth on medium lacking adenine (SD-ade). The numbers in the table reflect the percentage of variants obtained by infectivity assays after counting over 300 transformed colonies from more than three experiments for each temperature at which fibers were formed.

Rnq1PFD fibers formed at different temperatures are differentially stable- In the case of Sup35NM and the [*PSI*$^+$] prion, weaker variants have a longer amyloid core and stronger variants have a shorter amyloid core (25,26). The length of the core positively correlates with the stability of the amyloid fibers. Additionally, the more stable amyloid fibers with a longer core propagate weaker prion variants while less stable fibers with a shorter core propagate stronger prion variants.

We next asked if the stability of the amyloid fibers correlated to the [*RNQ*$^+$] variants induced in a manner similar to the observations with [*PSI*$^+$] and Sup35NM. Therefore, we used thermostability to determine the relative stability of Rnq1PFD fibers formed at different temperatures. We formed fibers at 18°C, 25°C, and 37°C and subjected them to increasing temperatures in 2% SDS. We then analyzed the soluble protein by SDS-PAGE and western blot. We found that fibers formed at 18°C were labile and showed ~50% disruption at 65°C (Fig. 3). Fibers formed at 25°C were slightly more stable and showed ~50% dissociation at 75°C. Rnq1PFD fibers formed at 37°C were the most stable and required 85°C to dissociate. Thus, stronger amyloid fibers yield weaker prion variants and this trend recapitulates the data observed previously for Sup35NM.

Transmission electron microscopy (TEM) reveals dramatic morphological differences in Rnq1PFD fibers- The observed dramatic differences in kinetics and stability of amyloid fibers of Rnq1PFD formed at different temperatures and their ability to induce different variants of [*RNQ*$^+$] led us to hypothesize that the morphology of the Rnq1PFD fibers formed at these temperatures may be distinct. In order to determine if there are gross morphological differences between the Rnq1PFD fibers formed at 18°C,

Figure 3

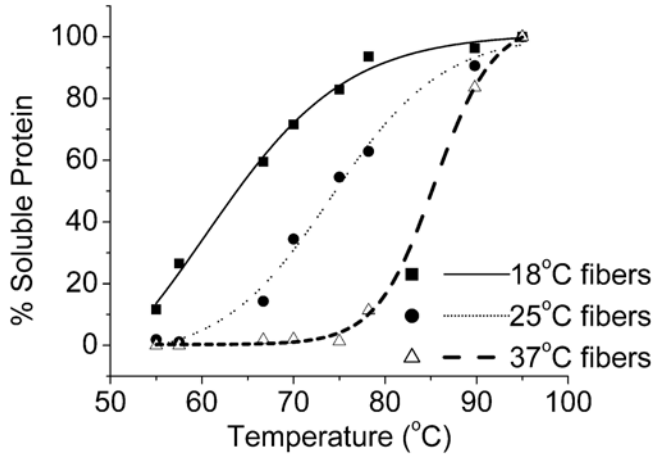

FIGURE 3. **Rnq1PFD fibers formed at higher temperatures are more stable.** Preformed fibers were treated across a temperature gradient in the presence of 2% SDS. Following SDS-PAGE and western blot, the amount of soluble Rnq1PFD was quantified and the results were graphed as a percentage of total protein at 95°C using OriginPro 6.1 with a sigmoidal fit function.

Figure 4

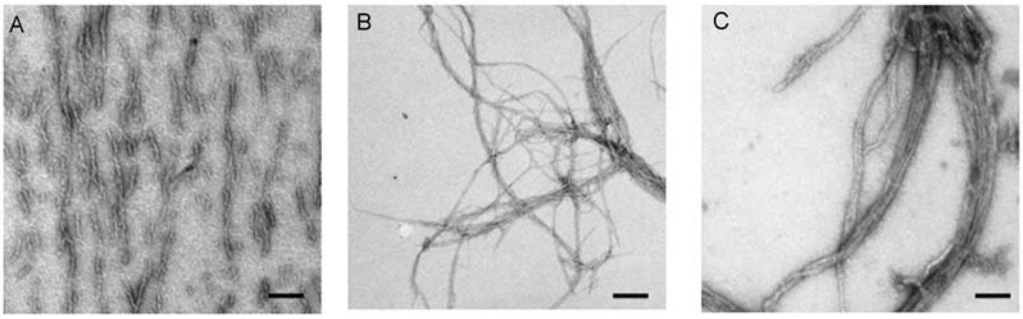

FIGURE 4. **The morphology of amyloid fibers formed from Rnq1PFD at different temperatures is distinct.** Amyloid fibers of Rnq1PFD formed in vitro were imaged by TEM. The scale bar represents 200 nm. (A) 18°C fibers are short and curly (B) 25°C fibers are long and curvy, and (C) 37°C fibers are long and bundled.

25°C, and 37°C we obtained TEM images of these amyloid fibers. In fact, we did observe significant differences in the morphology of the fibers formed at the different temperatures. We noted that the Rnq1PFD fibers formed at 18°C were short and curly (Fig. 4A) compared to the long fibers formed at 25°C (Fig. 4B). Lastly, the fibers formed at 37°C were also long and appeared to be more heavily bundled with one another as compared to the fibers formed at 25°C (Fig. 4C). These results indicate that temperature has a profound impact on the properties of the amyloid fibers formed by Rnq1PFD.

[*RNQ*$^+$] *prion variants have distinct protein aggregation and propagation properties in vivo* Variants of the [*PSI*$^+$] prion have differential abilities to faithfully propagate the prion through mitosis (24). We utilized the RRP marker to determine the relative mitotic stability of the [*RNQ*$^+$] prion variants. We grew the three different variants in liquid media overnight and plated them on rich media to assess [*RNQ*$^+$] stability by color. The colonies that did not maintain the prion through mitotic division turned red and were counted and plotted as a fraction of the total number of colonies (Fig. 5A). The strong [*RNQ*$^+$] prion variant propagated the prion with nearly 100% fidelity and rarely lost the prion phenotype. In comparison, the medium [*RNQ*$^+$] variant lost the prion in ~19% of the progeny and the weak [*RNQ*$^+$] variant lost the prion in almost 40% of the progeny. The loss of the [*RNQ*$^+$] prion was verified by conducting Rnq1p solubility assay on a subset of candidate [*rnq*$^-$] cells for each variant. Thus, the stability of prion propagation is correlated to the strength of the prion variant and is similar to what has been observed with the [*PSI*$^+$] prion.

Even though there are differences in mitotic stability, all prions should be transmitted in a non-Mendelian fashion via mating and meiosis (52). To verify that the

cells infected with in vitro formed fibers of Rnq1PFD truly harbor self-propagating prion elements, we tested the transmission of the prion. We mated the transformed cells harboring different variants of the [*RNQ*$^{+}$] prion to [*psi*$^{-}$] [*rnq*$^{-}$] cells. The diploids that we obtained were [*psi*$^{-}$] [*RNQ*$^{+}$] and red in color because wild type Sup35p does not aggregate with RRP and allows for faithful termination of translation (data not shown). We sporulated the diploids to determine if the [*RNQ*$^{+}$] prion variants were faithfully inherited in meiotic progeny as expected for the prion state. We then performed Rnq1p solubility assays on at least three complete tetrads from each strain. We noted that in each case, the [*RNQ*$^{+}$] prion was inherited in a non-Mendelian fashion with all four progeny being [*RNQ*$^{+}$] (data not shown).

Prion variants of both [*PSI*$^{+}$] and [*RNQ*$^{+}$] have also been shown to display differences in the ratio of soluble to aggregated protein (23,38). In order to determine whether the different [*RNQ*$^{+}$] variants that we had classified based on phenotype had corresponding biochemical differences, we performed Rnq1p solubility assays on the variants (Fig. 5B). In cells containing the weak [*RNQ*$^{+}$] variants, most of the protein was in the soluble fraction and a small amount of Rnq1p was in the pellet fraction. In the medium [*RNQ*$^{+}$] variants, a small portion of the protein was soluble, while most was found in the aggregated pellet fraction. However, in the strong [*RNQ*$^{+}$] variant, almost all of Rnq1p was aggregated and very little protein was found in the soluble fraction. Interestingly, this variant-dependent change in solubility was reproducible in fresh transformants but was not as apparent in new meiotic progeny (data not shown). However, the [*RNQ*$^{+}$] solubility assay has not always provided a robust measure of differences in prion variants (38,40).

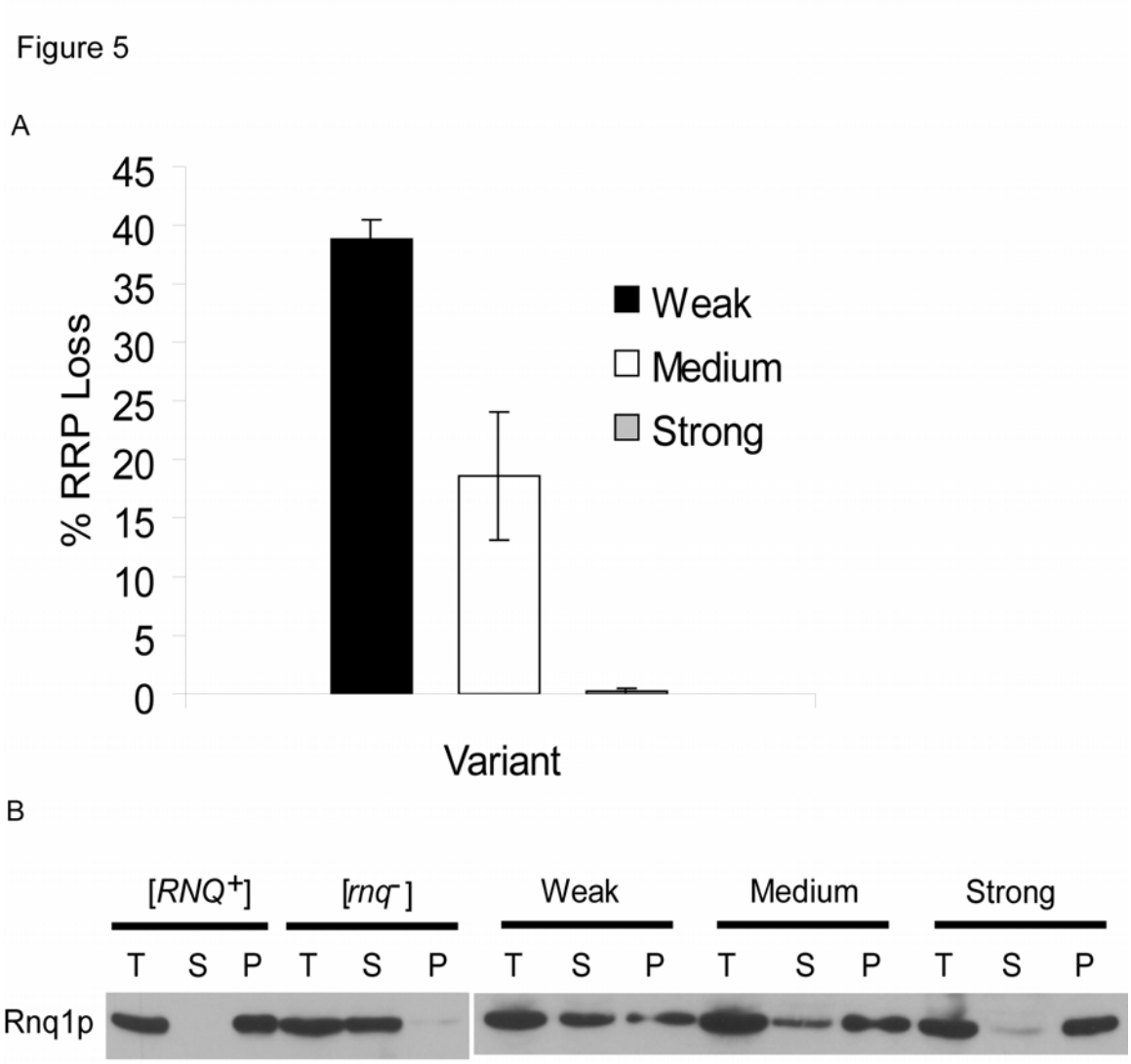

FIGURE 5. **Variants of the [*RNQ*$^+$] prion show distinct propagation and aggregation properties in vivo.** (A) Mitotic stability of the [*RNQ*$^+$] prion was dependent on the strength of the variant. The weak [*RNQ*$^+$] variant lost the prion in ~40% of the colonies (black bar), while medium [*RNQ*$^+$] lost the prion in ~19% of the colonies (white bar), and strong [*RNQ*$^+$] lost the prion in <1% of the colonies (grey bar). (B) Full length endogenous Rnq1p in lysates from different [*RNQ*$^+$] variants was fractionated by high speed centrifugation into total (T), supernatant (S), and pellet (P) fractions. The amount of protein in the supernatant fraction decreased as the strength of the variant increased. A representative blot from four independent experiments is shown.

Variants of [*RNQ*$^+$] *induce* [*PSI*$^+$] *with different efficiencies*- The only phenotype associated with the [*RNQ*$^+$] prion state is its ability to induce the [*PSI*$^+$] prion by acting as [*PIN*$^+$]. While other protein aggregates can act as [*PIN*$^+$], to date only [*RNQ*$^+$] has been found commonly in lab and wild strains (34,53,54) and as such, is likely the most common, naturally occurring [*PIN*$^+$] element. Since we observed that [*RNQ*$^+$] induced by protein transformation resulted in distinct variants based on nonsense suppression, we next wanted to test the ability of the variants to act as [*PIN*$^+$] and induce [*PSI*$^+$] (24,37). Red [*psi*$^-$] [*RNQ*$^+$] cells that were propagating different variants of the [*RNQ*$^+$] prion were obtained by mating and sporulation as described in the previous section. The progeny that expressed wild type *SUP35* and did not have the *RRP* reporter were transformed with a plasmid expressing a second copy of *SUP35* from its own promoter to induce [*PSI*$^+$]. Transformants were grown in selective media overnight to allow for Sup35p over-expression and then plated on YPD. The efficiency of [*PSI*$^+$] induction was determined by counting the number of colonies with light pink sectors and dividing that by the total number of colonies. In the [*rnq*$^-$] controls, we did not observe any induction of the [*PSI*$^+$] prion when *SUP35* was over-expressed in the cell, while in [*RNQ*$^+$] cells we obtained efficient induction of [*PSI*$^+$] (Fig. 6). As expected, the strong [*RNQ*$^+$] variants showed a high level of induction of [*PSI*$^+$], with > 60% of the colonies sectoring (Fig. 6). The medium [*RNQ*$^+$] variants had lower induction of [*PSI*$^+$] when compared to strong [*RNQ*$^+$]. Surprisingly, the weak [*RNQ*$^+$] variants demonstrated high levels of [*PSI*$^+$] induction (Fig. 6) that were comparable to the strong variants of [*RNQ*$^+$]. Interestingly, the induction of [*PSI*$^+$] we observed with our strong and weak [*RNQ*$^+$] variants were reminiscent of the

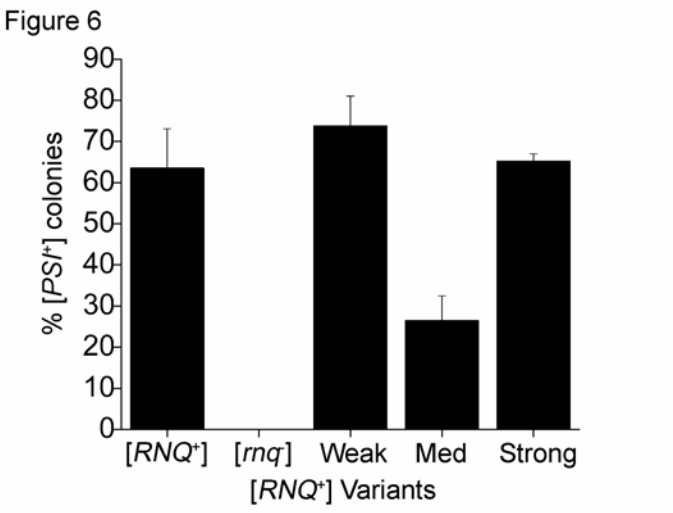

FIGURE 6. **The [*PSI*$^+$] induction capacity of the [*RNQ*$^+$] variants is distinct.** The over expression of Sup35p in the control [*RNQ*$^+$] strain induced [*PSI*$^+$] in ~62% of the colonies. [*PSI*$^+$] was not induced in [*rnq*$^-$] cells. Over expression of Sup35p in weak [*RNQ*$^+$] variants induced [*PSI*$^+$] in ~72% of the colonies, medium [*RNQ*$^+$] variants induced [*PSI*$^+$] in ~25% of the colonies, and strong [*RNQ*$^+$] variants induced [*PSI*$^+$] in ~65% of the colonies.

previously characterized high and very high [*PIN*$^+$] variants, respectively, that were previously published (38) and reconfirmed (data not shown).

DISCUSSION

The mechanism underlying the generation of prion variants was extensively investigated for only one yeast prion protein previously. Both the physical and structural basis for variant formation of the [*PSI*$^+$] prion from Sup35NM has been elucidated (25,26,29). Here, we created and characterized different variants of the [*RNQ*$^+$] prion. We assayed for prion variants in vivo using the chimeric protein RRP (40) that displayed distinct nonsense suppression phenotypes. We used changes in temperature as a means to generate different amyloid structures and correlated those to prion variant formation in vitro and in vivo. Rnq1PFD fibers formed at 18°C, 25°C, and 37°C have distinct biochemical and morphological properties. Interestingly, fibers formed at 37°C have a shorter lag phase when compared to the 25°C fibers. As expected, the stability of the fibers increased with the temperature at which the fibers were formed, which was also reflected by the morphology of the fibers observed by TEM. We speculate that the fibers formed at 18°C are the least stable because they are short. Fibers formed at 37°C appear to be the most stable and this may be due, in part, to the interactions between fibers. The more stable 37°C fibers also show reduced seeding capacity as compared to fibers formed at 25°C. The ability of 37°C Rnq1PFD fibers to seed new reactions was not enhanced by increased shearing, however (data not shown). Finally, fibers formed at 18°C, 25°C, or 37°C were transformed into [*rnq*$^-$] yeast cells and each resulted in distinct distributions of [*RNQ*$^+$] prion variants.

The correlation we observed between the length of the lag phase and the resulting [*RNQ*$^{+}$] prion variants, however, was not in accordance with previously observed properties of Sup35NM fibers and [*PSI*$^{+}$] variants. In the case of Sup35NM, fibers formed at 25°C have a longer lag phase when compared to 4°C fibers (55). When Sup35NM fibers are transformed into cells, strong [*PSI*$^{+}$] variants are generated from fibers with a short lag phase and weak [*PSI*$^{+}$] variants result from fibers that formed with a longer lag phase. In stark contrast, although Rnq1PFD fibers formed faster at 37°C, they induced weaker [*RNQ*$^{+}$] variants. Rnq1PFD fibers formed slower at 25°C and induced strong [*RNQ*$^{+}$] variants. We would like to note that unlike Sup35NM, Rnq1PFD was unable to form discernable amyloid fibers at 4°C (data not shown).

The correlation between the stability of Rnq1PFD amyloid fibers and the resulting prion variant distribution is similar to what was observed with Sup35NM and the [*PSI*$^{+}$] prion (47). We observed that an increase in the stability of the Rnq1PFD fibers correlated to an increase in weak [*RNQ*$^{+}$] variants and a decrease in strong [*RNQ*$^{+}$] variants. From this, we suggest that the stability of the fibers is a critical property in determining the previously proposed parameters that dictate prion variants. Since the rate of aggregation does not always correlate to the generation of specific prion variants, we suggest that this in vitro property cannot be generalized to determine the physical basis of variants in vivo. As the addition of new protein occurs at fiber ends (30), it follows that the most efficient propagation requires more free ends for templating. Faster aggregation, but slower disaggregation, would be unlikely to create strong variants, as is the case with Rnq1PFD fibers formed at 37°C. However, fast "disaggregation" or

shearing could compensate for some reduction in the rate of aggregation, as is the case with Rnq1PFD fibers formed at 25°C.

We were also able to determine the differences in the mitotic stability of the different [*RNQ*$^+$] variants using the convenient RRP marker. The ability to maintain the [*RNQ*$^+$] prion state was intimately linked to the strength of the prion, with strong [*RNQ*$^+$] being more stable than medium [*RNQ*$^+$], and medium [*RNQ*$^+$] being more stable than weak [*RNQ*$^+$]. The stability of the different variants could be related to the ratio of aggregated to soluble protein, the size of the aggregates, and the ability of Hsp104p and other chaperones to generate seeds that can be passed on to daughter cells.

We further characterized the [*RNQ*$^+$] variants by assaying their ability to act as [*PIN*$^+$] and induce [*PSI*$^+$]. Surprisingly, both weak [*RNQ*$^+$] and strong [*RNQ*$^+$] induced [*PSI*$^+$] at high efficiencies (> 60%) when compared to the medium [*RNQ*$^+$] variant. Interestingly, the weak [*RNQ*$^+$] variant was denoted as weak based on solubility of Rnq1p and low levels of nonsense suppression using RRP, but it maintained the greatest capacity to induce [*PSI*$^+$]. We compared our variant to the previously described variants of the [*RNQ*$^+$] prion that were obtained spontaneously (38). They were classified based on their ability to induce [*PSI*$^+$] into low, medium, high, and very high [*PIN*$^+$] variants. The extent of aggregation of Rnq1p correlated to an increase in [*PSI*$^+$] induction efficiency with the low, medium, and high variants. However, the very high [*PIN*$^+$] variant did not fit the trend as it showed the largest amount of soluble Rnq1p, but had the greatest capacity to induce [*PSI*$^+$]. Therefore, we propose that the weak [*RNQ*$^+$] variants we obtained by protein transformation are most similar to the previously obtained very high [*PIN*$^+$] variant (38). Since the RRP phenotype likely reflects co-aggregation with wild

type Rnq1p in the [*RNQ*$^+$] state and the induction of [*PSI*$^+$] likely reflects some transient physical interaction with Sup35p (40,56), we suggest that very high [*PIN*$^+$]/ weak [*RNQ*$^+$] forms a structure that affords less efficient self-templating but more efficient interaction with Sup35p than other variants. While the medium and strong [*RNQ*$^+$] variants correspond to medium and high [*PIN*$^+$], we note one important caveat in the interpretation of the differences in the ability to induce [*PSI*$^+$]. The reduced [*PSI*$^+$] induction we observed with medium [*RNQ*$^+$] is probably due in part to the decreased mitotic stability of medium [*RNQ*$^+$] when compared to high [*RNQ*$^+$]. This is not likely to explain the differences entirely, however, as different structures of Rnq1p in [*RNQ*$^+$] are likely to interact differently with Sup35p to induce [*PSI*$^+$].

Here, we have defined conditions for the aggregation of Rnq1PFD in vitro that result in the induction and propagation of specific [*RNQ*$^+$] variants in vivo. These data are consistent with a direct relationship between the biochemical properties of amyloid fibers and prion variants. The information gleaned from the generation of [*RNQ*$^+$] prion variants suggests that there may be some general properties dictating prion strain propagation, while others are unique to individual prion proteins. Using the [*RNQ*$^+$] variants and the ability to investigate their in vitro properties, we may be able to delineate the mechanisms involved in the self-seeding of Rnq1p to maintain variants of [*RNQ*$^+$] from those involved in cross-seeding Sup35p to induce [*PSI*$^+$]. Hence, this provides a tractable system to investigate mechanisms that impact protein aggregation and the onset of protein conformational disorders.

EXPERIMENTAL PROCEDURES

Protein purification- The $pHis_{10}$-Rnq1PD (amino acids 132-405) construct (39) was transformed into *Escherichia coli* BL21(DE3) cells. Resultant transformants were scraped to inoculate large cultures in CircleGrow media and the cells were grown to an OD_{600}~0.6. The expression of Rnq1PFD was induced with 1 mM IPTG for 6 hrs. The cells were harvested and incubated with agitation at room temperature for one hour in 20 mM Tris-HCl, 8 M Urea (Buffer A, pH 8). The cells were then further lysed by sonication. The lysate was cleared by spinning at 10,000 x *g* for 30 minutes. The supernatant was incubated with Ni^{2+}-Sepharose beads for two hours. Subsequently, the beads were packed in a column and washed with 25 column volumes (CV) Buffer A, pH 8. The beads were then washed successively with four CV each of Buffer A, pH 6.3 and Buffer A, pH 5.9, before eluting with Buffer A, pH 4.5. Rnq1p in the eluted fractions was verified for purity by SDS-PAGE and coomassie staining. The fractions containing the protein were filtered through a 100kD molecular weight cut off column (Amicon) and stored in methanol at -80°C.

Amyloid fiber formation- Kinetic assays of fiber formation were done in a SpectraMax M2e flourimeter microplate reader. Rnq1PFD fibers were diluted 75-fold from 7 M guanidine hydrochloride to a concentration of 4 μM in FFB buffer (150 mM NaCl, 5 mM KPO_4, 2 M Urea, pH 7.4) with 50-fold molar excess Thioflavin-T to initiate fiber formation in the presence of glass beads for agitation. The change in Thioflavin-T fluorescence over time was measured using an excitation wavelength of 450 nm and emission wavelength of 481 nm. The plate was agitated each minute prior to reading for ten seconds. Fibers were also formed in a rotator (end-over-end) at a monomer

concentration of 4 μM for thermostability assays and to obtain seeds for seeding experiments. For the seeded experiments, the fibers were seeded using 5% (w/w) seed.

Thermostability assay- Pre-formed fibers were treated with 2% SDS for five minutes at different temperatures (gradient from 55°C to 95°C, with 5-7°C increments). The treated samples were analyzed by SDS-PAGE and western blot using an anti-Rnq1p antibody. The bands were quantified using ImageJ software and values were normalized to the 95°C band. Results were plotted using Origin 6.1 statistical software.

Electron microscopy- Samples of fibrillar Rnq1PFD were allowed to settle onto freshly glow-discharged 200 mesh carbon-formvar coated copper grids for 10 minutes. Grids were then rinsed twice with water and stained with 1% uranyl acetate (Ted Pella) for one minute. Samples were viewed on a JEOL 1200EX transmission electron microscope (JEOL USA). *Protein transformation*- Transformation of Rnq1PFD fibers into a [*rnq*$^-$] 74-D694 (*ade1-14, ura3-52, leu2-3,112, trp1-289, his3-200*, *sup35::RRP*) yeast strain was conducted as described (44). The resulting colonies were replica plated onto rich media (YPD) plates to assay for colony color. Colonies that appeared to have acquired the prion state by nonsense suppression were picked and spotted on YPD, YPD containing 3 mM GdnHCl and SD-ade for phenotypic analyses.

Mitotic Stability of [*RNQ*$^+$]- Three independent protein transformants for each of the [*RNQ*$^+$] prion variants were grown in liquid YPD media overnight (~16 hours) to an OD_{600} of ~2.0. The cultures were diluted 8,000-fold in water and 250 μl were plated on 13 cm (diameter) YPD plates. Approximately 750 colonies for each transformant and a total of > 2,000 colonies were counted for each variant. The average and standard deviation is reported for each variant. The percentage of cells that lost the prion was

calculated by dividing the number of red cells by the total number of cells. The loss of the [*RNQ*$^+$] prion was confirmed by Rnq1p solubility assays for 10 representative colonies of each variant.

[*PSI*$^+$] *induction assay*- Yeast strains containing the [*RNQ*$^+$] prion were transformed with pEMBL-SUP2 (41) and plated on SD-ura. Transformants were grown in selective media to an OD_{600} of ~1.6 and plated on YPD. After 5 days of growth, [*PSI*$^+$] cells were counted as any cell with a light pink sector. Representative colonies were checked for curing by transient growth on media containing 3 mM GdnHCl.

[*RNQ*$^+$] *solubility assay*- The protocol was adapted from previously published work (34). The yeast cells were lysed in buffer containing 100 mM Tris-HCl, pH 7, 200 mM NaCl, 1 mM ethylendiaminetetraacetic acid (EDTA), 5% glycerol, 0.5% dithiothreitol (DTT), 50 mM N-ethyl malemide (NEM), 3 mM phenylmethanesulphonylfluoride, and EDTA-free complete Mini protease inhibitor cocktail (Roche). Lysis was performed by vortexing with glass beads. Following lysis, an equal volume of RIPA buffer (50 mM Tris-HCl, pH 7, 200 mM NaCl, 1% Triton X-100, 0.5% sodium deoxycholate, and 0.1% SDS) was added to the lysate and cell debris was cleared by centrifugation at 3,300 x *g* for 15 seconds. A portion of this cleared lysate was saved for the total protein sample. Aggregated protein was pelleted by centrifugation at 80,000 rpm in a Beckman TLA-100 rotor for 30 min. The supernatant containing the soluble protein was removed and the pellet was resuspended in a 1:1 mix of lysis buffer and RIPA buffer. The total, supernatant, and pellet fractions were subjected to SDS-PAGE, transferred to PVDF membrane, and probed with an anti-Rnq1p antibody.

FOOTNOTES

We thank Dr. J. Patrick Bardill for creating the RRP strain and plasmids used in this study. We thank Susan Liebman (University of Illinois, Chicago) for the $pHis_{10}$-Rnq1PD plasmid. We thank Wandy Beatty (EM core facility, Molecular Microbiology department, Washington University School of Medicine) for help with the TEM images and Dr. John Cooper for allowing us to use equipment and providing helpful advice. We thank members of the True Lab for helpful discussions and critical comments on the manuscript. This work was supported by NIH grant GM072228 (H.L.T) and the National Science Foundation.

The abbreviations used are: RRP, [RNQ^{+}] reporter protein; GdnHCl, guanidine hydrochloride; PFD, prion-forming domain; Th-T, Thioflavin-T; RFU, relative fluorescence units.

REFERENCES

1. Prusiner, S. B. (1998) *Proc Natl Acad Sci U S A* **95**, 13363-13383

2. Chesebro, B. (2003) *Br Med Bull* **66**, 1-20

3. Wadsworth, J. D., Hill, A. F., Beck, J. A., and Collinge, J. (2003) *Br Med Bull* **66**, 241-254

4. Prusiner, S. B. (1982) *Science* **216**, 136-144

5. Croes, E. A., Theuns, J., Houwing-Duistermaat, J. J., Dermaut, B., Sleegers, K., Roks, G., Van den Broeck, M., van Harten, B., van Swieten, J. C., Cruts, M., Van Broeckhoven, C., and van Duijn, C. M. (2004) *J Neurol Neurosurg Psychiatry* **75**, 1166-1170

6. King, A., Doey, L., Rossor, M., Mead, S., Collinge, J., and Lantos, P. (2003) *Neuropathol Appl Neurobiol* **29**, 98-105

7. Kovacs, G. G., Trabattoni, G., Hainfellner, J. A., Ironside, J. W., Knight, R. S., and Budka, H. (2002) *J Neurol* **249**, 1567-1582

8. Collinge, J. (2001) *Annu Rev Neurosci* **24**, 519-550

9. Du, Z., Park, K. W., Yu, H., Fan, Q., and Li, L. (2008) *Nat Genet* **40**, 460-465

10. Patel, B. K., Gavin-Smyth, J., and Liebman, S. W. (2009) *Nat Cell Biol* **11**, 344-349

11. Alberti, S., Halfmann, R., King, O., Kapila, A., and Lindquist, S. (2009) *Cell* **137**, 146-158

12. Nemecek, J., Nakayashiki, T., and Wickner, R. B. (2009) *Proc Natl Acad Sci U S A* **106**, 1892-1896

13. Brown, J. C., and Lindquist, S. (2009) *Genes Dev* **23**, 2320-2332

14. Uptain, S. M., and Lindquist, S. (2002) *Annu Rev Microbiol* **56**, 703-741

15. Wickner, R. B., Masison, D. C., and Edskes, H. K. (1995) *Yeast* **11**, 1671-1685

16. Wickner, R. B. (1994) *Science* **264**, 566-569

17. Paushkin, S. V., Kushnirov, V. V., Smirnov, V. N., and Ter-Avanesyan, M. D. (1996) *Embo J* **15**, 3127-3134

18. Patino, M. M., Liu, J. J., Glover, J. R., and Lindquist, S. (1996) *Science* **273**, 622-626

19. Zhouravleva, G., Frolova, L., Le Goff, X., Le Guellec, R., Inge-Vechtomov, S., Kisselev, L., and Philippe, M. (1995) *Embo J* **14**, 4065-4072

20. Stansfield, I., Jones, K. M., Kushnirov, V. V., Dagkesamanskaya, A. R., Poznyakovski, A. I., Paushkin, S. V., Nierras, C. R., Cox, B. S., Ter-Avanesyan, M. D., and Tuite, M. F. (1995) *Embo J* **14**, 4365-4373

21. Serio, T. R., and Lindquist, S. L. (1999) *Annu Rev Cell Dev Biol* **15**, 661-703

22. Kochneva-Pervukhova, N. V., Chechenova, M. B., Valouev, I. A., Kushnirov, V. V., Smirnov, V. N., and Ter-Avanesyan, M. D. (2001) *Yeast* **18**, 489-497

23. Uptain, S. M., Sawicki, G. J., Caughey, B., and Lindquist, S. (2001) *Embo J* **20**, 6236-6245

24. Derkatch, I. L., Chernoff, Y. O., Kushnirov, V. V., Inge-Vechtomov, S. G., and Liebman, S. W. (1996) *Genetics* **144**, 1375-1386

25. Krishnan, R., and Lindquist, S. L. (2005) *Nature* **435**, 765-772

26. Toyama, B. H., Kelly, M. J., Gross, J. D., and Weissman, J. S. (2007) *Nature* **449**, 233-237

27. Tessier, P. M., and Lindquist, S. (2007) *Nature* **447**, 556-561

28. Tanaka, M., Chien, P., Yonekura, K., and Weissman, J. S. (2005) *Cell* **121**, 49-62

29. Tanaka, M., Collins, S. R., Toyama, B. H., and Weissman, J. S. (2006) *Nature* **442**, 585-589

30. Collins, S. R., Douglass, A., Vale, R. D., and Weissman, J. S. (2004) *PLoS Biol* **2**, e321

31. Scheibel, T., Kowal, A. S., Bloom, J. D., and Lindquist, S. L. (2001) *Curr Biol* **11**, 366-369

32. Schlumpberger, M., Prusiner, S. B., and Herskowitz, I. (2001) *Mol Cell Biol* **21**, 7035-7046

33. Edskes, H. K., McCann, L. M., Hebert, A. M., and Wickner, R. B. (2009) *Genetics* **181**, 1159-1167

34. Sondheimer, N., and Lindquist, S. (2000) *Mol Cell* **5**, 163-172

35. Derkatch, I. L., Bradley, M. E., Hong, J. Y., and Liebman, S. W. (2001) *Cell* **106**, 171-182

36. Osherovich, L. Z., and Weissman, J. S. (2001) *Cell* **106**, 183-194

37. Derkatch, I. L., Bradley, M. E., Zhou, P., Chernoff, Y. O., and Liebman, S. W. (1997) *Genetics* **147**, 507-519

38. Bradley, M. E., Edskes, H. K., Hong, J. Y., Wickner, R. B., and Liebman, S. W. (2002) *Proc Natl Acad Sci U S A* **99 Suppl 4**, 16392-16399

39. Patel, B. K., and Liebman, S. W. (2007) *J Mol Biol* **365**, 773-782

40. Bardill, J. P., and True, H. L. (2009) *J Mol Biol* **388**, 583-596

41. Ter-Avanesyan, M. D., Kushnirov, V. V., Dagkesamanskaya, A. R., Didichenko, S. A., Chernoff, Y. O., Inge-Vechtomov, S. G., and Smirnov, V. N. (1993) *Mol Microbiol* **7**, 683-692

42. Vitrenko, Y. A., Pavon, M. E., Stone, S. I., and Liebman, S. W. (2007) *Curr Genet* **51**, 309-319

43. Bardill, J. P., Dulle, J. E., Fisher, J. R., and True, H. L. (2009) *Prion* **3**, 151-160

44. Harper, J. D., and Lansbury, P. T., Jr. (1997) *Annu Rev Biochem* **66**, 385-407

45. Perrett, S., and Jones, G. W. (2008) *Curr Opin Struct Biol* **18**, 52-59

46. Ohhashi, Y., Ito, K., Toyama, B. H., Weissman, J. S., and Tanaka, M. *Nat Chem Biol*

47. Tanaka, M., Chien, P., Naber, N., Cooke, R., and Weissman, J. S. (2004) *Nature* **428**, 323-328

48. Bradley, M. E., and Liebman, S. W. (2003) *Genetics* **165**, 1675-1685

49. Derkatch, I. L., Bradley, M. E., Masse, S. V., Zadorsky, S. P., Polozkov, G. V., Inge-Vechtomov, S. G., and Liebman, S. W. (2000) *Embo J* **19**, 1942-1952

50. Chien, P., DePace, A. H., Collins, S. R., and Weissman, J. S. (2003) *Nature* **424**, 948-951

51. Ferreira, P. C., Ness, F., Edwards, S. R., Cox, B. S., and Tuite, M. F. (2001) *Mol Microbiol* **40**, 1357-1369

52. Tuite, M. F., and Cox, B. S. (2003) *Nat Rev Mol Cell Biol* **4**, 878-890

53. Resende, C. G., Outeiro, T. F., Sands, L., Lindquist, S., and Tuite, M. F. (2003) *Mol Microbiol* **49**, 1005-1017

54. Nakayashiki, T., Kurtzman, C. P., Edskes, H. K., and Wickner, R. B. (2005) *Proc Natl Acad Sci U S A* **102**, 10575-10580

55. Serio, T. R., Cashikar, A. G., Kowal, A. S., Sawicki, G. J., Moslehi, J. J., Serpell, L., Arnsdorf, M. F., and Lindquist, S. L. (2000) *Science* **289**, 1317-1321

56. Vitrenko, Y. A., Gracheva, E. O., Richmond, J. E., and Liebman, S. W. (2007) *J Biol Chem* **282**, 1779-1787

Chapter 4: Infectious and non-infectious amyloid fibers formed by a mutation in the PFD of Rnq1p

Tejas Kalastavadi and Heather L. True

This work is a manuscript in preparation for publication.

SUMMARY

Prion diseases are unique neurodegenerative disorders that are transmitted by a misfolded and aggregated form of and endogenously expressed protein. Many lines of evidence suggest that the misfolded and aggregated forms of prion protein (PrP) form the infectious particles. Amyloid fibers formed by PrP share many of their biochemical and structural properties with fibers formed by other proteins that cause protein conformational disorders. However, the other proteins such as α-synuclein and amyloid-β, although capable of causing disease, do not appear to be infectious. The properties that confer infectivity to protein aggregates such that they act as "prions" are unclear, and this represents a major question. Yeast also harbor prions. One is termed [*RNQ*+], formed by aggregation of Rnq1p. In this study, we have used a deletion mutant in the prion-forming domain (PFD), of Rnq1p (Rnq1PFD, amino acids 133-405) termed Rnq1PFDΔHot (deletion of amino acids 284-317) to dissect biochemical and structural properties of infectious versus non-infectious amyloid. Rnq1PFDΔHot forms amyloid fibers at both 25°C and 37°C, as assayed by Thioflavin-T (Th-T) binding and transmission electron microscopy (TEM). These fibers also resist thermal denaturation. However, when the fibers are transformed into yeast cells, those formed at 37°C are infectious, whereas fibers formed at 25°C are not. We suggest that a conformational change caused by the assembly of the fibers formed at the two distinct temperatures is responsible for the change in the ability of the protein aggregates to be infectious. Biophysical experiments are currently underway to identify these structural differences between the infectious and non-infectious Rnq1PFDΔHot fibers.

Protein misfolding and aggregation has been associated with several diseases that affect many mammals including humans (1). Neurodegenerative diseases form a major subset of these protein conformational disorders (2). Most often, these diseases occur sporadically, but they can also be caused by mutations in the gene(s) associated with the disease (1). A common feature of neurodegenerative diseases such as Alzheimer's, Parkinson's and Huntington's is the deposition of amyloid fibers in the brain (3). Prion diseases are a unique class of neurodegenerative diseases in that they are also transmissible or infectious (4). The misfolded and aggregated material found in extracellular deposits in individuals affected with prion disease primarily consist of PrP aggregates (5). These aggregates are thought to be the agents of infection. It is not entirely clear if all protein aggregates are infectious or if there are certain special characteristics that allow PrP aggregates to become infectious.

Interestingly, many of the proteins or peptides implicated in neurodegenerative diseases such as amyloid-β (in Alzheimer's), α-synuclein (in Parkinson's), repeat expanded huntingtin exon-1 (in Huntington's), and PrP (Prion diseases) share many biochemical properties. They can all form amyloid fibers in vitro. Furthermore, they all seem to follow a similar kinetic pattern when converting from a denatured monomer to amyloid fiber with an initial lag phase, followed by an exponential growth phase and a final plateau phase (6,7). Additionally, "seeds" obtained from previously formed fibers, greatly enhance the conversion of protein monomers into fibers and either reduce or completely eliminate the lag phase, suggesting a nucleated conformational conversion model for polymerization (6,7). The ability of "seeds" to template polymerization in

vitro suggests that introduction of the misfolded conformation in organisms via transmission or infection may provide a means for onset and propagation of disease.

However, the only known cases of human epidemics involving amyloidogenic proteins are with PrP aggregates. Ritualistic cannibalism in the Fore tribe of Papua New Guinea and the cross-species transmission of bovine spongiform encephalopathy (BSE) into humans to cause variant Cruetzfeld-Jacob disease (vCJD) are two well-documented cases of transmission of disease by protein aggregates (8,9). There is new evidence however in model systems that suggests that other protein conformational disorders may also have the capacity to infect and propagate in a manner similar to prion diseases.

The most compelling case for infectivity of another disease that has prion-like features can be made for AA amyloidosis (10). However, in the disease model, the recipient mouse needs to be primed, for example by injecting silver nitrate, for elevated levels of serum Amyloid A in order for disease to be acquired by introduction of aggregated Amyloid A into the mouse (10). Additionally, there is evidence to suggest that transgenic mice used as an Alzheimer's disease model also accumulate plaques at an earlier time if injected with brain homogenate from mice with amyloid-β plaques (11). Furthermore, experiments in cell culture show that protein aggregates introduced into the culture media, can be taken up by the cell, thus providing a potential means for propagation of disease (12,13).

It is, important to note however, that there are many issues that need to be considered before a disease can truly be considered to transmit via a prion-like mechanism. These issues include temporal and topological pattern of expression of the protein and localization of the protein in a cell. We suggest that, in addition to the

specific requirements mentioned above, there are structural and biochemical features that permit a protein to become infectious. Important factors to consider when determining the ability of a protein to be infectious include 1) the ability of a misfolded protein to faithfully template the conversion of monomer into a specific conformation and then aggregate and 2) the ability of the protein aggregates to disaggregate to further template conversion.

In this study, we have made use of a mutant form of the yeast prion protein Rnq1p that can form amyloid fibers that are both infectious and non-infectious. The Rnq1 protein has no known function in its soluble state, but when it aggregates to form the [*RNQ*+] prion, it enhances the induction another yeast prion, called [*PSI*+] (14,15). The PFD of Rnq1p extends from amino acids 153-405. The mutant form of Rnq1PFD we used contains a deletion of the amino acids 284-317 (Rnq1PFDΔHot) (16-19).

This deletion mutant was previously generated in our lab while determining regions of Rnq1p that were important for the maintenance of the [*RNQ*+] prion (16). In this study (16), a PCR mutagenesis of the PFD of RNQ1 was conducted to identify mutants that failed to propagate the [*RNQ*+] prion. A significantly larger number of mutants that were identified fell between amino acids 284-317. Therefore, this region, identified as a hotspot for mutants in RNQ1 PFD that failed to propagate the [*RNQ*+] prion was deleted (Rnq1ΔHot) to further investigate its role in prion propagation. The Rnq1ΔHot mutant was able to propagate low and medium variants of [*RNQ*+]. It was however unable to propagate the high [*RNQ*+] variant.

We show that Rnq1PFDΔHot can form amyloid fibers in vitro with typical kinetics as observed by Th-T assay at both 25°C and 37°C. Seeds obtained from fibers

formed at either temperature were able to substantially enhance the polymerization of monomeric protein. We were able to identify subtle differences in morphology, in the fibers at the two temperatures by TEM. Fibers formed at both temperatures were resistant to thermal denaturation. However, when the fibers were transformed into [*rnq*-] yeast cells, only fibers formed at 37°C were able to induce the [*RNQ*+] prion state. Fibers formed at 25°C were unable to infect the cells and induce the prion state. We suggest that the Rnq1pPFDΔHot fibers formed at 25°C have acquired a conformation that is unable to infect yeast and propagate the [*RNQ*+] prion. In contrast, 37°C fibers have a conformation that is infectious. We propose that this model could be used to obtain structural signatures that may represent the ability of a protein aggregate to be infectious or benign.

RESULTS

Temperature has a profound impact on the kinetics of Rnq1PFDΔHot fiber formation- We purified recombinant Rnq1PFDΔHot in 8 M Urea as described in experimental procedures. The purified Rnq1PFDΔHot protein formed amyloid fibers when diluted out of denaturant. The length of the lag phase of fiber formation is a parameter that can be used to measure the ability of the protein to aggregate and is a difference commonly found between amyloid fibers of different morphologies; a longer lag phase indicates a reduced ability to aggregate. We used different temperatures to generate structural variation in the fibers of Rnq1PFDΔHot. We followed fiber formation of Rnq1PFDΔHot at 25°C and 37°C using a Thioflavin-T fluorescence assay. At 25°C, Rnq1PFDΔHot fibers had a lag phase of ~450 minutes followed by a logarithmic growth

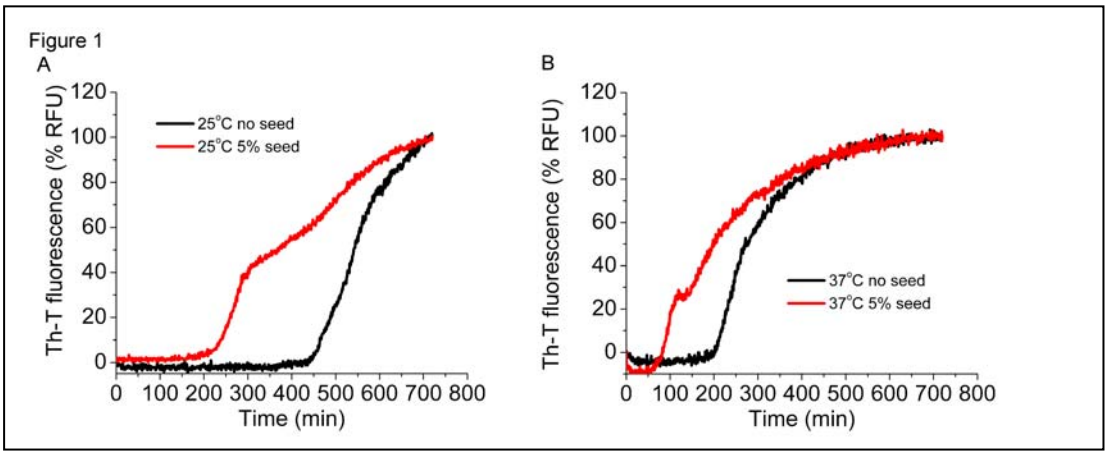

FIGURE 1. **Fiber formation of Rnq1PFDΔHot is faster at higher temperatures and enhanced by the addition of pre-formed seeds.** Purified Rnq1PFDΔHot was diluted from denaturant (75-fold) to 4 μM and fiber formation was followed using Th-T fluorescence. Graphs are plotted as %RFU (relative fluorescence units) versus time. (A) Rnq1PFDΔHot unseeded at 25°C (black) and seeded with 5% seeds (red). (B) Rnq1PFDΔHot fiber formation at 37°C unseeded (black), and with 5% seeds (red).

phase (Fig. 1A). In contrast, fiber formation of Rnq1PFDΔHot at 37°C had a shorter lag phase of ~200 minutes (Fig. 1B).

The ability of seeds to enhance the conversion of monomeric protein into fibers is an important feature of nucleated conformational conversion for amyloid fiber formation (7,20). We formed Rnq1PFDΔHot fibers at 25°C and 37°C and tested the ability of the fibers to act as seeds and template the addition of freshly diluted monomeric Rnq1PFDΔHot. The seeds obtained from fibers formed at 25°C, as well as those formed at 37°C, were capable of templating new fiber formation at 25°C and 37°C, respectively (Fig. 1A and 1B).

Rnq1PFDΔHot fibers formed at 37°C infect yeast cells to induce the [*RNQ+*] *prion but those formed at 25°C are not infectious*- The prion hypothesis suggests that when purified recombinant prion protein is made to aggregate in vitro and introduced into an organism the aggregates should infect the organism and propagate. Only very recently infectious material from a recombinant source for PrP has been shown to fulfill this hypothesis (21). However, significant advancement to provide this ultimate proof for the "prion hypothesis" hypothesis was facilitated by the study of fungal prions. HET-s a prion protein of the fungus *Podospora anserina*, Sup35p, Ure2p and Rnq1p, both prions of the yeast *S. cerevisiae* have been shown to produce infectious prion particles when purified recombinant protein is assembled in vitro to form amyloid fibers (17,22-24).

Here we used a yeast strain that expressed the [*RNQ+*] reporter protein (RRP) to assay infectivity of amyloid fibers formed by Rnq1PFDΔHot (16,18). The RRP is a fusion of amino acids 133-405 from Rnq1p to the N-terminus of the middle and C-terminal domain Sup35p (amino acids 124-685). Sup35p is the eukaryotic release factor

Table 2.

		Distribution of strains (%)		
		Weak	Medium	Strong
Rnq1 PFD ΔHot	25 ° C	0	0	0
	37 ° C	15	84	0

Table 1. **Ability of Rnq1PFDΔHot to infect yeast**. Yeast colonies that resulted from infection of Rnq1PFDΔHot fibers formed at 25°C, and 37°C were grouped into weak, medium, and strong [*RNQ*$^+$] strains based on RRP-mediated colony color (on YPD) and growth on medium lacking adenine (SD-ade). The numbers in the table reflect the percentage of variants obtained by infectivity assays after counting over 3,000 transformed colonies for infection of fibers formed at 25°C and 300 colonies for 37°C fibers from more than three experiments for 37°C and 10 experiments for 25°C fibers.

3 and is important for translation termination at stop codons. The RRP fusion protein reports on the prion status of Rnq1p. The RRP presumably co-aggregates with Rnq1p in the [*RNQ*+] state and allows for readthrough of premature stop codons in the aggregated state. The allele *ade1-14*, contains a premature stop codon. Increased read through of stop codons (as would be the case in [*RNQ*+] cells) turns cells white and faithful termination turns cells red in color. Therefore, we were able to use a red/white colony color assay to determine the prion status of Rnq1p in cells.

We transformed yeast cells with amyloid fibers formed in potassium phosphate buffer, pH 7.4, 150 mM sodium chloride and 2 M urea, with end-over-end agitation, with Rnq1PFDΔHot at 25°C and 37°C and assayed for the induction of [*RNQ*+]. We have identified Rnq1PFDΔHot as a protein that is presumably capable of infecting in one conformation and not another. As shown in Table 1, fibers of Rnq1PFDΔHot formed at 37°C infect cells and induce weak and medium variants of the [*RNQ*+] prion, but when fibers are formed at 25°C, they cannot infect yeast cells to induce [*RNQ*+].

Rnq1PFDΔHot fibers formed at different temperatures are differentially stable- The stability of the amyloid fibers has proven to be predictive of prion variants they induce when transformed into yeast. More stable amyloid fibers have a longer core and propagate weaker prion variants while less stable fibers with a shorter core propagate stronger prion variants (25-27).

We next asked if the stability of the infectious amyloid fibers of Rnq1PFDΔHot differed from those that were not able to induce the [*RNQ*+] prion. We used thermostability to determine the relative stability of Rnq1PFDΔHot fibers formed at different temperatures. We formed fibers at 18°C, 25°C, and 37°C and subjected them to

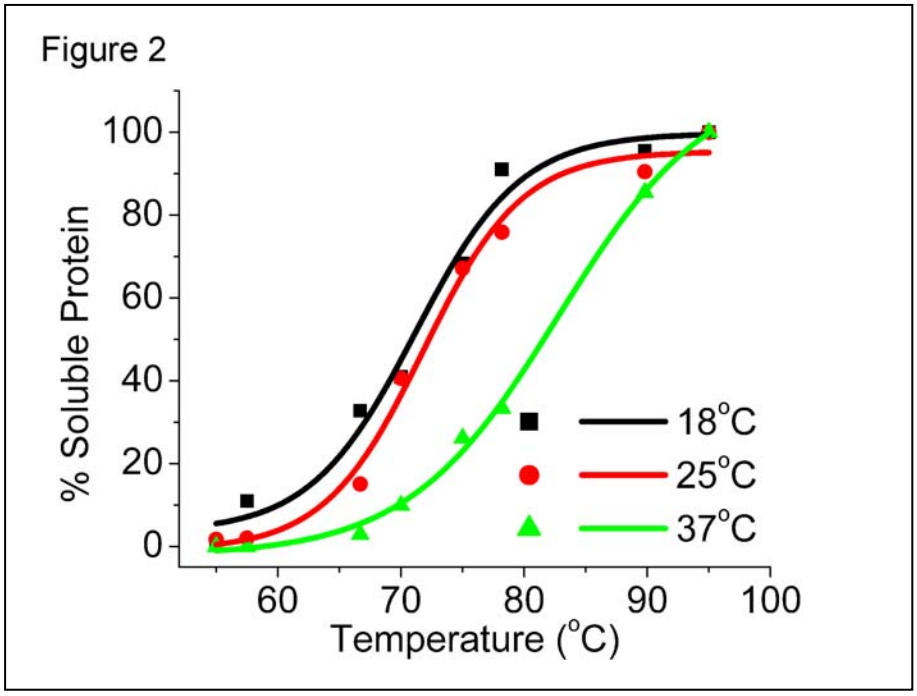

FIGURE 2. **Rnq1PFDΔHot fibers formed at higher temperatures are more stable.** Preformed fibers were treated across a temperature gradient in the presence of 2% SDS. Following SDS-PAGE and western blot, the amount of soluble Rnq1PFDΔHot was quantified and the results were graphed as a percentage of total protein at 95°C using OriginPro 6.1 with a sigmoidal fit function.

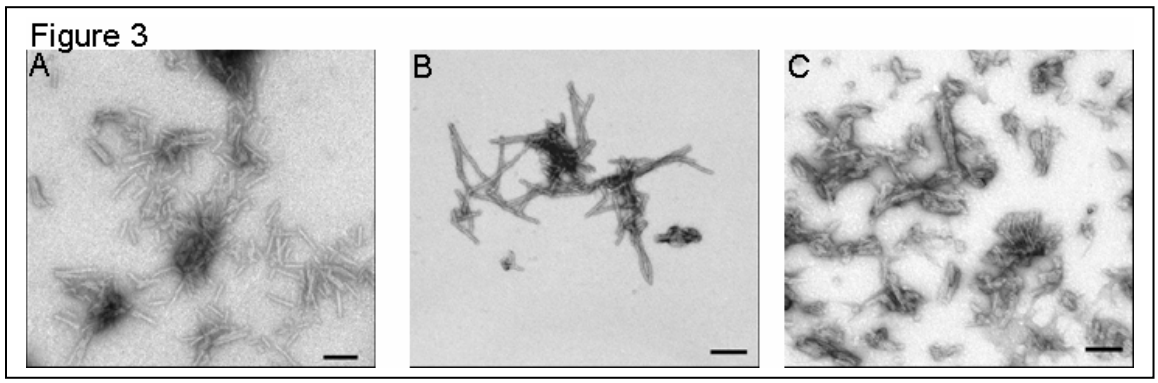

FIGURE 3. **The morphology of amyloid fibers formed from Rnq1PFDΔHot at different temperatures shows subtle changes.** Amyloid fibers of Rnq1PFDΔHot formed in vitro were imaged by TEM. The scale bar represents 200 nm. (A) 18°C fibers are short and thin (B) 25°C fibers are short and thin, and (C) 37°C fibers are lwider.

increasing temperatures in 2% SDS. We then analyzed the soluble protein by SDS-PAGE and western blot. We found that fibers formed at 18°C and 25°C were more labile and showed ~50% disruption at 71°C (Fig. 2). Fibers formed at 37°C were significantly more stable and showed ~50% dissociation at 81°C. Thus, the stronger amyloid fibers formed at 37°C yield amyloid fibers that were able to infect yeast and the benign fibers that were formed at 25°C were weaker.

Transmission electron microscopy (TEM) reveals subtle morphological differences in Rnq1PFDΔHot fibers- The observed differences in kinetics and stability of amyloid fibers of Rnq1PFDΔHot formed at different temperatures and their ability to infect yeast cells to induce the [*RNQ*+] prion led us to hypothesize that the morphology of the Rnq1PFDΔHot fibers formed at these temperatures may be distinct. In order to determine if there were any morphological differences between the Rnq1PFDΔHot fibers formed at 18°C, 25°C, and 37°C we obtained TEM images of these amyloid fibers. In fact, we did observe subtle differences in the morphology of the fibers formed at the different temperatures. Rnq1PFDΔHot fibers formed at 18°C, 25°C and 37°C are all short (Figure 3). There appeared to be subtle changes in the width of the amyloid fibers formed at each of these temperatures however. Fibers formed at 37°C appeared slightly thicker than those formed at 18°C and 25°C. .

DISCUSSION

The hypothesis that an infectious agent may contain only protein and no nucleic acid was received with much skepticism initially (4). However, since then, there has been considerable evidence in mammalian systems (4,21) and compelling evidence in fungal prion systems to suggest that protein infectious particles or "prions" to prove this

hypothesis true (27). However, considering that there are other proteins that are implicated in disease such as the amyloid-β peptide, α-synuclein and Huntington exon 1 share many biochemical and structural characteristics that are similar to PrP and prion disease, it has been proposed that these proteins too, given the opportunity, may be infectious (12,28). There is some evidence to suggest that many of the protein misfolding and aggregation diseases may have prion-like properties. However, to date, only prion disease caused by PrP protein aggregates has been shown to be capable of being truly infectious.

Here, we have identified a unique protein fragment, Rnq1PFDΔHot that can form amyloid fibers that capable of forming both infectious amyloids and those that are not. We were able to modify the infectivity of the Rnq1PFDΔHot fibers by changing the temperature of assembly. Rnq1PFDΔHot fibers formed faster at 37°C as compared to 25°C. Furthermore, fibers formed at both temperatures were able to act as seeds and enhance polymerization of monomeric Rnq1PFDΔHot protein. Surprisingly, however, when Rnq1PFDΔHot fibers formed at 25°C were transformed into yeast cells, they did not infect cells. The fibers formed at 37°C, in contrast, were capable of infecting cells. The 37°C Rnq1PFDΔHot fibers induced medium and weak variants of the [*RNQ*+] prion. Interestingly, Rnq1ΔHot protein (Full length Rnq1p with amino acids 284-317 deleted) does not maintain high [*RNQ*+] in vivo either. Therefore the fibers formed in vitro presumably acquire conformations that appear to be pertinent to the in vivo aggregate structure. We characterized the thermal stability of the amyloid fibers formed at different temperatures and found that 37°C fibers were more stable than those formed at either 25°C or 18°C . Finally, in sharp contrast to the differences in the ability of the fibers to

infect yeast cells, we found that the fibers had similar morphologies, as visualized by TEM.

We suggest that changes in the intra- and inter-molecular contacts made during fiber assembly cause significant differences that result in their differential ability to infect yeast cells. These changes in contacts may not result in supra-molecular changes to the morphology of the fibers, but may change other biochemical properties and finer structural properties. We propose to use the Rnq1PFDΔHot model polypeptide to identify structural features that correlate infectious versus non-infectious protein aggregates.

One possible explanation for the ability of a specific protein to form infectious or non-infectious aggregates, is based on the ability to propagate as different "prion strains". For a protein to be infectious, not only does it need to be capable of efficiently aggregating, but it also needs to be able to faithfully convert soluble species or other monomers to an aggregated state. Furthermore, once the aggregates are formed, they need to be sheared in order to increase the number of sites for the templating reaction to occur efficiently. The ability to shear an aggregate and increase the number of sites for propagation of the amyloid conformation is presumably as crucial as the initial structural conversion. Therefore, we suggest that protein aggregates that not transmissible are conformations that form very unstable variants.

The unstable variant conformations of yeast prions are inefficient at transmitting "seeds" from mother cell to daughter cells (29). Rnq1PFDΔHot fibers formed at 25°C may be in a conformation that is unstable in vivo because the templating is inefficient. Additionally, the 25°C Rnq1PFDΔHot fibers are also fairly stable and this may prevent

the shearing of aggregated protein in vivo and decrease the number of templating sites and transmissible seeds. In combination, this may create a situation in vivo that results in unstable propagation of the prion state, resulting in rapid loss of the prion state altogether. On the other hand, the conformation of the fibers formed at 37°C produce weaker variants that are more stable in vivo because the fibers are more efficient at aggregating as compared to 25°C fibers. Although this conformation is more stable, the efficiency of aggregation may compensate for the potential reduction in shearing of the aggregated protein.

Other models to explain the lack of infectivity by Rnq1PFDΔHot fibers formed at 25°C include the possibility that this conformation is in fact an extremely strong variant of [*RNQ*+]. The high rate of aggregation in the strong variant may render the chaperone machinery inefficient to disaggregate the protein. It is also possible that the specific conformation adapted at 25°C is either not recognized at all by the chaperone machinery, hence, preventing the generation of seeds. Alternatively the chaperones may be very efficient at clearing the aggregates formed at 25°C and prevent aggregation altogether.

We suggest that the difference in the ability of the amyloid fibers formed at 37°C to infect and 25°C to not infect cells is due to conformational changes in the monomer when it forms the amyloid fibers at the two different temperatures. We propose future work using biophysical techniques to identify these structural changes. Understanding the specific interactions of amino acids in the two different conformations may provide clues toward understanding properties that make certain protein aggregates infectious and others benign.

Here, we have defined conditions for the aggregation of Rnq1PFDΔHot in vitro that yeild two different conformations of amyloid fibers, one that is infectious and another that is not. The data obtained here is consistent with a hypothesis that proposes direct relationship between the biochemical and structural properties of amyloid fibers and their ability to be infectious. The information gleaned from the infection of yeast cells to induce the prion state suggests that there we may be able to identify some general properties that dictate infectivity of amyloid fibers. Using the different conformations of Rnq1PFDΔHot to investigate their in vitro properties, we may be able to delineate the mechanisms and structural features necessary for infectivity. Thus [*RNQ*+] yeast prion system provides a tractable system to investigate a major, controversial and highly debated question in the field of protein misfolding and aggregation.

EXPERIMENTAL PROCEDURES

Protein purification- The $pHis_{10}$-Rnq1PFDΔHot construct was transformed into *Escherichia coli* BL21 (DE3) cells. The resulting transformants were scraped and used to inoculate large cultures in CircleGrow media. The cells were grown to an OD_{600}~0.6. The expression of Rnq1PFDΔHot was induced with 1 mM IPTG for 6 hrs. The cells were harvested and incubated with agitation at room temperature for one hour in 20 mM Tris-HCl, 8 M Urea (Buffer A, pH 8) and lysed by sonication. The lysate was cleared by spinning at 10,000 x *g* for 30 minutes. The supernatant was incubated with Ni^{2+}-Sepharose beads for two hours. Subsequently, the beads were packed in a column and washed with 25 column volumes (CV) Buffer A, pH 8. The beads were then washed successively with four CV each of Buffer A, pH 6.3 and Buffer A, pH 5.9, before eluting with Buffer A, pH 4.5. Rnq1PFDΔHot in the eluted fractions was verified for purity by

SDS-PAGE and coomassie staining. The fractions containing the protein were filtered through a 100kD molecular weight cut off column (Amicon) and stored in methanol at -80°C.

Amyloid fiber formation- Kinetic assays of fiber formation were done in a SpectraMax M2e fluorimeter microplate reader. Rnq1PFDΔHot fibers were diluted 75-fold from 7 M guanidine hydrochloride to a concentration of 4 μM in FFB buffer (150 mM NaCl, 5 mM KPO_4, 2 M Urea, pH 7.4) with 50-fold molar excess Thioflavin-T to initiate fiber formation in the presence of glass beads for agitation. The change in Thioflavin-T fluorescence over time was measured using an excitation wavelength of 450 nm and emission wavelength of 481 nm. The plate was agitated each minute prior to reading for ten seconds. Fibers were also formed in a rotator (end-over-end) at a monomer concentration of 4 μM for thermostability assays and to obtain seeds for seeding experiments and for protein transformation experiments. For the seeded experiments, the fibers were seeded using 5% (w/w) seed.

Thermostability assay- Pre-formed fibers were treated with 2% SDS for five minutes at different temperatures (gradient from 55°C to 95°C, with 5-7°C increments). The treated samples were analyzed by SDS-PAGE and western blot using an anti-Rnq1p antibody. The bands were quantified using ImageJ software and values were normalized to the 95°C band. Results were plotted using Origin 6.1 statistical software.

Electron microscopy- Samples of fibrillar Rnq1PFDΔHot were allowed to settle onto freshly glow-discharged 200 mesh carbon-formvar coated copper grids for 10 minutes. Grids were then rinsed twice with water and stained with 1% uranyl acetate

(Ted Pella) for one minute. Samples were viewed on a JEOL 1200EX transmission electron microscope (JEOL USA).

Protein transformation- Transformation of Rnq1PFDΔHot fibers into a [*rnq*$^{-}$] 74-D694 (*ade1-14, ura3-52, leu2-3,112, trp1-289, his3-200*, *sup35::RRP*) yeast strain was conducted as described. The resulting colonies were replica plated onto rich media (YPD) plates to assay for colony color. Colonies that appeared to have acquired the prion state by nonsense suppression were picked and spotted on YPD, YPD containing 3 mM GdnHCl and SD-ade for phenotypic analyses.

REFERENCES

1. Chiti, F., and Dobson, C. M. (2006) *Annu Rev Biochem* **75**, 333-366

2. Koo, E. H., Lansbury, P. T., Jr., and Kelly, J. W. (1999) *Proc Natl Acad Sci U S A* **96**, 9989-9990

3. Rostagno, A., Holton, J. L., Lashley, T., Revesz, T., and Ghiso, J. *Cell Mol Life Sci* **67**, 581-600

4. Prusiner, S. B. (1998) *Proc Natl Acad Sci U S A* **95**, 13363-13383

5. Prusiner, S. B. (1991) *Science* **252**, 1515-1522

6. Jarrett, J. T., and Lansbury, P. T., Jr. (1993) *Cell* **73**, 1055-1058

7. Serio, T. R., Cashikar, A. G., Kowal, A. S., Sawicki, G. J., Moslehi, J. J., Serpell, L., Arnsdorf, M. F., and Lindquist, S. L. (2000) *Science* **289**, 1317-1321

8. Gajdusek, D. C. (1977) *Science* **197**, 943-960

9. Collinge, J. (2001) *Annu Rev Neurosci* **24**, 519-550

10. Aguzzi, A., and Calella, A. M. (2009) *Physiol Rev* **89**, 1105-1152

11. Lundmark, K., Westermark, G. T., Nystrom, S., Murphy, C. L., Solomon, A., and Westermark, P. (2002) *Proc Natl Acad Sci U S A* **99**, 6979-6984

12. Frost, B., Jacks, R. L., and Diamond, M. I. (2009) *J Biol Chem* **284**, 12845-12852

13. Ren, P. H., Lauckner, J. E., Kachirskaia, I., Heuser, J. E., Melki, R., and Kopito, R. R. (2009) *Nat Cell Biol* **11**, 219-225

14. Derkatch, I. L., Bradley, M. E., Masse, S. V., Zadorsky, S. P., Polozkov, G. V., Inge-Vechtomov, S. G., and Liebman, S. W. (2000) *EMBO J* **19**, 1942-1952

15. Derkatch, I. L., Bradley, M. E., Zhou, P., Chernoff, Y. O., and Liebman, S. W. (1997) *Genetics* **147**, 507-519

16. Bardill, J. P., and True, H. L. (2009) *J Mol Biol* **388**, 583-596

17. Patel, B. K., and Liebman, S. W. (2007) *J Mol Biol* **365**, 773-782

18. Sondheimer, N., and Lindquist, S. (2000) *Mol Cell* **5**, 163-172

19. Vitrenko, Y. A., Gracheva, E. O., Richmond, J. E., and Liebman, S. W. (2007) *J Biol Chem* **282**, 1779-1787

20. Harper, J. D., and Lansbury, P. T., Jr. (1997) *Annu Rev Biochem* **66**, 385-407

21. Wang, F., Wang, X., Yuan, C. G., and Ma, J. *Science* **327**, 1132-1135

22. Sparrer, H. E., Santoso, A., Szoka, F. C., Jr., and Weissman, J. S. (2000) *Science* **289**, 595-599

23. Maddelein, M. L., Dos Reis, S., Duvezin-Caubet, S., Coulary-Salin, B., and Saupe, S. J. (2002) *Proc Natl Acad Sci U S A* **99**, 7402-7407

24. Brachmann, A., Baxa, U., and Wickner, R. B. (2005) *EMBO J* **24**, 3082-3092

25. Krishnan, R., and Lindquist, S. L. (2005) *Nature* **435**, 765-772

26. Tanaka, M., Chien, P., Naber, N., Cooke, R., and Weissman, J. S. (2004) *Nature* **428**, 323-328

27. Tessier, P. M., and Lindquist, S. (2009) *Nat Struct Mol Biol* **16**, 598-605

28. Baxa, U. (2008) *Curr Alzheimer Res* **5**, 308-318

29. Tanaka, M., Collins, S. R., Toyama, B. H., and Weissman, J. S. (2006) *Nature* **442**, 585-589

Chapter 5: Environmental conditions affect amyloid fiber properties of Sup35NM and Rnq1PFD

This work is a manuscript in preparation for publication

SUMMARY

We have established an efficient assay to study the effect that a variety of different conditions have on amyloid fiber formation. We have used Sup35NM and Rnq1PFD, the prion forming domains (PFD) of the yeast proteins Sup35p and Rnq1p respectively, as model amyloidogenic proteins. Sup35p and Rnq1p aggregate in vivo to determine the yeast prions [*PSI*+] and [*RNQ*+] respectively and their PFDs have been shown to form amyloid fibers in vitro. Fibers formed at physiological pH (7.4) differ in kinetics of assembly and stability depending on the presence of denaturant (urea), salt (NaCl), divalent cation ($MgCl_2$), osmolyte (sorbitol), molecular crowding agent (polyethylene glycol, PEG) and viscous liquid (glycerol) in the solution. The effect of the different conditions on the kinetics of fiber formation was profound and rather disparate for Sup35NM and Rnq1PFD. The stability of the fibers formed in different conditions was dramatically affected for Sup35NM but only subtly affected for Rnq1PFD fibers. We are currently testing the ability of Sup35NM and Rnq1PFD fibers formed in the different conditions to induce [*PSI*+] and [*RNQ*+], respectively. We are also in the process of analyzing the morphology of the fibers using transmission electron microscopy (TEM) and atomic force microscopy (AFM). We hypothesize that variation in the structure of the amyloid fibers formed by Sup35NM and Rnq1PFD is a result of the interactions of the two proteins with the solvent conditions. Based on our kinetic data, we suggest that the interaction of the polypeptide with the solvent is sequence - dependent and that the same solvent conditions may have drastically different effects on different amyloidogenic polypeptides. Fibrillar polymorphism has been

reported for many different proteins and may have various biological consequences including forming the basis for variation in disease pathology and transmissibility.

The amyloid fiber has been suggested to be a structure that most if not all, polypeptides and proteins can access if given the right conditions (1). Deposition of amyloid fibers formed from a variety of proteins has been associated with many neurodegenerative diseases such as Alzheimer's, Parkinson's and prion diseases (2-4). Amyloid fibers formed from various proteins and peptides have been used to obtain the molecular structure of these ordered aggregates. Techniques such as solid state NMR and X-ray diffraction have provided breakthroughs towards obtaining an atomic resolution structure for amyloid fibers (5-8). Furthermore, an atomic resolution model for the basis of structural variation and the resulting polymorphism in amyloid fibers has also been proposed (9). Previous work done by our laboratory (Kalastavadi and True, JBC, In Revision) and others using yeast prion proteins as a model has provided evidence to link variation in the morphology and biochemical properties of the amyloid fibers to prion strain formation (10,11). Work done by others on yeast prion strains (called variants in yeast) has also shown differences in inter- and intra-molecular contacts between monomers that form the fiber in different variants, hence suggesting a role for monomer-monomer interactions in generating the structural polymorphisms observed with amyloid fibers (12,13). Polymorphisms in amyloid fibers have also been observed in protein deposits found in protein misfolding diseases (14). Although significant work has been done toward understanding the structural basis for the polymorphisms, not much is known about how different environmental conditions interact with different amyloidogenic proteins to create amyloid fiber polymorphism. Recent studies have

reported the effect of solvent conditions on fiber morphology (15,16), but these systems lack the ability to assay the phenotypic consequences of the diverse morphologies and properties inside a cell.

In this study, we have used two different yeast prion proteins, Sup35NM and Rnq1PFD, to dissect the effect that solvent conditions have on amyloid fiber morphology and prion phenotype (for a review on yeast prions (17)). Both Sup35NM and Rnq1PFD form amyloid fibers in vitro when diluted out of denaturant (18-20). Sup35NM has been shown to form ordered amyloid fibers in a potassium phosphate buffer (5 mM at pH 7.4) containing 150 mM sodium chloride (FFB) (18). Rnq1PFD has been shown to form amyloid fibers in the same buffer, but in the presence of 2 or 4 M urea (FFB + 2 M Urea) ((21) and True and Kalastavadi, JBC, in revision). We have investigated the effect of concentrations of denaturant (urea), salt (NaCl), divalent cation ($MgCl_2$), osmotic stress (sorbitol), molecular crowding agent (PEG) and viscous agent (glycerol) on amyloid fiber formation of both Sup35NM and Rnq1PFD. We found that solvent conditions dramatically affected the rate of fiber formation and stability for Sup35NM. Rnq1PFD fiber formation kinetics was also influenced dramatically by the various solvent conditions, but the effect on stability was more subtle. We propose to assay morphology of these fibers by EM and AFM, and differences in their secondary structure using thioflavin-T (Th-T) fluorescence spectra, CD, and FTIR spectra. We are currently in the process of determining what prion variants are induced by Sup35NM and Rnq1PFD fibers formed in the different solvent conditions. Our preliminary results suggest that solvent conditions do not uniformly affect fiber formation kinetics and stability for

different amyloidogenic proteins, rather, specific and in fact, sometimes opposite effects occur with different proteins.

RESULTS

Urea inhibits fiber formation of Sup35NM to a larger extent than it does with Rnq1PFD- Previous studies have used high concentrations of urea as a standard component in buffers for fiber formation of Rnq1PFD (21). Sup35NM fiber formation does not require urea (18,19). Considering Sup35NM and Rnq1PFD are both the QN-rich domains (26% for Sup35NM and 40% for Rnq1PFD is made of Q/N) of their respective yeast prion proteins Sup35p and Rnq1p and have a high degree of similarity in amino acid composition; we asked if there was a difference in the ability of a denaturant to suppress the aggregation propensity of either of the proteins. Surprisingly, we noticed that increasing the urea concentration in Sup35NM fiber formation reactions greatly suppressed aggregation (Figure 1A). Sup35NM has a lag phase of ~100 minutes in the absence of urea, which increases to ~300, ~400 and ~650 minutes in the presence of 0.5 M, 1.0 M and 1.5 M urea. Sup35NM was unable to form fibers in 2M urea in the time period assayed (data not shown). Rnq1PFD fiber formation did not have an appreciable lag phase for fiber formation in the absence of urea. Fibers formed in 0.5M urea with less than a 50 minute lag phase and in 1.0M urea this increased to ~ 100 minute lag phase. Interestingly, in low concentrations of urea, the Rnq1PFD fibers tended to have significant amounts of noise in the Th-T fluorescence signal. When Rnq1PFD fibers were formed in, however, the noise in the data was almost absent and the fiber formation showed an appreciable lag phase of ~ 275 minutes.

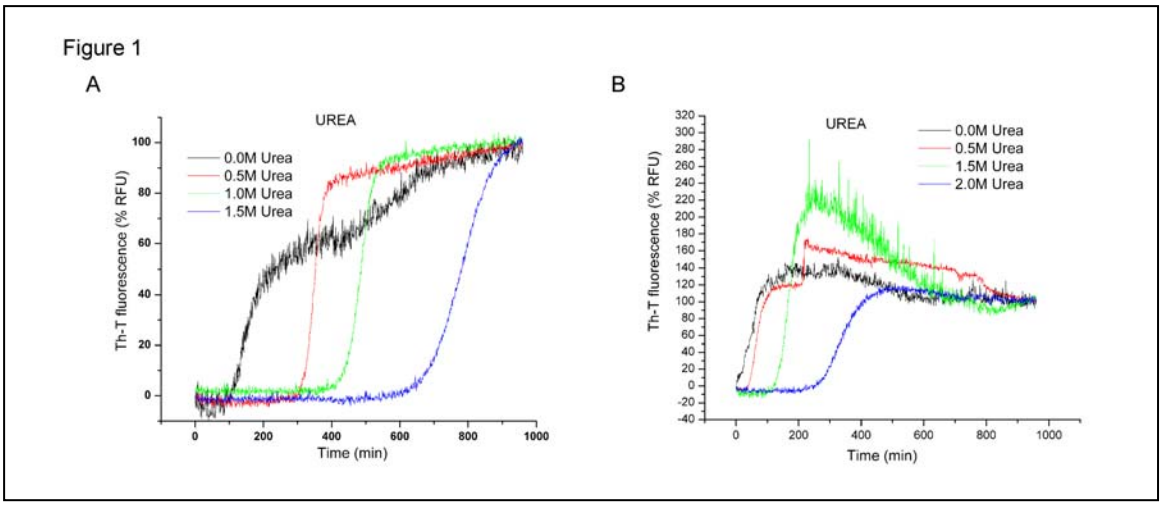

Figure 1: Urea inhibits rate of amyloid fiber formation in (A) Sup35NM and (B) Rnq1PFD. Sup35NM fiber formation was initiated by diluting (120-fold) the protein from 6 M GdHCl to a final concentration of 2.5μM in the reaction and Rnq1PFD fiber formation was initiated by diluting (75 fold) the protein from 7 M GdHCl to a final concentration of 4μM in the reaction. Fiber formation was assayed by measuring Thioflavin-T fluorescence present in 100-fold excess.

Since Rnq1PFD fiber formation showed an appreciable lag phase with little noise in Th-T fluorescence assays only in the presence of 2 M urea, we performed experiments to test the effects of other solvent conditions on Rnq1PFD fiber formation in the presence of 2M urea. Since Sup35NM formed fibers with an appreciable lag phase and with little noise in the absence of urea, we did not add urea to test the effect of other solvent conditions for Sup35NM.

Solvent conditions dramatically affect kinetics of amyloid fiber formation- We then asked what effect changing solvent conditions had on the kinetics of amyloid fiber formation. To this end, we analyzed increasing concentrations of salt, divalent cations, osmotic stress agents and molecular crowding agents for an effect on the lag phase as a measure of the propensity to form amyloid fibers.

We noted that the lag phase for fiber formation of Sup35NM did not change with increasing concentrations of NaCl and the lag phase was ~180 minutes for all concentrations of NaCl added to the reaction (Figure 2A). For Rnq1PFD fiber formation, however, increasing the concentration of NaCl greatly decreased the lag phase and enhanced fiber formation. The lag phase for Rnq1PFD fiber formation in reactions containing 100mM NaCl was ~400 minutes (Figure 3A). This decreased to ~ 350 and ~300 minutes when the concentration of NaCl was increased incrementally to 250mM and 500mM respectively. Further increase in the concentration of NaCl to 750mM and 1000mM decreased the lag phase to ~275 and ~200 minutes respectively (Figure 3A).

Increasing the concentration of divalent cations ($MgCl_2$) resulted in an increase in the lag phase for both Sup35NM and Rnq1PFD, suggesting partial inhibition of fiber formation. Sup35NM fiber formation lag phase increased from ~ 200 to ~250 minutes,

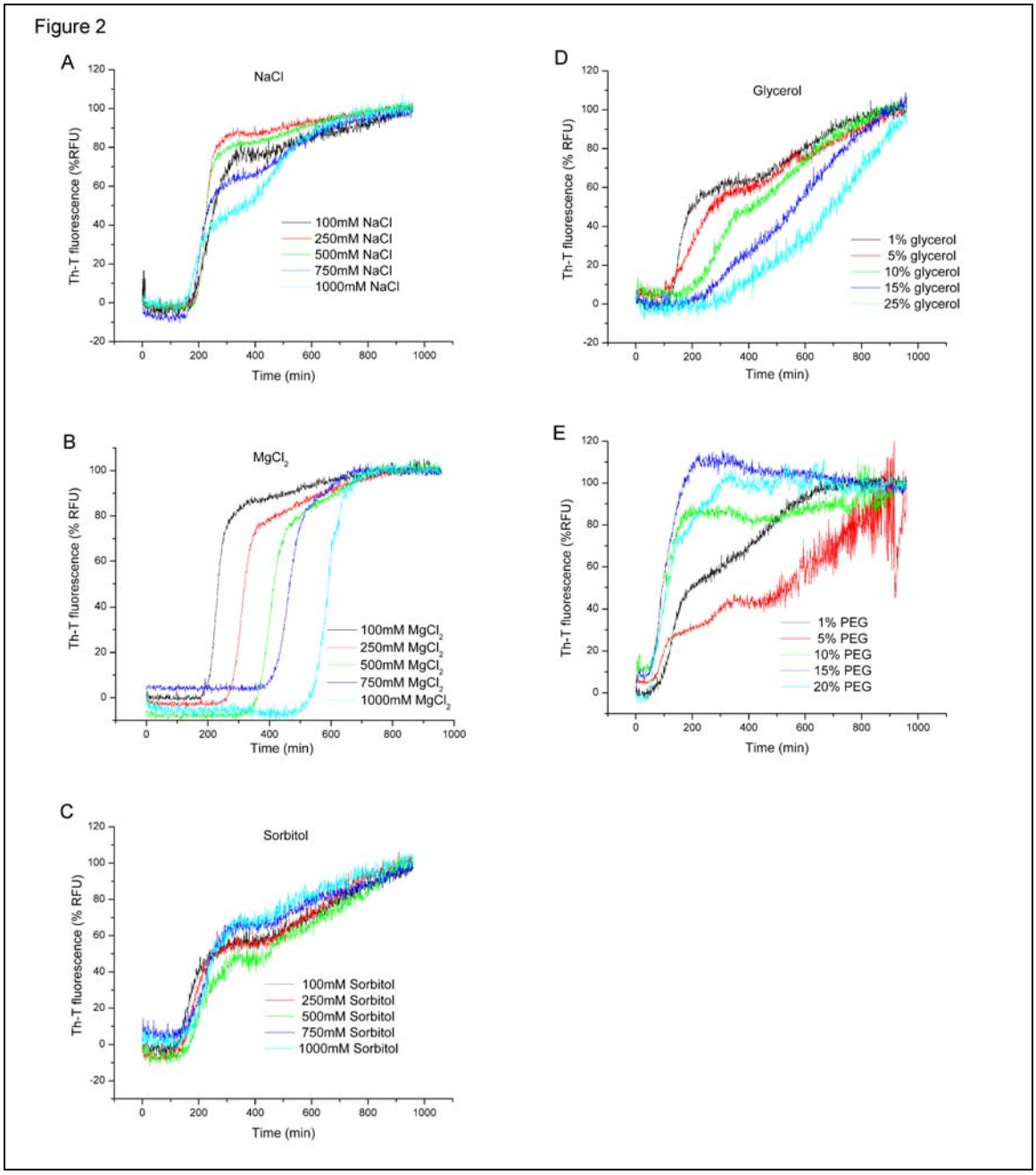

Figure 2. Sup35NM fiber formation kinetics is differentially affected by different solvent conditions (A) Sodium Chloride (NaCl), (B) Magnesium Chloride ($MgCl_2$) (C) Sorbitol (D) Glycerol and (E) PEG. Sup35NM fiber formation was performed at 2.5μM concentration (120 fold dilution from denaturant) in followed by Th-T fluorescence (50 fold excess). These experiments have been done twice and representative graphs are shown.

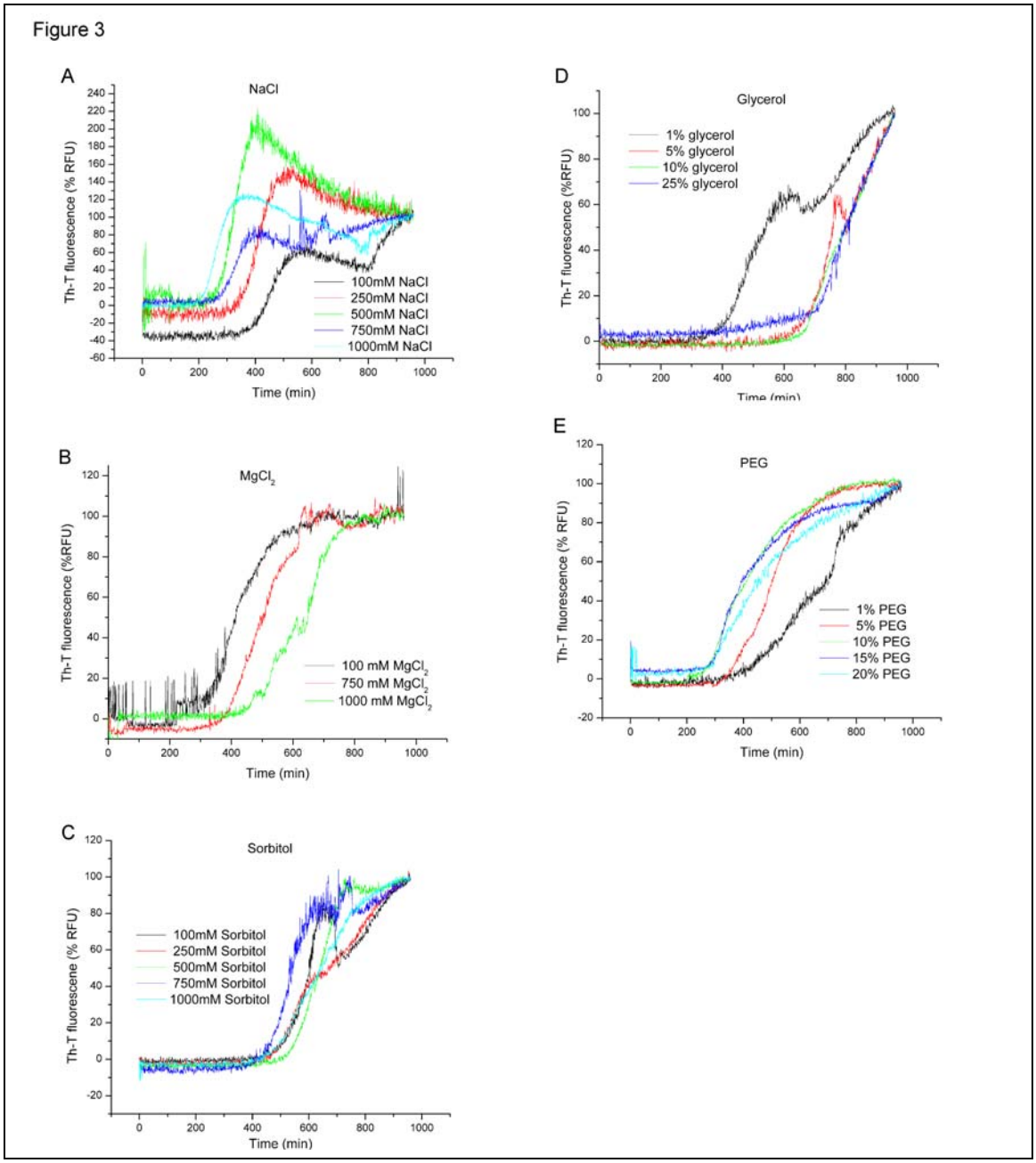

Figure 3. Rnq1PFD fiber formation kinetics is differentially affect with different solvent conditions (A) Sodium Chloride (NaCl), (B) Magnesium Chloride ($MgCl_2$) (C) Sorbitol (D) Glycerol and (E) PEG. Rnq1PFD fiber formation was performed at 4 µM concentration (75-fold dilution from denaturant) and followed by Th-T fluorescence (50 fold excess). These experiments have been done twice and representative graphs are shown.

with an increase in concentration of $MgCl_2$ to 100mM and 250mM. The lag phase further increased to ~350, ~400 and ~525 minutes at concentrations of 500mM, 750mM and 1M $MgCl_2$ respectively (Figure 2B). We saw a similar effect of increased lag phase for Rnq1PFD fiber formation from ~300 minutes in 100mM $MgCl_2$ to ~400 and ~500 minutes with 750mM and 1000mM $MgCl_2$ (Figure 3B).

An increase in the concentration of sorbitol did not affect lag phase of fiber formation for both Sup35NM and Rnq1PFD proteins. Sup35NM had a lag phase of ~170 minutes in the presence of all the concentrations of sorbitol used (100mM – 1M) (Figure 2C). For Rnq1PFD, the lag phase of fiber formation varied subtly from 480 minutes to 520 minutes (Figure 3C) with no correlation to concentration of sorbitol.

We next tested the ability of the two proteins to aggregate in the presence of glycerol. We used glycerol to assay the effect of solvent viscosity on amyloid fiber formation. We saw that with both Sup35NM and Rnq1PFD increasing the solvent viscosity increased the lag phase of fiber formation. The Sup35NM lag phase was ~150 minutes at 1% glycerol and 5% glycerol. It increased to ~200, ~250 and ~320 minutes at 10%, 15% and 25% glycerol concentrations (Figure 2D) respectively. With Rnq1PFD, the lag phase was ~400 minutes with 1% glycerol. It increased to ~670 minutes with 5% and 10% glycerol. The lag phase was further increased to ~730 minutes with 15% glycerol (Figure 3D).

Finally, we tested the effect of molecular crowding on amyloid fiber formation with Sup35NM and Rnq1PFD. With both the proteins we observed that, PEG, which was used as the molecular crowding agent, decreased the lag phase, presumably enhancing the ability of the protein to aggregate. We noted that with Sup35NM the lag

phase was ~120 minutes with 1% PEG. It decreased to ~75 minutes with 5% PEG and to ~50 minutes with 10%, 15% and 20% PEG (Figure 2E). With Rnq1PFD, the length of the lag phase was ~475 minutes in 1% PEG. It decreased to 350 minutes with 5% PEG. This further decreased to ~300 minutes with 10%, 15% and 20% PEG.

Sup35NM and Rnq1PFD fibers formed in various solvent conditions have different thermostabilities- The differences in the thermal stabilities of amyloid fibers can be used as an indicator of differences in the structure of the fibers. We identified specific concentrations of the various conditions used previously for kinetic characterization to determine whether these were changes in the thermostability of the fibers formed in those conditions. We chose concentrations in each condition at which there was a significant change in the kinetics as compared to the control fiber formation buffers (FFB or FFB + 2 M urea) for each protein. Fibers of Sup35NM and Rnq1PFD were formed in the chosen solvent conditions. Subsequently, the fibers were then incubated in the presence of 2% SDS and individual samples were treated to increasing temperatures from 25°C to 95°C (in 10°C intervals). The treated samples were then assayed by SDS-PAGE, western blot and the protein bands were quantified. There were significant differences in the thermostabilities of the fibers formed in the different conditions for Sup35NM (Figure 4A) and subtle differences for Rnq1PFD (Figure 4B).

We noted that the variation in stability of Sup35NM was much greater when compared to Rnq1PFD (Figure 4). In fact, Sup35NM fibers formed in 1.0M urea were completely thermolabile and did not show any resistance to thermal denaturation (Figure 4A). The addition of sodium chloride, PEG, sorbitol and magnesium chloride all increased the stability of fibers formed with Sup35NM (Figure 4A). With Rnq1PFD

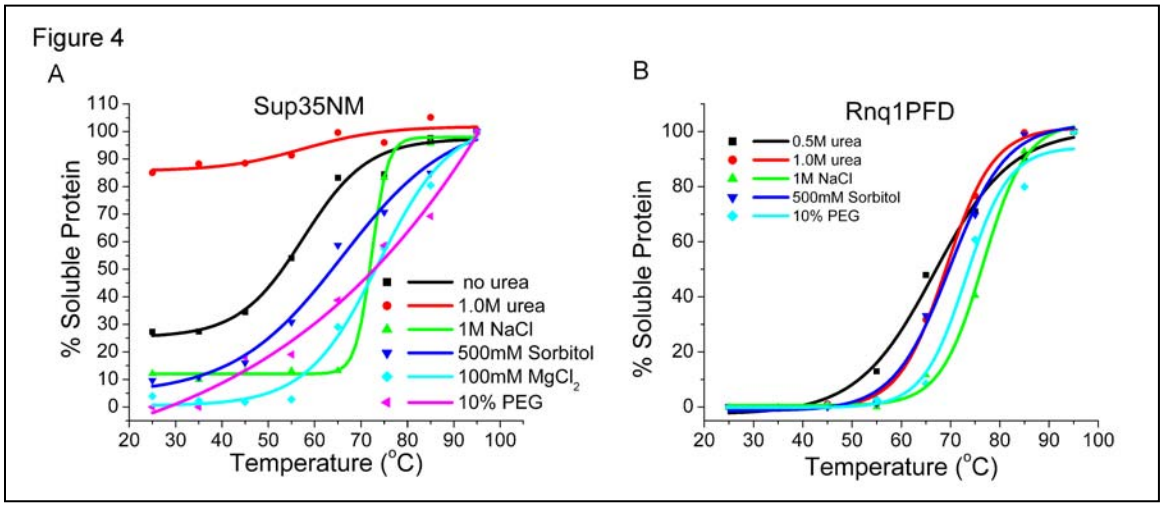

Figure 4. Thermostability of amyloid fibers formed by (A) Sup35NM and (B) Rnq1PFD varies significantly when they are assembled in different solvent conditions. Fibers were formed end over end rotation for 3 days at 2.5 μM concentration for Sup35NM and 4μM concentration for Rnq1PFD. This experiment has been done once and needs to be repeated for Sup35NM and has been done two times for Rnq1PFD.

fibers, we also saw an increase in stability of the fibers with the addition of sodium chloride, sorbitol and PEG (Figure 4B). Surprisingly, we noted that in sharp contrast to Sup35NM, increasing the concentration of urea in the fiber formation buffer actually enhanced the stability of Rnq1PFD fibers. Fibers formed in 0.5 M urea had a $t_{1/2}$~60°C as compared to fibers formed in 1M urea, which had a $t_{1/2}$~70°C. Fibers of Sup35NM and Rnq1PFD formed in NaCl however increased the stability of the fibers to the greatest degree amongst all tested conditions for both polypeptides. Sup35NM fibers formed in 1M NaCl had a $t_{1/2}$~73°C and Rnq1PFD fibers in 1M NaCl had a $t_{1/2}$~76°C. Although sorbitol did not affect the lag phase of fiber formation for either Sup35NM or Rnq1PFD, fibers formed in 500mM sorbitol had significantly enhanced the stabilities of the fibers.

DISCUSSION

The yeast prion proteins, Sup35NM and Rnq1PFD, have both been shown to readily form amyloid fibers at physiological pH. Sup35NM forms ordered amyloid fibers in a potassium phosphate buffer, pH 7.4, with 150 mM sodium chloride when diluted from a denatured state. With Rnq1PFD, however, the presence of urea in the buffer is desired to obtain a majority of ordered amyloid fibers. We suggest that Rnq1PFD forms many non-specific aggregates in the absence of urea and that the denaturant either prevents the formation of the non-specific aggregates or renders them unstable, thereby allowing for more protein to participate in ordered amyloid fiber formation. Non-specific aggregation of Rnq1PFD in the absence of urea may be due to an increase in the inherent ability of the protein to aggregate as compared to Sup35NM. The lower aggregation propensity of Sup35NM is also reflected in the inability of this protein to form amyloid fibers in the presence of high concentrations of denaturant.

Previous work has shown the prevalence of a high degree of structural polymorphism of various amyloidogenic proteins both at different and within the same solvent conditions (22,23). In this study, we have utilized the two polypeptides, Sup35NM and Rnq1PFD, with differential propensities to aggregate to decipher the interplay between solvent conditions, kinetics, stability, and fibrillar morphology. We modulated the rate of fiber formation of the proteins by changing solvent conditions with an expectation that this would change the morphology of the fibers. We assayed changes to the structure of the amyloid fibers using a thermal stability assay. We will further characterize differences in the morphology of the fibers using AFM and TEM techniques, Th-T fluorescence, FTIR and CD spectra.

The relationship between amyloid fiber formation and the various solvent conditions is complex. Surprisingly, we observed that for certain conditions, the Sup35NM and Rnq1PFD kinetics behaved differently and for other conditions they behaved similarly. For example, sorbitol did not have an effect on lag phase of fiber formation for either protein, but sodium chloride increased the lag phase of fiber formation for Rnq1PFD and had no effect on the lag phase for Sup35NM fiber formation. Therefore, we suggest that the interaction of the amyloid fiber forming peptide and the solvent is sequence-dependent. This interaction may influence intra- and inter-molecular interactions of the monomeric subunits of the proteins that form amyloid fibers. The pathway that a protein follows to convert from a monomer to an amyloid fiber may also be influenced by the solvent conditions. These and other effects that the solvent conditions have on fiber formation may be avenues that a protein utilizes to generate polymorphisms in the resulting amyloid fiber.

Our data show that there is no definitive correlation between the length of lag phase of fiber formation and fiber stability. For example, 10% PEG decreased the length of lag phase when compared to control fiber formation conditions and increased the stability of these fibers for both Sup35NM and Rnq1PFD. In contrast, 100mM $MgCl_2$ increased the length of lag phase, but this condition also increased the stability of the fibers for both proteins. It is yet to be determined if there is a correlation between length of lag phase and stability of fibers at different concentrations of the variable component in a specific solvent condition.

Previous work has explored the effect of salts on the aggregation propensity of Alzheimer's Aβ (1-40), α-synuclein, glucagon, insulin and β2-microglobulin (15,24-26). Aβ(1-40) showed a trend where aggregation became more favorable with the increasing salt concentrations of both NaCl and $MgCl_2$ (25). $MgCl_2$ enhanced fiber formation for both Rnq1PFD and Sup35NM. However, NaCl enhanced fiber formation only for Rnq1PFD and had no effect on Sup35NM. The effect of salts on aggregation may be due to either peptide-salt interactions or via changes in the water structure (surface tension). Considering we observed a mixed effect on aggregation with the different salts, we suggest that the kinetics of fiber formation is depended on a combination of both effects of salts in a solvent.

Sorbitol has been shown previously to act as a stabilizing osmolyte and specifically counteract the effect of urea on fiber formation of immunoglobulin light chain (27). The mechanism of the stabilizing osmolytes is thought to be non-specific. With Sup35NM and Rnq1PFD, we did not observe stabilizing effects by sorbitol. This

may be presumably due to the fact that both these proteins have already been denatured and therefore are not capable of being stabilized by the osmolytes.

Glycerol which is another solvent condition, tested, that we noted that it inhibited fiber formation for both Sup35NM and Rnq1PFD. However, previously, it has been shown to act as an hydrating agent and enhance the aggregation of Aβ (28) as well as to inhibit the conversion of PrP^C to PrPSc (29,30) by acting as a chemical chaperone and stabilizing the native conformation. We propose that in Sup35NM and Rnq1PFD, glycerol is acting as a chemical chaperone to inhibit fiber formation. We suggest that the concentrations of glycerol that have been used in the experiments may not be sufficient to cause the inhibition by increasing the viscosity based on the experiments conducted with α-synuclein (31). However it is theoretically possible that the effect of viscosity is greater for Sup35NM and Rnq1PFD fiber assembly than is for α-synuclein.

PEG is a polymer commonly used to simulate molecular crowding (32). Previous studies have shown PEG to accelerate amyloid fiber formation of α-synuclein and apolipoprotein C-II (31,32). As proposed previously, we suggest that the acceleration in fiber formation observed for Sup35NM and Rnq1PFD is due to excluded volume effects and decreased solubility of the protein (31).

An ongoing experiment that may provide very interesting results is in regard to the influence that the various conditions may have on the the fibers in inducing yeast prion variants in vivo. To this end, we have transformed the fibers formed in the different conditions into [*prion*-] yeast cells. We will determine the prion variants of [*PSI*+] and [*RNQ*+] that the fibers induce and further investigate their in vivo and in vitro properties. We will then attempt to draw correlations between the solvent conditions,

biochemical properties of the fibers, and in vivo properties of the prion variants. The ability to study the properties of the amyloid fibers in vitro and then investigate their in vivo aggregation and resultant phenotype, is a powerful tool to investigate novel features of protein aggregation. Further, the in vivo studies will help us correlate the in vitro fiber properties to their biological relevance in a cellular context.

We propose that these data and ongoing and future experiments will help us determine correlations between different solvent conditions and their influence on amyloid fiber formation and polymorphism. This information may provide clues toward understanding the cell and tissue specificity of protein aggregation diseases. Additionally, understanding the underlying principles of amyloid polymorphisms may help elucidate the mechanisms of strains in "protein-only" diseases. Finally, differentially stable amyloid fibers may provide novel avenues to develop tailored polymers for use as materials.

EXPERIMENTAL PROCEDURES

Protein expression and purification of recombinant proteins – Sup35NM was purified as reported previously (33).

The $pHis_{10}$-Rnq1PD (amino acids 132-405) construct (21) was transformed into *Escherichia coli* BL21(DE3) cells. Resultant transformants were scraped to inoculate large cultures in CircleGrow media and the cells were grown to an OD_{600}~0.6. The expression of Rnq1PFD was induced with 1 mM IPTG for 6 hrs. The cells were harvested and incubated with agitation at room temperature for one hour in 20 mM Tris-HCl, 8 M Urea (Buffer A, pH 8). The cells were then further lysed by sonication. The lysate was cleared by spinning at 10,000 x *g* for 30 minutes. The supernatant was

incubated with Ni^{2+}-Sepharose beads for two hours. Subsequently, the beads were packed in a column and washed with 25 column volumes (CV) Buffer A, pH 8. The beads were then washed successively with four CV each of Buffer A, pH 6.3 and Buffer A, pH 5.9, before eluting with Buffer A, pH 4.5. Rnq1p in the eluted fractions was verified for purity by SDS-PAGE and coomassie staining. The fractions containing the protein were filtered through a 100kD molecular weight cut off column (Amicon) and stored in methanol at -80°C.

Amyloid fiber formation- Kinetic assays of fiber formation were done in a SpectraMax M2e flourimeter microplate reader. Sup35NM monomers were diluted 120-fold from 6 M guanidine hydrochloride to a concentration of 2.5 μM in FFB buffer (150 mM NaCl, 5 mM KPO_4) and Rnq1PFD monomers were diluted 75-fold from 7 M guanidine hydrochloride to a concentration of 4 μM in FFB + 2M Urea buffer (150 mM NaCl, 5 mM KPO_4, 2 M Urea, pH 7.4) with 50-fold molar excess Thioflavin-T to initiate fiber formation in the presence of glass beads for agitation. The change in Thioflavin-T fluorescence over time was measured using an excitation wavelength of 450 nm and emission wavelength of 481 nm. The plate was agitated each minute prior to reading for ten seconds.

For the various other buffer conditions, except when concentration of urea itself was varied, the other agents were added to the mentioned to the final concentration to FFB buffer and FFB + 2M urea buffer for Sup35NM and Rnq1PFD respectively.

Thermostability assay- Pre-formed fibers were treated with 2% SDS for five minutes at different temperatures (gradient from 25°C to 95°C, with 10°C increments). The treated samples were analyzed by SDS-PAGE and western blot using an anti-Rnq1p or anti-

Sup35p antibodies. The bands were quantified using ImageJ software and values were normalized to the 95°C band. Results were plotted using Origin 6.1 statistical software.

REFERENCES:

1. Dobson, C. M. (1999) *Trends Biochem Sci* **24**, 329-332

2. Prusiner, S. B. (1998) *Proc Natl Acad Sci U S A* **95**, 13363-13383

3. Chiti, F., and Dobson, C. M. (2006) *Annu Rev Biochem* **75**, 333-366

4. Harper, J. D., and Lansbury, P. T., Jr. (1997) *Annu Rev Biochem* **66**, 385-407

5. Nelson, R., Sawaya, M. R., Balbirnie, M., Madsen, A. O., Riekel, C., Grothe, R., and Eisenberg, D. (2005) *Nature* **435**, 773-778

6. Jaroniec, C. P., MacPhee, C. E., Astrof, N. S., Dobson, C. M., and Griffin, R. G. (2002) *Proc Natl Acad Sci U S A* **99**, 16748-16753

7. Makin, O. S., Atkins, E., Sikorski, P., Johansson, J., and Serpell, L. C. (2005) *Proc Natl Acad Sci U S A* **102**, 315-320

8. Petkova, A. T., Ishii, Y., Balbach, J. J., Antzutkin, O. N., Leapman, R. D., Delaglio, F., and Tycko, R. (2002) *Proc Natl Acad Sci U S A* **99**, 16742-16747

9. Sawaya, M. R., Sambashivan, S., Nelson, R., Ivanova, M. I., Sievers, S. A., Apostol, M. I., Thompson, M. J., Balbirnie, M., Wiltzius, J. J., McFarlane, H. T., Madsen, A. O., Riekel, C., and Eisenberg, D. (2007) *Nature* **447**, 453-457

10. Tanaka, M., Chien, P., Naber, N., Cooke, R., and Weissman, J. S. (2004) *Nature* **428**, 323-328

11. Tanaka, M., Collins, S. R., Toyama, B. H., and Weissman, J. S. (2006) *Nature* **442**, 585-589

12. Krishnan, R., and Lindquist, S. L. (2005) *Nature* **435**, 765-772

13. Toyama, B. H., Kelly, M. J., Gross, J. D., and Weissman, J. S. (2007) *Nature* **449**, 233-237

14. Jimenez, J. L., Tennent, G., Pepys, M., and Saibil, H. R. (2001) *J Mol Biol* **311**, 241-247

15. Pedersen, J. S., Dikov, D., Flink, J. L., Hjuler, H. A., Christiansen, G., and Otzen, D. E. (2006) *J Mol Biol* **355**, 501-523

16. Piazza, R., Pierno, M., Iacopini, S., Mangione, P., Esposito, G., and Bellotti, V. (2006) *Eur Biophys J* **35**, 439-445

17. Tuite, M. F., and Cox, B. S. (2003) *Nat Rev Mol Cell Biol* **4**, 878-890

18. Glover, J. R., Kowal, A. S., Schirmer, E. C., Patino, M. M., Liu, J. J., and Lindquist, S. (1997) *Cell* **89**, 811-819

19. King, C. Y., Tittmann, P., Gross, H., Gebert, R., Aebi, M., and Wuthrich, K. (1997) *Proc Natl Acad Sci U S A* **94**, 6618-6622

20. Sondheimer, N., and Lindquist, S. (2000) *Mol Cell* **5**, 163-172

21. Patel, B. K., and Liebman, S. W. (2007) *J Mol Biol* **365**, 773-782

22. Anderson, M., Bocharova, O. V., Makarava, N., Breydo, L., Salnikov, V. V., and Baskakov, I. V. (2006) *J Mol Biol* **358**, 580-596

23. Petkova, A. T., Leapman, R. D., Guo, Z., Yau, W. M., Mattson, M. P., and Tycko, R. (2005) *Science* **307**, 262-265

24. Grudzielanek, S., Smirnovas, V., and Winter, R. (2006) *J Mol Biol* **356**, 497-509

25. Klement, K., Wieligmann, K., Meinhardt, J., Hortschansky, P., Richter, W., and Fandrich, M. (2007) *J Mol Biol* **373**, 1321-1333

26. Munishkina, L. A., Henriques, J., Uversky, V. N., and Fink, A. L. (2004) *Biochemistry* **43**, 3289-3300

27. Kim, Y. S., Cape, S. P., Chi, E., Raffen, R., Wilkins-Stevens, P., Stevens, F. J., Manning, M. C., Randolph, T. W., Solomon, A., and Carpenter, J. F. (2001) *J Biol Chem* **276**, 1626-1633

28. Yang, D. S., Yip, C. M., Huang, T. H., Chakrabartty, A., and Fraser, P. E. (1999) *J Biol Chem* **274**, 32970-32974

29. DebBurman, S. K., Raymond, G. J., Caughey, B., and Lindquist, S. (1997) *Proc Natl Acad Sci U S A* **94**, 13938-13943

30. Tatzelt, J., Prusiner, S. B., and Welch, W. J. (1996) *EMBO J* **15**, 6363-6373

31. Munishkina, L. A., Cooper, E. M., Uversky, V. N., and Fink, A. L. (2004) *J Mol Recognit* **17**, 456-464

32. Hatters, D. M., Minton, A. P., and Howlett, G. J. (2002) *J Biol Chem* **277**, 7824-7830

33. Tanaka, M., and Weissman, J. S. (2006) *Methods Enzymol* **412**, 185-200

Chapter 6: Conclusions and Future Directions

6.1 Sup35-PrP chimeras future directions

Summary

The reason for the onset of a subset of the inherited forms of prion disease is suggested to be due to the ability of the mutation in the gene to destabilize the native conformation of the protein and presumably enhance its ability to induce the prion state (1). In the case of repeat expansion mutations in prion disease, previous studies have observed a correlation between the length of expansion and age of onset (2). Additionally, previous work done in our lab demonstrated that the repeat-expanded fusion protein of Sup35p and PrP maintain a stronger variant of the [*PSI*+] prion in yeast cells (3). Therefore, we hypothesized that the repeat expansions may play a role in increasing the inherent capacity of the protein to aggregate. Purified recombinant chimeric proteins of Sup35-PrP did in fact show an ability to aggregate in vitro, however, the chimeras did not show a correlative increase in the stabilities of the aggregated conformation.

Determine the amyloid core of SP14NM variants

Another interesting observation we made with a specific repeat expansion of Sup35-PrP fusion which contained 14 octapeptide repeats was the ability of this fusion to switch between prion variants (3). We observed that in vivo, the SP14 prion was capable of converting from a strong variant to a weak variant and back at a high frequency. This ability to switch between prion variants was not observed for [*PSI*+] formed from the wild type Sup35p or the shorter repeat expansions. In Chapter 2, I demonstrate that SP14NM can form amyloid fibers in vitro and, when transformed into yeast cells, they induce the prion state.

Preliminary experiments have shown that when SP14NM fibers are formed at different temperatures and transformed into yeast they produce different variants of the [*PSI*+] in vivo. The physical basis for prion variants has been proposed based on the ability of Sup35NM fibers formed at different temperatures to induce distinct variants in vivo (4,5). However, in contrast to the variants maintained by SP14NM, these variants are stable and do not switch between strong and weak variants with a high frequency. I hypothesize that the ability of the SP14 chimeric protein based variants are able to allow for the high frequency switch between variants is based on the conformation that the SP14 monomers adopt when they aggregate. I speculate that the structural difference between two strains formed from the SP14 protein is very little when compared to the structural differences between two strains based on Sup35p.

In order to address this hypothesis, I made reagents that may prove useful in investigating the structural variation between the strains of SP14NM fibers formed at different temperatures. I took advantage of the fact that SP14NM does not contain any endogenous cysteine residues and introduced single cysteine mutants that spanned the SP14NM protein fragment. I made eight cysteine substitution mutations in SP14NM to interrogate the orientation of different regions of the protein based on fluorescence labeling techniques used previously for Sup35NM (6). I suggest that future experiments be focused on labeling the recombinant cysteine mutants of SP14NM with fluorophors such as pyrene, acrylodan and alexa fluor-488 (or others) in order to determine the environment of the amino acid labeled in SP14NM. Both pyrene and acrylodan are sensitive to the solution environment and produce a shift in fluorescence based on their surrounding polar or non-polar environment. This property will be useful in identifying

regions of the protein that are exposed or buried to the solvent. Additionally, pyrene also has the ability to form excimers with neighboring pyrene molecules. This property of pyrene will be useful to determine inter-molecular sites of interactions by measuring excimer formation of two different labeled cysteine mutants mixed together.

Elucidating the structure of SP14NM in amyloid fibers created at different temperatures may provide a means to understand mechanisms behind the phenotypic variability observed in neurodegenerative diseases. Furthermore, it may provide clues toward elucidating the reason why SP14NM is capable of forming amyloid fibers at a much greater efficiency when compared to the wild type Sup35NM and non-repeat-expanded SP5NM proteins.

We also observed, as mentioned in Chapter 2, that the morphology of the amyloid fibers was significantly different for the different chimeras. We observed that SP5NM (chimera with wild type number of repeats) fibers were ordered and did not form a meshwork or clumps of fibers. The repeat expanded chimeras, SP8NM, SP11NM and SP14NM however all formed a meshwork or clumps of fibers. It is important to note that only the repeat-expanded chimeras are associated with inherited prion disease and cause pathology. Understanding conformational differences between the wild type chimera and the repeat-expanded chimera using techniques proposed in this chapter or using H/D exchange NMR techniques used for Sup35NM previously (7) may prove important in understanding conformational differences between aggregates that are associated with pathology and those that are not. This is especially biologically significant because protein aggregation has been shown to be present in the absence of disease, suggesting that there may be certain forms of aggregates that are not pathological (8).

Another independent reason for the phenotypic variability seen in [*SP14*+] cells may be due the prion state actually being lost and then SP14 protein aggregating *de novo* to form a novel variant. It is plausible that in yeast cells that the *de novo* aggregation of the already aggregation-prone SP14 protein may be facilitated by [*RNQ*+]. The interaction of the aggregated Rnq1p with SP14 may allow for phenotypic variability. This interaction may prove to be a useful model in elucidating the nature of the interaction between amylodogenic proteins in disease to cause phenotypic variability in humans. Recent reports have provided evidence to suggest that the aggregation of one protein may template the aggregation of a different protein in various diseases and disease models (9,10). One avenue for disease onset and phenotypic variability may be the cross-talk between two aggregation prone proteins and Rnq1p and SP14/ SP14NM may provide a useful model to elucidate these mechanisms both in vivo and in vitro.

Conclusions

The Sup35-PrP chimera with various disease-associated repeat expansion substitutions provides a genetically tractable and biochemical means to assay multiple aspects of protein aggregation and amyloid fiber formation. The ability to understand the structural properties of the disease-associated mutants and then transform those aggregates into cells provides a powerful tool to decipher the relationship between structural changes and phenotype or disease. The above experiments proposed are aimed at understanding the molecular basis of variation in phenotypes and co-aggregation of proteins in various progressive and fatal diseases in humans.

6.2 Structure of Rnq1PFD in prion variants of [*RNQ*+]

Summary

One of the most intriguing properties of proteins that form amyloid fibers is their ability to access multiple stable conformations. These conformations are also capable of faithfully templating their structure onto unconverted monomeric forms of the protein. Yeast prions can also propagate with multiple conformations. A physical basis for the existence of yeast prion strains has been proposed based solely on the experiments done with Sup35NM (5). In chapter 3, I have done work toward identifying common and distinct features that are shared between [*RNQ*+] and [*PSI*+] prion variants. The molecular structure of the prion variants generated by forming amyloid fibers with Sup35NM has been studied in detail using multiple approaches (6,7,11). However, not much is known about the amyloid structure of Rnq1PFD or its variants.

Determine the amyloid core of Rnq1PFD variants

In order to elucidate the amyloid core of the Rnq1PFD variants, I have generated 15 cysteine mutants that span the sequence of this protein. Future experiments will include using techniques used previously (6) to determine what regions of the protein that are involved in forming the amyloid core as well as amino acids in Rnq1PFD that are involved in inter-molecular interactions. Further structural characterization of the variants could include 3D fiber topology determination using AFM and spectroscopic methods such as FTIR and EPR to determine secondary structure content differences (4,12).

Determine specific sites of interaction between Sup35NM and Rnq1PFD

Based on the heterologous cross-seeding model for enhanced [*PSI*+] induction in the presence of [*RNQ*+], the aggregates of Rnq1p template the aggregation of Sup35p resulting in the induction of [*PSI*+] (13). Although there is significant amount of data to suggest an interaction between Sup35p and Rnq1p, the specific physical interaction between the two proteins is at best correlative (13-16). Future experiments using reagents generated to determine the structural properties of Rnq1PFD as mentioned in this chapter along with reagents used to determine structural properties for Sup35NM by Krishnan and Lindquist (6) may provide a means to elucidate the specific interaction domains between the two protein fragments. Experiments with different pairs of cysteine mutant proteins in cross-linking will provide information regarding interactions that are agonists and antagonists of cross-seeding. Additionally, previous reports have suggested specific interactions between variants of [*PSI*+] and [*RNQ*+], with certain variants of one prion destabilizing the propagation of variants of another prion (17). This may occur due to specific templating interactions may induce specific variants and destroy other variants. The cross-linking of cysteine residues between monomers of Sup35NM and Rnq1PFD may provide information about interactions that lead to the production of specific variants.

Conclusions

The etiology of most cases of protein misfolding disorders is unknown and therefore classified as being "sporadic". I suggest that some of the sporadic cases may be caused by initial misfolding of proteins that are unrelated directly to disease pathology, but are indirectly involved in cross-seeding other aggregation prone proteins to cause

disease. Understanding the molecular and structural basis for the interaction between two different proteins that are known to interact in vivo may provide clues towards understanding the mechanisms that cause certain sporadic cases of protein misfolding diseases. Additionally, cross-seeding of multiple proteins may also play a role in explaining the phenotypic diversity observed in some protein misfolding diseases (9). The experiments proposed above provide a platform where we may be able to start answering these very important disease mechanisms.

Determine the interaction between Rnq1PFD and the yeast chaperone system

The role that molecular chaperones, specifically heat-shock proteins, play in prion propagation has been well studied in vivo (18,19). Hsp104p is a chaperone in yeast that is required for the propagation of both [*PSI*+] and [*RNQ*+] (20,21). Deletion of *HSP104* cures yeast cells of the prion state. Intriguingly, over expression of Hsp104p only cures the [*PSI*+] prion and not the [*RNQ*+] prion (20). Although the mechanism of the action of Hsp104p and other chaperones on amyloid fibers formed with Sup35NM has been well-studied in vitro (22,23), the reason for the differential effects of the chaperone system on [*PSI*+] and [*RNQ*+] has not been investigated.

I propose that using already established protocols in the lab to purify Hsp104p and the ability to make Rnq1PFD fibers will allow us to understand the mechanism of [*RNQ*+] prion propagation and the differential effects that Hsp104p has on different prions. Future experiments that can be conducted include the effect that different concentrations of Hsp104p has on the lag phase of fiber formation and the variants of Rnq1PFD that are formed. Additionally, experiments can be designed to detect the ability of Hsp104p to disaggregate Rnq1PFD fibers.

Conclusions

The ability of chaperones to modulate the aggregation and disaggregation of yeast prions provides a tantalizing avenue to explore therapeutic approaches that do the same in human diseases. Hsp104 itself is not conserved in humans and therefore could be developed as a therapeutic agent (24). More importantly, understanding the mechanism of how chaperones modulate protein aggregation will provide inspiration to develop synthetic agents with similar mechanism for use in either preventing the progress or curing protein misfolding disorders.

6.3 Structural differences between infectious and non-infectious amyloid aggregates

Summary

In chapter 4, we have begun to explore properties that make an amyloid fiber infectious versus non-infectious. We used the deletion mutant of Rnq1PFD termed Rnq1PFDΔHot that formed infectious fibers when assembled at 37°C, whereas, fibers formed at 25°C were not able to infect yeast cells to induce the [*RNQ*+] prion. We have characterized the mutant biochemically (Th-T fluorescence and thermal stability assays). However, the variation in structure of the mutant when assembled at the two different temperatures remains to be determined.

Determine the structural differences between Rnq1PFDΔHot fibers formed at 25°C and 37°C

The initial experiments to determine structural differences between the infectious and non-infectious variants of Rnq1PFDΔHot involve the use of various spectroscopic techniques. Fibers formed at the different temperatures can be assayed using CD spectra,

FTIR and EPR to determine the secondary structure. Additionally, using AFM will allow the identification of morphological differences between fibers formed at the different temperatures that were not easily discernable using TEM.

The subsequent experiments should concentrate on investigating the differences in the structure of the protein in the fibers at a higher resolution. The use of HD-exchange NMR or biophysical techniques to identify the orientation of regions of the protein as used in the studies referenced (6,7) will provide useful information regarding the structural signatures that determine the infectivity of an amyloid fiber. The generation of cysteine mutants that span the Rnq1PFDΔHot region will be a critical step toward doing the experiments proposed above.

An alternative reason for the differences in the ability of the two variants to induce the prion in vivo may be due to differences in the effect of various chaperones on the amyloid fibers. Therefore, experiments designed to elucidate the effect of Hsp104p and other yeast Hsps may provide critical details that help differentiate between infectious and non-infectious amyloid fibers. To characterize the effect of chaperones on Rnq1PFDΔHot fibers, Th-T fiber formation assays and fiber disaggregation assays can be conducted by treating the fibers with increasing concentrations of Hsp104p in combination with other yeast chaperones.

Conclusions

The proposal that all protein aggregates that form amyloid fibers can be infectious is a currently hotly debated and investigated area of research (25-28). Since, most amyloid fibers seem to undergo a "nucleated polymerization model" for fiber formation, it is conceivable that all of them are infectious. However, I hypothesize that differences

in the rates of nucleation, aggregation and fragmentation of the fibers will determine the ability of an amyloid fiber to be infectious and that the specific conformation that a monomer acquires when it becomes part of an aggregate plays a major role in determining these properties. The Rnq1PFDΔHot protein fragment and the [*RNQ*+] yeast prion provides us with a unique model system to interrogate the differences between infectious and non-infectious amyloids in both in vitro and the in vivo conditions.

6.4 Correlation between amyloid fiber morphology and solvent conditions

Summary

The polymorphism in amyloid fiber preparations can be readily observed using techniques such as AFM or TEM (29-31). Protein aggregates in disease have also shown morphological differences when observed by cryo-EM (32). Various possibilities may cause the differences in the structure of the amyloid fibers, including differences in the assembly of individual amyloid fibers into bundles and variations in the inter- and intra-molecular contacts that the monomers make during polymerization. Environmental changes could play a major role in influencing the distribution in morphology of the fibers. In chapter 5 of this thesis, we have used Sup35NM and Rnq1PFD to dissect the interaction between amyloid fiber polymorphism and solvent conditions.

Morphological characterization of amyloid fibers

Experiments described in chapter 5 of this thesis have provided evidence to suggest that amyloid fibers of Sup35NM and Rnq1PFD formed in different solvent conditions have distinct biochemical properties. In addition, Sup35NM and Rnq1PFD seem to interact differently with the solvents, suggesting that the biochemical properties

and morphologies of amyloid fibers may be a consequence of both protein sequence and environmental conditions. The goal of this chapter is to draw correlations between solvent conditions, amyloid fiber morphologies and prion variant creation. In order to determine the structural differences between the amyloid fibers formed in various solvent conditions, future experiments will use spectroscopic techniques such as CD, FTIR and EPR to determine secondary structure content. Additionally, the supra-molecular structural differences will be determined using AFM and TEM imaging.

Additional experiments that correlate morphologies of amyloid fibers to the prion variants they induce in vivo will be done using yeast protein transformation techniques. It will be interesting to identify weather there are any correlations between amyloid morphologies, prion variants and infectivity.

Future directions could also include testing the tensile strength of the fibers formed from the different proteins in different conditions using the AFM. The data obtained from these experiments could provide valuable information regarding potential material properties of the fibers. Using these properties as a guide, one can envision developing conditions that can tailor the physical properties of fibers formed from various proteins to use as a source for materials.

Conclusions

Understanding the basis for polymorphism in the structure of amyloid fibers and developing techniques to control the morphology of amyloid fibers has implications both in understanding phenotypic variation in disease and in developing biodegradable tailor-made materials for various applications. By using Sup35NM and Rnq1PFD as model amyloidogenic proteins, we hope to elucidate the interactions between solvent conditions

and amyloid fibers. Furthermore, we anticipate identifying sequence-specific differential interactions between solvent conditions and amyloidogenic proteins. These studies may also facilitate identification of environments risk factors for protein misfolding diseases.

REFERENCES:

1. Collinge, J. (2001) *Annu Rev Neurosci* **24**, 519-550

2. Croes, E. A., Theuns, J., Houwing-Duistermaat, J. J., Dermaut, B., Sleegers, K., Roks, G., Van den Broeck, M., van Harten, B., van Swieten, J. C., Cruts, M., Van Broeckhoven, C., and van Duijn, C. M. (2004) *J Neurol Neurosurg Psychiatry* **75**, 1166-1170

3. Tank, E. M., Harris, D. A., Desai, A. A., and True, H. L. (2007) *Mol Cell Biol* **27**, 5445-5455

4. Tanaka, M., Chien, P., Naber, N., Cooke, R., and Weissman, J. S. (2004) *Nature* **428**, 323-328

5. Tanaka, M., Collins, S. R., Toyama, B. H., and Weissman, J. S. (2006) *Nature* **442**, 585-589

6. Krishnan, R., and Lindquist, S. L. (2005) *Nature* **435**, 765-772

7. Toyama, B. H., Kelly, M. J., Gross, J. D., and Weissman, J. S. (2007) *Nature* **449**, 233-237

8. Slow, E. J., Graham, R. K., Osmand, A. P., Devon, R. S., Lu, G., Deng, Y., Pearson, J., Vaid, K., Bissada, N., Wetzel, R., Leavitt, B. R., and Hayden, M. R. (2005) *Proc Natl Acad Sci U S A* **102**, 11402-11407

9. Giasson, B. I., Lee, V. M., and Trojanowski, J. Q. (2003) *Neuromolecular Med* **4**, 49-58

10. Morales, R., Estrada, L. D., Diaz-Espinoza, R., Morales-Scheihing, D., Jara, M. C., Castilla, J., and Soto, C. *J Neurosci* **30**, 4528-4535

11. Shewmaker, F., Wickner, R. B., and Tycko, R. (2006) *Proc Natl Acad Sci U S A* **103**, 19754-19759

12. Tanaka, M., Chien, P., Yonekura, K., and Weissman, J. S. (2005) *Cell* **121**, 49-62

13. Derkatch, I. L., Bradley, M. E., Hong, J. Y., and Liebman, S. W. (2001) *Cell* **106**, 171-182

14. Derkatch, I. L., Bradley, M. E., Zhou, P., Chernoff, Y. O., and Liebman, S. W. (1997) *Genetics* **147**, 507-519

15. Derkatch, I. L., Chernoff, Y. O., Kushnirov, V. V., Inge-Vechtomov, S. G., and Liebman, S. W. (1996) *Genetics* **144**, 1375-1386

16. Vitrenko, Y. A., Gracheva, E. O., Richmond, J. E., and Liebman, S. W. (2007) *J Biol Chem* **282**, 1779-1787

17. Bradley, M. E., and Liebman, S. W. (2003) *Genetics* **165**, 1675-1685

18. Jones, G. W., and Tuite, M. F. (2005) *Bioessays* **27**, 823-832

19. Rikhvanov, E. G., Romanova, N. V., and Chernoff, Y. O. (2007) *Prion* **1**, 217-222

20. Chernoff, Y. O., Lindquist, S. L., Ono, B., Inge-Vechtomov, S. G., and Liebman, S. W. (1995) *Science* **268**, 880-884

21. Sondheimer, N., and Lindquist, S. (2000) *Mol Cell* **5**, 163-172

22. Shorter, J., and Lindquist, S. (2004) *Science* **304**, 1793-1797

23. Shorter, J., and Lindquist, S. (2006) *Mol Cell* **23**, 425-438

24. Vashist, S., Cushman, M., and Shorter, J. *Biochem Cell Biol* **88**, 1-13

25. Baxa, U. (2008) *Curr Alzheimer Res* **5**, 308-318

26. Lundmark, K., Westermark, G. T., Nystrom, S., Murphy, C. L., Solomon, A., and Westermark, P. (2002) *Proc Natl Acad Sci U S A* **99**, 6979-6984

27. Zhang, B., Une, Y., Fu, X., Yan, J., Ge, F., Yao, J., Sawashita, J., Mori, M., Tomozawa, H., Kametani, F., and Higuchi, K. (2008) *Proc Natl Acad Sci U S A* **105**, 7263-7268

28. Frost, B., Jacks, R. L., and Diamond, M. I. (2009) *J Biol Chem* **284**, 12845-12852

29. Anderson, M., Bocharova, O. V., Makarava, N., Breydo, L., Salnikov, V. V., and Baskakov, I. V. (2006) *J Mol Biol* **358**, 580-596

30. Klement, K., Wieligmann, K., Meinhardt, J., Hortschansky, P., Richter, W., and Fandrich, M. (2007) *J Mol Biol* **373**, 1321-1333

31. Pedersen, J. S., Dikov, D., Flink, J. L., Hjuler, H. A., Christiansen, G., and Otzen, D. E. (2006) *J Mol Biol* **355**, 501-523

32. Jimenez, J. L., Tennent, G., Pepys, M., and Saibil, H. R. (2001) *J Mol Biol* **311**, 241-247